Synthesis and Biological Activity of Vasopressin Analogs

Master's Thesis by Birgit Höger

Submitted to the Faculty of
Technical Chemistry, Chemical & Process Engineering and Biotechnology
at Graz University of Technology
in partial fulfillment of the requirements for the degree of Master of Science
in Biochemistry and Molecular Biomedical Sciences

External Supervisor:
Dr. Maja Köhn
Genome Biology Unit
EMBL Heidelberg

Supervisor:
Prof. Dr. Peter Macheroux
Institute of Biochemistry
Graz University of Technology

Submitted December 2011

EIDESSTATTLICHE ERKLÄRUNG

Ich erkläre an Eides statt, dass ich die vorliegende Arbeit selbstständig verfasst, andere als die angegebenen Quellen/Hilfsmittel nicht benutzt, und die den benutzten Quellen wörtlich und inhaltlich entnommene Stellen als solche kenntlich gemacht habe.

Graz, am ....
(Unterschrift)

STATUTORY DECLARATION

I declare that I have authored this thesis independently, that I have not used other than the declared sources/resources, and that I have explicitly marked all material which has been quoted either literally or by content from the used sources.

....
(date) (signature)

The herein presented work is the final report of my master's thesis project that has been carried out at the European Molecular Biology Laboratory EMBL in Heidelberg, Germany, under the supervision of Dr. Maja Köhn.

The work has been supported by the KUWI Stipendium from Graz University of Technology and the Auslandsstudienbeihilfe des Landes Steiermark.

Acknowledgment

I would like to cordially thank my two supervisors, first of all Maja Köhn for giving me the opportunity to come to Heidelberg to work in her lab and for the great support and motivation she gave me during these months, secondly Peter Macheroux for enabling and encouraging me to perform this thesis abroad and for supervising me throughout my studies at university.
I sincerely thank all my colleagues from the Köhn lab for supporting me and giving me helpful suggestions and for the cheerful atmosphere that made me enjoy my stay so much. Special thanks are dedicated to Karolina Pavic for helping me getting started, Pablo Rios for assisting me during cloning and Christoph Meyer for supervising me in the past.
I further thank Gregor Reither from the Schultz lab for familiarizing me with the world of microscopy.
Furthermore, I want to thank my “old” colleagues from the Macheroux lab for supervising me during my studies and helping me with all sorts of problems.
Last but not least I want to express my gratitude to my family for making life so easy and enjoyable and above all to my dear parents for enabling everything in my life and for their constant support.

Abstract

During the past 50 years, a lot of attention has been paid to the analysis of physiology and pathophysiology of the neuropeptide hormone vasopressin. Substantial efforts were undertaken to develop peptide and non-peptide agonists and antagonists of the vasopressin receptors in order to investigate the underlying signaling mechanism(s), as well as to treat various vasopressin-related diseases.

Disulfide bond-engineering of peptide analogs is an important strategy to stabilize peptides against proteolytic degradation. To date, various such engineered vasopressin analogs already have been synthesized. In the course of this thesis, 1-carba- and 6-carba-thioether analogs of vasopressin (AVP) and the vasopressin-analog desmopressin (dDAVP) have been synthesized by solid-phase peptide synthesis, followed by UV-induced thiol-ene reaction of a cysteine residue with an alkene moiety that was incorporated into the peptides. This strategy enables for the first time the exchange of both respective sulfur atoms by a carbon atom and therefore represents peptide engineering on single atom level. The double bond-holding L-vinylglycine residue has been synthesized racemization-free by water-elimination of an L-homoserine residue. Cyclic and linear 1-carba-dDAVP were synthesized successfully. An unintended side-product of 1-carba-dDAVP-synthesis turned out to be a dimer of the peptide. We were therefore able to induce selective dimerization, an interesting finding worth further investigations.

The thioether analogs have been tested for their biological activities against vasopressin receptors AVPR1a, AVPR2 and the oxytocin receptor OTR of the closely related peptide hormone oxytocin by two different assay approaches. 1-carba-dDAVP turned out to be inactive towards all tested receptors in the measured concentration range, indicating that these structural changes led to a drastic decrease or even loss of agonistic activity. Interestingly, linear 1-carba-dDAVP showed increasing activity against AVPR2 at higher concentrations with an EC_{50} value of > 1600 nM, suggesting *in situ*-folding into a pseudocyclic conformation, like it was also the case for reduced dDAVP (EC_{50} 1.48 nM). The uncharacterized 1-carba-AVP analogs did not show any activity against any of the receptors.

Zusammenfassung

Während der letzten fünfzig Jahre wurde großes Interesse in Physiologie und Pathophysiologie des Neuropeptid-Hormons Vasopressin gelegt. Für die Entwicklung von Peptid- und Nichtpeptid-Agonisten und -Antagonisten der Vasopressinrezeptoren wurden große Anstrengungen unternommen, einerseits um die zugrundeliegenden Signalmechanismen zu studieren, und andererseits für die Behandlung verschiedener Vasopressin-bezogener Krankheiten. Disulfidbrücken-Engineering von Peptid-Analoga ist eine wichtige Strategie, um Peptide gegen proteolytischen Abbau zu schützen. Bis heute wurden einige solcher Vasopressin-Analoga synthetisiert. In der hier präsentierten Masterarbeit wurden 1-carba- und 6-carba-Thioether-Analoga von Vasopressin (AVP) und dem Vasopressin-Analogon Desmopressin (dDAVP) durch Festphasenpeptidsynthese synthetisiert, gefolgt von UV-induzierter Thiol-en-Reaktion eines Cysteins mit einer vorher in das Peptid eingebrachten Alkengruppe. Diese Strategie erlaubte zum ersten Mal den Austausch beider entsprechender Schwefelatome durch ein Kohlenstoffatom und repräsentiert daher Peptidmodulierung an einzelnen Atomen. Das Doppelbindungs-tragende L-Vinylglycin wurde durch racemisierungsfreie Wasserelimination von L-Homoserin hergestellt. Zyklisches und lineares 1-carba-dDAVP wurden erfolgreich hergestellt. Ein unbeabsichtigtes Nebenprodukt der 1-carba-dDAVP-Synthese stellte sich als Dimer des Peptids heraus. Wir konnten also eine selektive Dimerisierung herbeiführen; eine interessante Entwicklung, die weitere Untersuchungen wert ist.

Die Thioether-Analoga wurden auf deren biologische Aktivität gegen die Vasopressinrezeptoren AVPR1a, AVPR2 und den Oxytocinrezeptor OTR des verwandten Hormons Oxytocin mittels zwei verschiedener Assaymethoden untersucht. 1-carba-dDAVP stellte sich als inaktiv gegen alle Rezeptoren im untersuchten Konzentrationsbereich heraus, was darauf hindeutet, dass die strukturelle Änderung zu einem drastischen Abfall oder gar Verlust der agonistischen Aktivität führte. Interessanterweise zeigte lineares 1-carba-dDAVP beginnende Aktivität gegen AVPR2 in den höheren Konzentrationen mit einem EC_{50}-Wert von > 1600 nM, was *in situ*-Faltung in eine pseudozyklische Konformation vorschlägt, wie es auch für reduziertes dDAVP (EC_{50} 1.48 nM) der Fall war. Die uncharakterisierten 1-carba-AVP-Analoga zeigten keinerlei Aktivität gegenüber irgendeinen der Rezeptoren.

Index

Chapter 1

Introduction

1 Introduction

1.1 Vasopressin – hormone and neuropeptide

Vasopressin, in mammals also known as arginine vasopressin (AVP) or antidiuretic hormone (ADH), is a nonapeptide synthesized by neurons in hypothalamic subregions of the brain[1,2]. It exerts a wide variety of physiological and behavioral effects, acting both as a hormone in the periphery as well as regulating higher brain functions as a neuropeptide[1,3].

The peptide consists of nine amino acids with residues one and six forming a six-membered ring structure *via* a disulfide bond between the two cysteine residues, and a three-membered C-terminal flexible tail structure with an amidated carboxylic acid moiety (Figure 1).

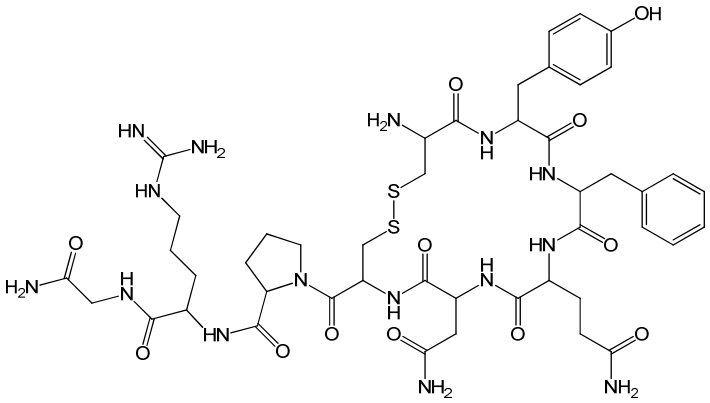

Figure 1: Structure of the nonapeptide vasopressin.

Vasopressin is biosynthesized in special neuron clusters of the paraventricular and supraoptic nuclei of the hypothalamus[1]. The peptide is synthesized as a prepropeptide together with neurophysin II and the glycoprotein copeptin[4]. Vasopressin is cleaved from its precursor during cotranslational translocation into the rough endoplasmic reticulum, accompanied by formation of its disulfide bond. The biologically active peptide is formed in the Golgi apparatus and processed and stored in vesicles[5], bound to its carrier protein neurophysin[6]. Upon osmotic stress, vasopressin is released axonally and secreted into the blood stream to perform its hormonal action. Somatodendritic release into the brain's extracellular fluid defines its function as a neuromodulator[1].

For proper hormonal and neuropeptidic function, the release of vasopressin from its storage vesicles is tightly regulated by, for example, volume-, baro- and osmoreceptors sensing changes in blood properties[44,45], or hormones like estrogens regulating AVP-mediated social recognition abilities[1].

1.2 Vasopressin receptors and pharmacological properties

Vasopressin can act on four different receptors, each belonging to the class of G-protein coupled receptors: the three vasopressin receptor subtypes AVPR1a, AVPR1b and AVPR2, and the receptor of the closely related neurohypophyseal peptide hormone oxytocin, OTR[7].
AVPR1a is found in a variety of body tissues, mediating vascular effects by inducing vasoconstriction[7], regulating glucose homeostasis[8] and protein catabolism[9], mediating aldosterone release from adrenal gland cells[10], modulating lipid metabolism[11] and mediating platelet aggregation[12]. AVPR1b receptors are present in pituitary cells mediating the release of ACTH (adrenocorticotropic hormone) into the circulation followed by release of steroid hormones like cortisol from the adrenal glands[13] and in the pancreas inducing insulin release from islet cells[14]. AVPR2 receptors are mainly present in the kidney in cells of the renal collecting duct, exerting the antidiuretic effects by regulating water and sodium retention[12].
Centrally, vasopressin plays a role in a variety of behavioral effects like influencing social memory[15] and bonding[16,17], emotionality[3] and anxiety[1]. It is also involved in stress response[18] and pain perception[19]. AVPR1a is the primary receptor in the brain[20], however, AVPR1b is also expressed to a lesser extent[21].
A further putative vasodilating vasopressin receptor AVPR1c has been suggested after findings of hypotensive AVP agonists[22].
Because of structural similarities, vasopressin is also able to activate the oxytocin receptor OTR like its actual natural ligand oxytocin (for comparison of the hormones see Figure 4), mediating uterine contraction and milk-ejection in females[23] and showing importance in reproductive and social behaviours[23,24].

Besides varying distribution patterns in various tissues, the different pharmacological properties of the receptors arise from the use of different second messenger signaling molecules[1]. Binding of vasopressin to receptor AVPR2 induces activation of adenylyl cyclase and production of cAMP as second messenger. Binding to AVPR1a, AVPR1b and OTR leads to activation of phospholipase C, phosphatidylinositol turnover and increase in intracellular Ca^{2+} levels[7,25].

1.3 G-protein coupled receptor signaling

G-protein coupled receptors (GPCRs) represent the largest class of hormone receptors and the biggest group of validated pharmacological targets[26,27]. The receptors, consisting of seven

transmembrane-spanning α-helices, transduce extracellular signals (like neurotransmitters, hormones, growth factors, small molecule odorants and light[28]) to intracellular effectors, controlling several diverse physiological functions and being involved in multiple diseases[29].

GPCRs are activated upon extracellular ligand binding, thereby undergoing a conformational change that triggers the recruitment and activation of G-protein trimers (αβγ) on the intracellular side. The Gα subunit exchanges the previously, in its inactive state bound GDP to the now more favored GTP. This leads to dissociation of Gα-GTP and the also activated Gβγ dimer. The active G-protein subunits can now activate multiple effectors, depending of the family of the subunits. The primary effectors further transduce the signal, leading to a cellular response. Termination of the signal is achieved by the intrinsic GTPase activity of Gα, hydrolyzing GTP to GDP which leads to reformation of the inactive trimer Gαβγ. This process is supported by RGS proteins (regulators of G-protein signaling) like GAP (GTPase activating protein). Furthermore, GEFs (guanine nucleotide exchange factors) and GDIs (guanine nucleotide dissociation inhibitors) modulate G-protein cycles by enhancing or inhibiting the exchange of GDP to GTP during the activation process, respectively[30,31,32].

Gα subunits can be divided into four families – $G\alpha_s$, $G\alpha_i$, $G\alpha_{q/11}$ and $G\alpha_{12/13}$. $G\alpha_s$ stimulates adenylyl cyclase and thereby the production of cAMP which can futher activate protein kinase A[33,30], and it also affects tubulin polymerization[34]. $G\alpha_i$, on the other hand, inhibits adenylyl cyclase and the subsequent steps[33] and modulates ion channels[35]. $G\alpha_{q/11}$ activates phospholipase Cβ which hydrolyzes phosphatidylinositol-(4,5)-bisphosphate (PIP_2) resulting in inositol triphosphate (IP_3) and diacylglycerol (DAG). DAG then stimulates protein kinase C, whereas IP_3 leads to the release of Ca^{2+} out of intracellular stores[33,30]. Downstream effectors of $G\alpha_{12/13}$ are, among others, Rho GTPases which mediate cytosceletal rearrangements[33,36]. Activated protein kinases and Ca^{2+} can then influence various cell biological aspects like, for example, protein expression.

The activated Gβγ subunit exerts a variety of effects, on the one hand activating some of the same effectors as Gα, like adenylyl cyclase[37] and phospholipase C[38], on the other hand activating other effectors including potassium channels[39] and Map kinases[40].

The great diversity of GPCR signaling derives not only from the use of different Gα subunits, but also from different Gβ and Gγ subunits and is therefore the result of various combinations of the respective subunits and the differing effector molecules of the different G proteins[41]. Figure 2 summarizes the classification and mechanism of action of G-proteins.

GPCR mediated signaling can also occur independently of the activation of G-proteins, for example by phosphorylation of ligand-bound GPCRs by GRKs (G-protein receptor kinases) which leads to recruitment of arrestins to the phosphorylated sites, subsequent binding of clathrin and internalization of the receptor-ligand complex into endosomes, a process leading to desensitization and therefore termination of G-protein mediated signaling[42]. It has also been shown that GPCR signaling can prolong and even commence after receptor internalization into endosomes[43], and that GPCRs can also directly interact with numerous proteins[33].

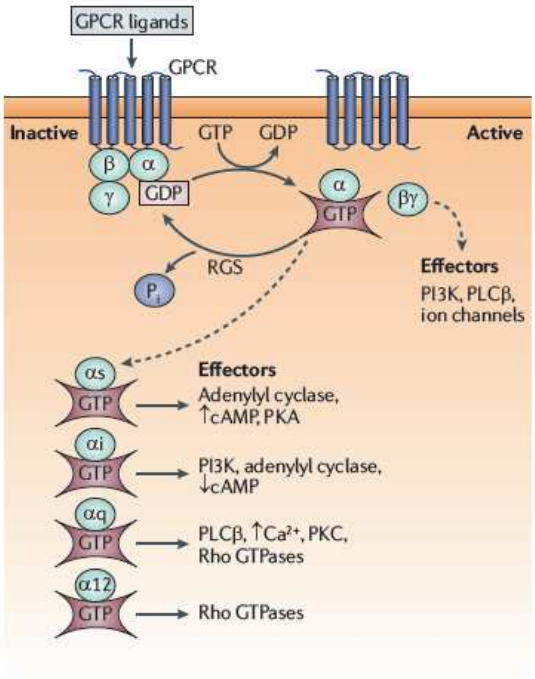

Figure 2: GPCR signaling mediated by G-proteins, according to Lappano and Maggiolini[29]. Upon ligand binding to GPCRs, G-proteins become activated resulting in dissociation of the Gβγ subunit and the Gα subunit now binding GTP instead of GDP bound to the inactive Gαβγ. The various activated Gα subunits and the activated Gβγ subunit trigger activation of various effector molecules. RGS proteins terminate the signal by enhancing the GTPase activity of the Gα subunit, leading to inactive Gαβγ-GDP.

1.4 Vasopressin and water homeostasis – physiology and pathophysiology

Regulation of the body's water balance is an essential survival aspect for terrestrial animals and humans. Both water intake and water excretion are tightly regulated. Vascular volume- and baroreceptors as well as osmoreceptors sense changes in blood volume and osmolarity, mediating the release of vasopressin into the blood stream[44,45]. The hormone exerts its antidiuretic action on cells of the renal collecting duct, inducing final urine concentration. By binding to AVPR2 receptors present in the basolateral membrane of collecting duct cells, cAMP production is activated *via* adenylyl cyclase, which triggers activation of protein kinase

A (PKA). This leads to phosphorylation and subsequent translocation of homotetrameric aquaporin-2 channels (AQP2) – newly expressed or from intracellular stores – to the apical plasma membrane. Water can now enter the cell due to the osmotic gradient and leaves at the basolateral membrane through constitutively expressed aquaporin channels AQP3 and -4. The signal is terminated when isotonicity is restored and hence blood vasopressin levels are depleting, leading to internalization of AQP2 channels. Additionally, several hormones play a role as antagonists of the vasopressin-induced signal. Moreover, further signaling events may play important roles inside the cell, including the protein Epac (exchange protein directly activated by cAMP) (review[46]). Figure 3 shows the vasopressin-regulated water reabsorption in renal collecting duct cells.

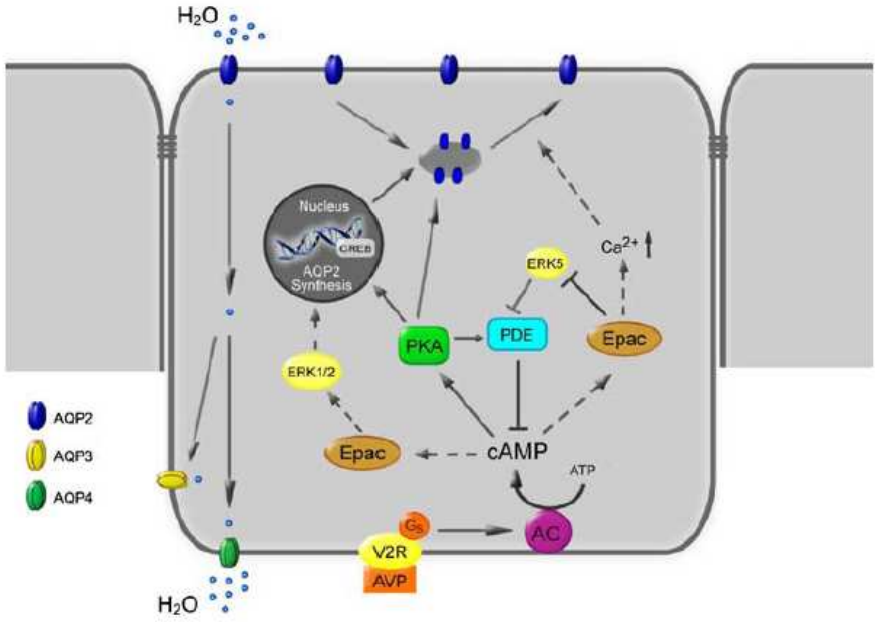

Figure 3: Vasopressin-regulated water reabsorption in renal collecting duct cells, according to Boone and Deen[46]. Binding of AVP to receptor AVPR2 activates adenylyl cyclase (AC) and further protein kinase A (PKA) *via* the second messenger cAMP, inducing translocation of newly expressed or in vesicels stored aquaporin channels AQP2 to the apical plasma membrane (top). Water now enters the cell and leaves at the basolateral membrane (bottom) through constitutively expressed aquaporins AQP3 and -4. Epac may also play a role in inducing the signal.

Vasopressin levels and AQP2 water channels play a role in a number of pathophysiologic conditions of water homeostasis with enhanced or impaired water reabsorption like congestive heart failure or diabetes insipidus, respectively[47,48]. Diabetes insipidus (DI) is characterized by serious polyuria due to inadequate water reabsorption, caused by either insufficient secretion of vasopressin into the blood stream (central diabetes insipidus, CDI) or inefficient response to the hormone in collecting duct cells of the kidney (nephrogenic diabetes insipidus, NDI) and can be both acquired or inherited (congenital/familial)[1]. Acquired CDI can be caused

from inflammation, trauma after surgery or tumors. The congenital form can result from a variety of mutations in the vasopressin prepropeptide, leading to improper processing and therefore accumulation of the dysfunctional peptide[49,50]. Causes for acquired NDI are electrolyte disturbances, renal diseases, multiple myeloma or pregnancy[51]. Congenital NDI can be caused from mutations in the AVPR2 receptor, resulting in disturbed signal transduction[52], or from mutations in the AQP2 channel, leading to misfolding of the protein and retention in the endoplasmic reticulum[53].

It is evident that only CDI-derived inabilities to concentrate urine can be treated with vasopressin-derived drugs like the commonly used AVPR2 agonist desmopressin (1-deamino-8-D-arginine-vasopressin), since CDI is characterized by insufficient vasopressin secretion and insufficient blood hormone levels that can therefore easily be overcome with designed vasopressin analogs. This treatment is not adequate for NDI having sufficient vasopressin levels but inefficient signal transduction abilities[51].

1.5 Structural aspects of vasopressin, receptors and ligand-receptor interactions

Turns are common structural recognition motifs found in cyclic peptides targeting GPCRs like vasopressin and oxytocin due to stabilization by cyclic ring moieties[33]. Figure 4 presents turn motifs found in deamino-oxytocin and shows the structural similarity of the two hypophyseal hormones oxytocin and vasopressin, differing only in amino acid positions 3 (Phe in vasopressin, Ile in oxytocin) and 8 (Arg in vasopressin, Leu in oxytocin).

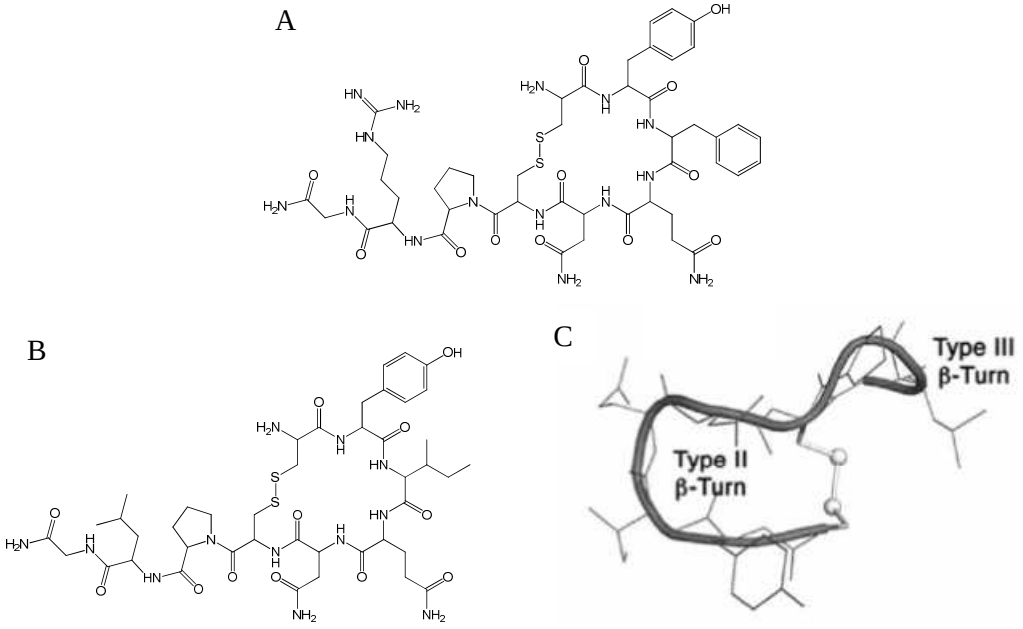

Figure 4: Structural comparison of vasopressin (A) and oxytocin (B) and turn motifs found in deamino-oxytocin (C, according to Gruber *et.al.*[33]).

Several studies showed the existence of various turn motifs present in vasopressin and oxytocin (analogs), revealed by crystal structure or NMR analysis[54,55,56,57,58]. It has been proven that vasopressin possesses conformational flexibility in solution and that it can adopt a large number of conformations, differing with the solvents used and even within the same solvent. Generally spoken, "the cyclic moiety consists of some sort of turn structure with a highly flexible acyclic tail" [6]. It has to be pointed out that those structures have been determined in solution or as crystals devoid of complexes with receptors, therefore assumptions that they represent the same structure in ligand-receptor complexes have to be taken with severe precaution. Nevertheless, it can be speculated that the receptor-bound structures might not be totally different[6]. Since crystal structures of transmembrane-receptors (like GPCRs) together with their ligands are hard to accomplish, one has to rely on solution structures of the ligands and modeling studies, like it has been done for vasopressin bound to the receptors AVPR1a, AVPR2 and OTR[59]: Figure 5 shows a representation of the AVP binding pocket in receptors AVPR2, AVPR1a and OTR.

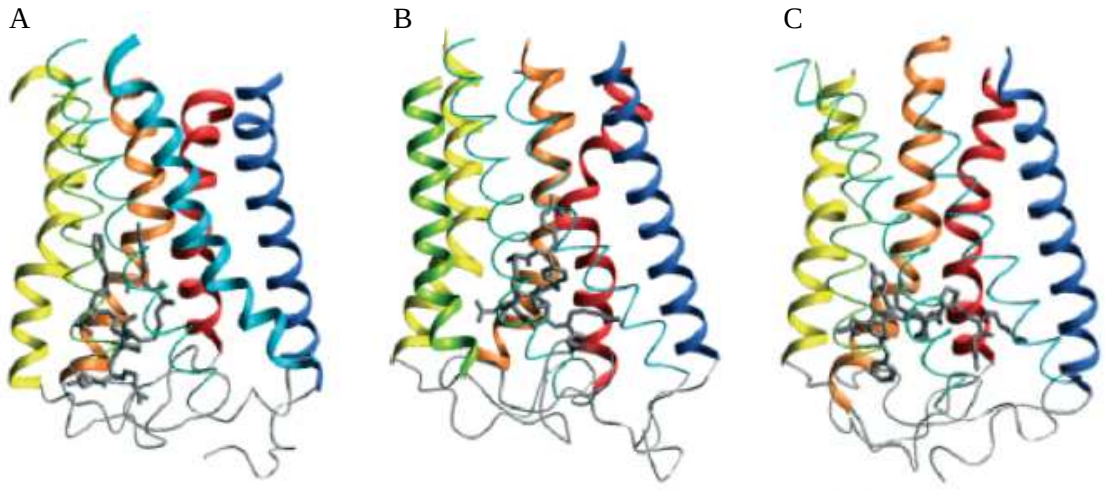

Figure 5: Vasopressin (dark gray) bound to AVPR2 (A), AVPR1a (B) and OTR (C), according to Slusarz *et.al*.[59]. Transmembrane helices are colored from blue (TM1) to red (TM7). Extracellular loops are shown in light gray.

The membrane-spanning GPCRs consist of seven transmembrane α-helices (TM1 to TM7), connected by extracellular and intracellular loops, with an extracellular N-terminus and a cytoplysmic C-terminus[60]. The vasopressin binding pocket has been shown to be located inside the cavity of the helices, close to the extracellular part. The location of the hormone differs in each receptor. It is vertical in AVPR2 and AVPR1a and horizontal in OTR (see Figure 5)[59]. This suggests different mechanisms of vasopressin binding to its receptors. The binding residues important for ligand binding have been examined in several studies using either site-directed mutagenesis methods and/or peptide analogs of the hormones. Figure 6

presents a representation of AVPR1a residues involved in binding of AVP. Most interactions result from hydrogen bonds and salt bridges. Several conserved glutamine residues have been shown to represent main anchor residues for vasopressin inside the receptors. A strong hydrogen bond between one glutamine residue and positively charged Arg8 of vasopressin has been identified[59]. Interactions of Arg8 (vasopressin) and D-Arg8 (desmopressin, an AVPR2 agonist) with non-conserved residues in the first extracellular loop (tyrosine in AVPR1a, aspartate in AVPR2) have been found to be crucial for selectivity of agonist binding, respectively[61,62]. Aromatic residues localized at the bottom of the AVPR1a binding pocket have been shown to have no effect on AVP and agonist affinity, but to be important for antagonist binding[63]. Molecular interactions between antagonists and receptors have been found to be different than those between agonists and receptors[64]. It is thought that each ligand (agonist or antagonist) has its own unique set of interactions with each receptor. Nevertheless, also structurally very different agonists or antagonists (including peptides and non-peptidic small molecules) can interact with common sets of residues, respectively[63].

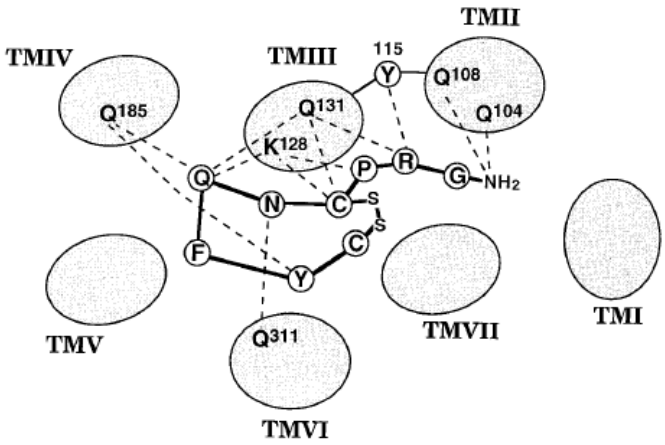

Figure 6: Schematic representation of AVPR1a residues involved in binding of AVP, according to Barberis *et.al*. [65]. Transmembrane helices (TMI-TMVII) are indicated as spheres (top-view), hydrogen bonds as dashed lines.

All mentioned structural studies have been done with receptors AVPR1a, AVPR2 and OTR. Information on the structure of vasopressin receptor AVPR1b is rare.

1.6 Rationale for the synthesis of vasopressin analogs

Two different approaches are in wide use for studies on ligand-receptor interactions: mutagenesis studies on receptors and chemical modifications of ligands. While mutagenesis experiments are important to reveal interacting residues important for ligand binding and signal transduction, ligand modifications have the additional goal to create analogs that act as

antagonists or agonists and that therefore can be used not only for basic research on the biology of the system, but also for treatment of diseases related to the action of the hormones, by blocking or stimulating the respective receptors.

As already mentioned in chapter 1.4, desmopressin is such an analog of vasopressin, acting as agonist of the human AVPR2 receptor (although also found to be an agonist for human receptor AVPR1b, as shown by Saito *et.al.*[66]) and being widely used for the treatment of diabetes insipidus, haemophilia A and von Willebrand's disease[6]. This peptide has been developed through structural modifications of vasopressin, yielding 1-desamino-8-D-arginine-vasopressin[67]. Since vasopressin plays an important role in many physiological processes (see chapter 1.2), many malfunctions involved in these can be overcome by drugs acting as agonists or antagonists for the respective receptors. Antagonists are important tools for the treatment of pathologies characterized by increased vasopressin levels like congestive heart failure and liver cirrhosis, showing excessive water uptake[46,47] (AVPR2 antagonists). Oxytocin receptor antagonists are therapeutically interesting for the prevention of premature labour[68], while AVPR1a antagonists have clinical potential for treatment of hypertension[69]. Agonists are important for treatment of pathologies characterized by decreased hormone levels like the one mentioned above in this chapter for decreased vasopressin levels and inefficient water uptake (AVPR2 agonists).

To date, a wide variety of different agonists and antagonists for the vasopressin and oxytocin receptors have been designed, ranging from cyclic or linear, fluorescent, radiolabelled or bivalent peptide analogs to non-peptide analogs (summarized by Manning *et.al.*[70]). Figure 7 shows structures of some vasopressin analogs. Many of the synthesized peptide analogs contain unnatural or non-proteinergic (amino) acids like ornithine or aminobutyric acid (derivatives), tetrahydroisoquinoline, methylated amino acid residues or other derivatives, deaminated N-terminal residues, D-amino acids or bulky groups like in cyclohexylalanine[70]. These are methods to maintain structural similarity to the native hormones and therefore maintaining binding affinity to the receptors, while making them more stable against proteolytic degradation and increasing their half-lifes[71], and trying to enhance selectivity for one of the receptors. Changes in ring sizes of the cyclic moiety of oxytocin, on the other hand, led to drastic or complete loss in activity[72].

The advantage of peptide analogs compared to non-peptide analogs is, on the one hand, the water solubility of peptides, making them easier research and pharmacological tools. On the other hand, non-peptide analogs are derived from excessive library screens of small molecule compounds against receptors, therefore the rational design of peptide analogs having the

natural hormones as starting point is far less time- and reagent-consuming. Nevertheless, non-peptide analogs like the vaptans as class of AVPR2-antagonists became important for research and are being investigated in (pre)-clinical tests. Only one non-peptide analog, Conivaptan, has been approved for clinical use so far. It has to be pointed out that also only a handful of peptide analogs are currently in therapeutical usage[70].

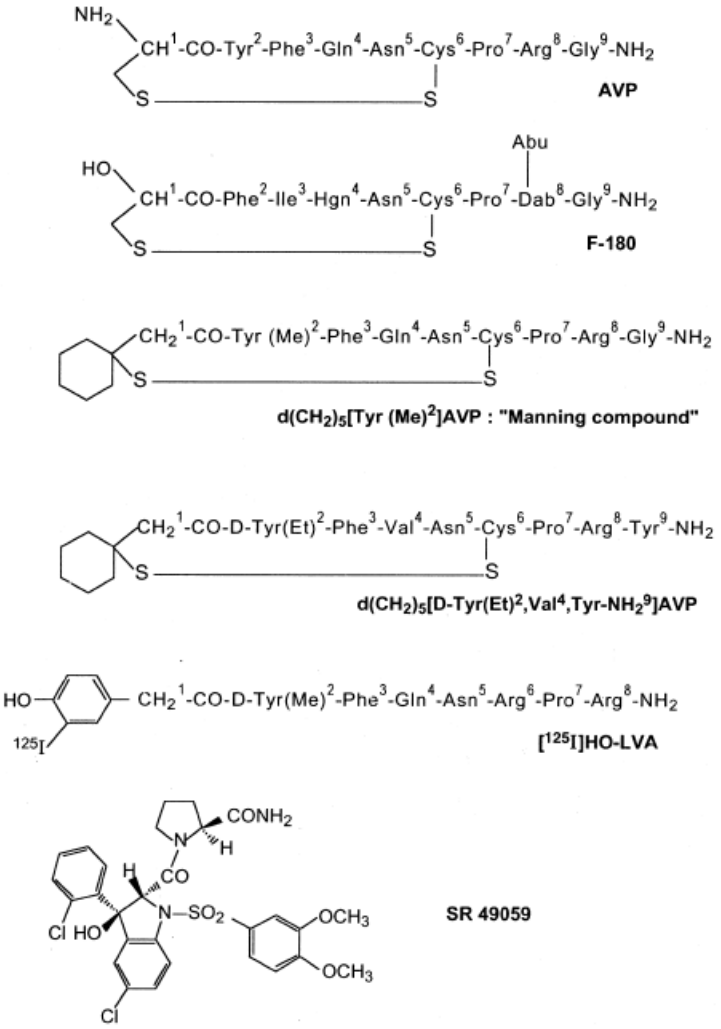

Figure 7: Structure of AVP and some agonist and antagonist analogs for AVPR1a, according to Cotte *et.al.*[63]. AVP and F-180 are peptide agonists, all others are peptide or non-peptide (SR 49059) antagonists. Dab, diaminobutyric acid; Abu, aminobutyric acid; Hgn, homoglutamine.

Selectivity against only one of the possible receptors is a main goal in developing hormone analogs. Nevertheless, this is a difficult task for analogs of the vasopressin/oxytocin receptors, since all receptor subtypes AVPR1a, AVPR1b, AVPR2 and OTR show high sequence homologies – which is crucial for vasopressin to be able to bind to all receptors and to fulfill its diverse functions – and peptide analogs are chemically very similar. To date, selective peptide agonists and antagonists have been developed for all four human receptors. For rat

receptors, no selective antagonist has been found for AVPR1b and OTR. Another problem for the design of selective analogs is differences of the receptors between various animal species. Some ligands shown to be selective for a receptor in one species turned out to be non-selective in another (like it has been shown to be the case for desmopressin wich is selective for AVPR2 in rats, but not in humans[66]). Hence, development of selective analogs demands screening of all receptors of one or more species and forecasts of pharmacological properties cannot be made between different species[73].

1.7 Disulfide bond-engineered peptide analogs

Another possibility to increase proteolytic stability, half-life and bioavailability of peptides additionally to the methods described in the previous chapter is engineering of the hormones' disulfide bond[71]. Disulfide bonds stabilize the tertiary structure of peptides by constraining the flexibility of the polypeptide chain, hence they are crucial for agonistic activity of the neurohypophyseal hormones[74]. However, they are susceptible to reduction by thiol-containing biomolecules like glutathione, serum albumin or oxido-reductases. In order to avoid these inactivating processes, disulfide bond engineering represents an approach to protect the peptides while only minimally perturbing the structure of the native peptide. It has been proven that these peptides are stable to reduction and alkylation conditions [71].

With its chirality, disulfide bonds show a characteristic feature important for structure and activity of biomolecules. The C-S-S-C linkage possesses optical activity due to a dihedral angle of approximately + or – 90°, as shown in Figure 8, giving two not superimposable conformers[75]. It has been shown that vasopressin and its analogs can have different conformational properties concerning the dihedral angle of the disulfide bond, which is + 90° for vasopressin. Therefore, this conformational variability could be one factor for activity variabilities[56].

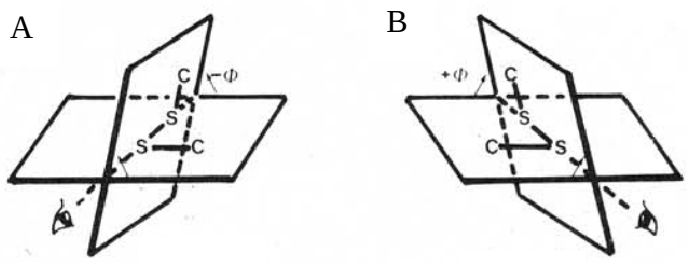

Figure 8: Dihedral angles of disulfide bonds with left-handed (A) or right-handed (B) screw sense, according to Panijpan[75].

Analyses of disulfide-engineered peptide analogs can examine the importance of the disulfide bond for hormone activity. Since replacement of one or both sulfur atoms changes the characteristics of the bond, changes in the structure of the whole peptide and therefore in its activity are possible. Bond angles of C-S-S in disulfides are about 100° [75]. The bond angle for C-S-C, for example, is about 90° and therefore quite different from the one of the disulfide bond.

Some of the disulfide-engineered oxytocin analogs developed so far are presented in Figure 9. Substitution of the disulfide bond of oxytocin and -analogs by various carbon linkages revealed carbocyclic peptide analogs with antagonistic properties[76]. Muttenthaler *et. al.* synthesized various analogs of oxytocin by replacing one or two sulfur atoms with selenium, tellurium or carbon atoms, forming selenylsulfide, diselenide, ditelluride and thioether bonds, respectively, gaining analogs with retained, but in its potency altered biological activities[71]. Dicarba-dAVP synthesized by Hase and Morikawa showed to be biologically active[77].

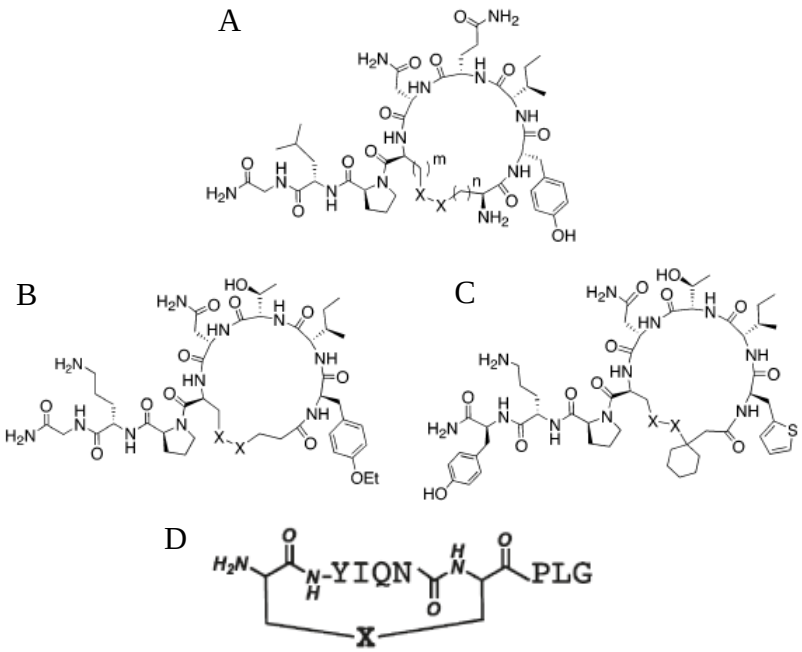

Figure 9: Disulfide-engineered analogs of oxytocin (A, D), oxytocin-analog antisoban (B) and an oxytocin antagonist (C), according to Muttenthaler *et.al.* [71]. X-X being CH_2-CH_2 (B, C) or CH=CH (A, B)[76], X being S, CH_2-S, Se-S, S-Se, Se-Se or Te-Te (D).

Several thioether analogs of oxytocin, desmopressin and vasopressin analogs have been made using different procedures. Mayer *et.al.* synthesized biologically active 1-carba-OT by reaction of an internal cysteine thiol with an N-terminal bromo-homoalanine in 5 % N-methylmorpholine/DMF[78]. 1-carba-dOT was synthesized by Rudinger and Jost *via* reaction of an internal 3-carboxypropyl-cysteine residue with N-terminal Tyr8 by treatment with N-ethyl-

5-phenylisoxazolium-3'-sulfonate, yielding the active analog[79]. 6-carba-dDAVP – synthesized by cyclization of internal 2-carboxyethyl-homocysteine with N-terminal Tyr8 at 50 °C under N_2 atmosphere – showed increased antidiuretic activity (rat) in comparison to desmopressin itself. 6-carba-dAVP showed pressor- and antidiuretic activity (rat) of the same level as dAVP[80].

Thioether analogs of different biological peptides have been made, for example, by creating a thioether containing Fmoc-cystathionine building block out of Fmoc-cysteine and Aloc-homoalanine, subsequent incorporation of this building block into the peptide during solid-phase synthesis, and final head-to-side-chain cyclization[81]. Another procedure for making thioether building-blocks for incorporation into peptides during solid-phase synthesis was the synthesis of S-acetyl (homo-)cysteine and S-propionyl (homo-) cysteine[82].

All above mentioned studies on the activities of disulfide-engineered analogs of vasopressin and oxytocin revealed that maintenance of the original disulfide bond is not crucial for biological activity, since some analogs with one or both sulfur atoms replaced by other atoms showed retained or even enhanced agonistic activities. Nevertheless, not all synthesized analogs revealed to be agonists.

1.8 Solid-phase peptide synthesis

Since the first introduction of solid-phase peptide synthesis (SPPS) by Merrifield in 1963[83], synthesis of peptides has become extremely simplified and a widely used routine practice.

The principal strategy is formation of a peptide bond between two amino acid residues by attack of the amino group of one residue at the carboxyl carbon atom of the other residue that has been activated by introduction of an electron-withdrawing group X (Figure 10).

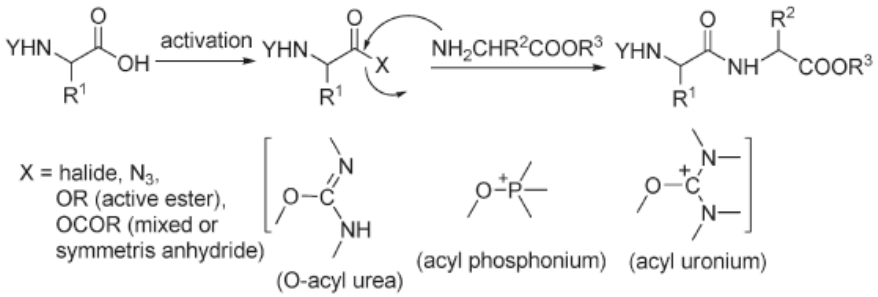

Figure 10: Principle of amide bond formation in peptide synthesis, according to El-Faham and Albericio[84]. Elextron-withdrawing groups X are indicated.

The big advantage of solid-phase synthesis with regard to the synthesis in solution is the avoidance of extensive purification steps after each single coupling reaction, the possibility to automatization and the accessibility of large peptides. This is achieved by coupling the C-terminal amino acid to a polymeric solid support bearing a linker (resin) and successively coupling the subsequent amino acids from the C- to the N-terminal part, only interrupted by washing steps[83]. The principle is depicted in Figure 11. Loading of the first N^{α}- and side-chain protected amino acid to the resin *via* an ester- or amide linkage is followed by repetitive cycles of N^{α} deprotection and amino acid coupling reactions. The functional groups of amino acids-to-be-coupled are masked by N^{α}- and, if necessary, side-chain protecting groups itself, in order to avoid side-reactions and to create a controllable reaction procedure. The temporary N^{α}-protecting groups are removed during the start of the subsequent cycles, whereas the permanent side-chain protecting groups are stable throughout the whole synthesis. After each coupling step, excess of reagents is removed by filtration and washing. Finally, the peptide is cleaved from the resin with simultaneous removing of side-chain protecting groups[85].

Modern solid-phase peptide synthesis encompasses two different approaches: The N-Boc- and the N-Fmoc-strategy. Due to the dangerous conditions and the need for special equipment when handling HF during Boc-peptide synthesis, the Fmoc-strategy is the most common approach used today.[86].

Different matrix polymers can be used as solid supports, of which polystyrene resins are the most common ones.

The different resins are functionalized with different linkers, depending on the needs for the respective peptides, leaving either peptide-amides or peptide acids as C-terminal functional groups after cleavage from the solid support. Figure 12 shows some possible linkers for Fmoc-based SPPS. To date, a variety of different linkers has been developed for each individual need, as reviewed by Moss[87]. Among the different linkers, Rink-amide linker creates C-terminal amides that can be cleaved under strong acidic conditions with simultaneous deprotection of the side-chains. Other linkers that are cleaved by weak acidic conditions are chosen when side-chain protecting groups have to be stable upon cleavage from the resin, e.g. for further C-terminal modifications[86].

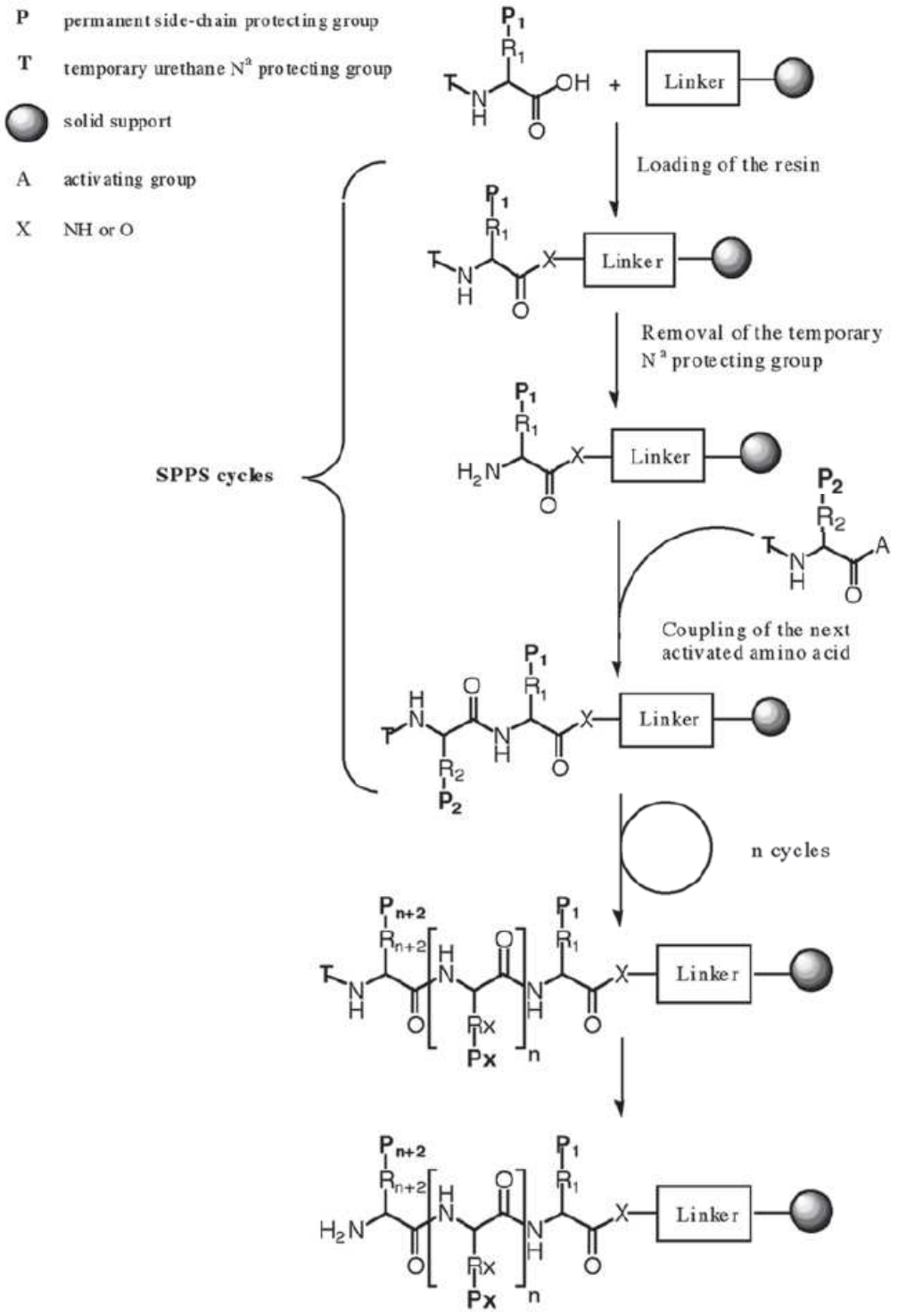

Figure 11: General principle for solid-phase peptide synthesis (SPPS), according to Amblard *et.al.*[85].

Coupling reactions are performed by activating the carboxylic group of the amino acid-to-be-coupled *via* introduction of an electron-withdrawing group, as already shown in Figure 10. A wide variety of different coupling reagents exists to date, with uronium-based reagents like HBTU being of the most commonly used[84].

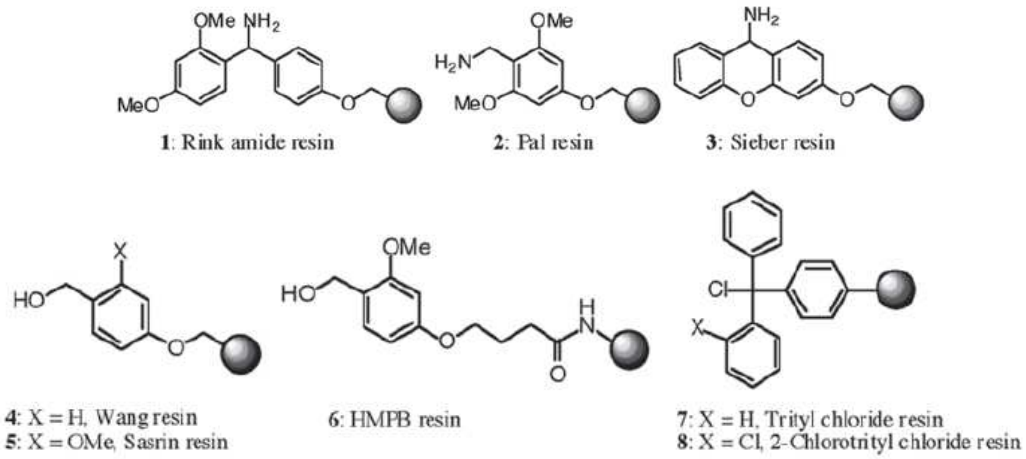

Figure 12: Linker structures for peptide amide (1-3) and peptide acid (4-8) synthesis, according to Amblard *et.al.*[85].

These reagents convert N-protected amino acids into their OBt esters in the presence of a base like diisopropylethylamine (DIPEA). Other additives like HOBt can additionally be used for active ester formation[85,86].

Side-chain protecting groups for amino acids are chosen according to the individual peptides. For routine Fmoc-based solid-phase synthesis, protecting groups labile to strong acids are generally used, getting simultaneously removed with cleavage from the resin. Protecting groups labile to mild acids are used when side-chain modifications are generated directly on-resin[86].

Generally spoken, solid-phase peptide synthesis has become routine use, allowing individual strategies for every single case due to the great variability of resins, reagents and protecting groups existing so far.

1.9 Aim of this project – vasopressin analogs *via* thiol-ene reaction

Since the first synthesis of the neurohypophyseal peptide hormone vasopressin in 1954[88], the number of synthetic peptide analogs has been immensely increased. To date, various analogs of vasopressin and the closely related oxytocin have been synthesized, allowing detailed studies of their biological roles. An important issue for the development of such peptide analogs for research as well as clinical use is plasma-stability and bioavailability. Since the two peptide hormones contain an intramolecular disulfide bond, they are prone to reduction reactions abolishing their functions by subsequent degradation[71]. In order to avoid these processes, disulfide bond-engineering is an important task for stabilizing such peptides.

In the course of this master's thesis project, the aim was to synthesize disulfide-bond engineered peptide analogs of vasopressin, utilizing a new approach for thioether-containing peptides.

The thiol-ene reaction is a simple method for racemization-free synthesis of S-alkylated cysteines, encompassing the radical-initiated addition of a thiol to an alkene, yielding a thioether bond (Figure 13). The reaction can be initiated by UV light radiation (254/365 nm) or radical initiators[89].

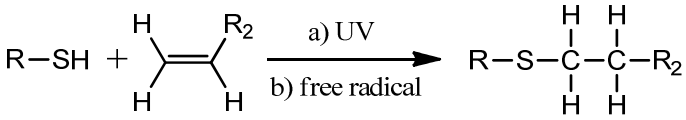

Figure 13: Scheme of thiol-ene reaction by a) UV or b) free radical initiation.

This reaction is in use for many synthetic approaches, including substrate surface modifications, photolithography, dendrimer formation, polymer functionalization, crosslinking and network-formation, as well as for bioorganic functionalization like cysteine-modifications and peptide macrocyclizations[90,91,92]. It belongs to the so-called "click" reactions, defined as site-specific conjugation of two functional groups with high yields, no or easily removable side-products, regio- and stereospecificity and compatibility with aqueous conditions[93].

In order to apply the thiol-ene principle on the synthesis of thioether analogs of vasopressin and desmopressin (1-deamino-8-D-arginine-vasopressin) having each one of the two sulfur atoms substituted by a carbon atom, respectively, an (amino) acid residue holding a double bond has to be introduced into each peptide during solid-phase peptide synthesis. Since an L-amino acid having a double bond in the right position is not available, the synthesis of optically pure Fmoc-protected L-vinylglycine out of L-homoserine by a procedure adapted from Pellicciari et.al. was developed in this work[94]. Figure 14 shows the thioether analogs of vasopressin and desmopressin planned to synthesize *via* thiol-ene reactions, resulting in each two possibilities for thioether bond-formation. The thiol-ene reaction would thereby enable for the first time to exactly replace a sulfur atom by a carbon atom in each position of the disulfide bond. This strategy would give insight into the importance of the disulfide bond's respective sulfur atoms for hormonal activity. The principle of synthesizing thioether-analogs of the neurohypophyseal hormones with unaltered ring size of the cyclic moiety by use of the thiol-ene reaction has not been reported so far.

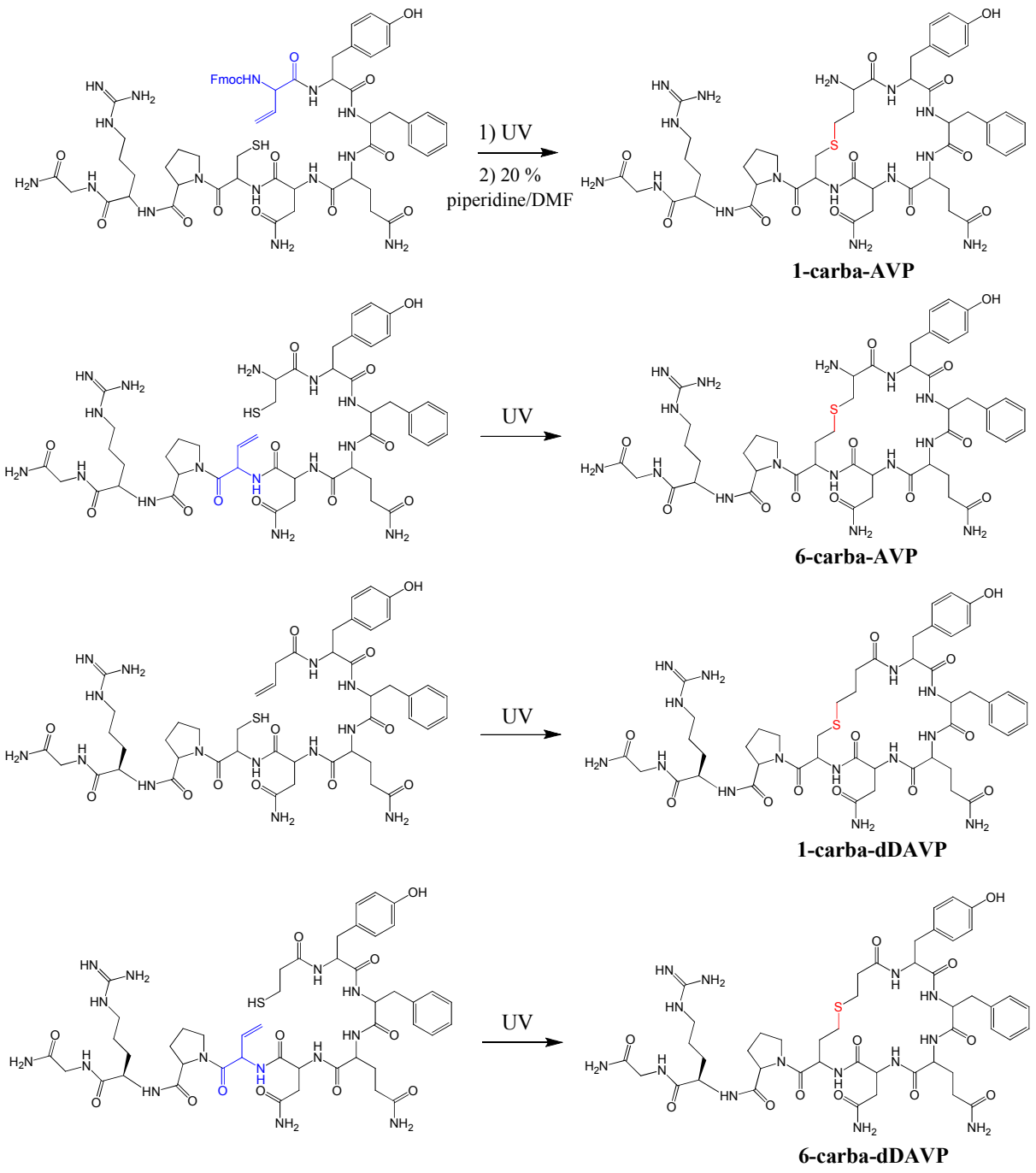

Figure 14: Thioether analogs of vasopressin (1-carba-AVP, 6-carba-AVP) and desmopressin (1-carba-dDAVP, 6-carba-dDAVP) by thiol-ene reactions. Vinylglycine residues are blue, thioether bonds are red.

As seen in Figure 14 , L-vinylglycine is needed for synthesis of both vasopressin analogs and one of the desmopressin analogs (6-carba-dDAVP). Synthesis of 1-carba-AVP requires Fmoc-protection of the peptide until successful thioether bond-formation due to risk of racemization of the terminal vinylglycine residue. The desmopressin analog with sulfur-to-carbon substitution in the respective upper position (1-carba-dDAVP) does not require incorporation of vinylglycine due to the lack of an N-terminal amino group. Instead, 3-butenoic acid is incorporated. Synthesis of the two analogs holding the vinylglycine residue in position 6 (6-

carba-AVP, 6-carba-dDAVP) cannot be accomplished by direct coupling of Fmoc-vinylglycine during peptide synthesis, since subsequent base-mediated removing of the Fmoc-protecting group would lead to racemization or isomerization of the double bond. Hence, these two peptides would have to be synthesized with homoserine in position 6 and converting it to vinylglycine on the solid support according to the same principle as for Fmoc-L-vinylglycine synthesis (Figure 15).

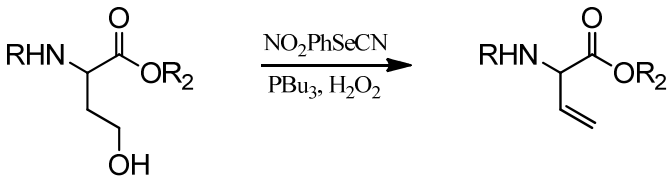

Figure 15: Synthesis of L-vinylglycine from L-homoserine, according to Pellicciari *et.al.*[94].

The synthesized vasopressin and desmopressin analogs were then to be analyzed for biological activity against human receptors AVPR2, AVPR1a and OTR by two different approaches both measuring second messenger production, in order to investigate the effect of the thioether-modifications on hormone activity, as well as for studying the importance of each sulfur atom for receptor activation.

Chapter 2

Materials and equipment

2 Materials and equipment

2.1 Chemistry

All chemicals and solvents were purchased of highest grade commercially available and used without further purification.
Fmoc-protected amino acids, Fmoc-OSu, Rink amide AM resin (200-400 mesh, 0.62 mmol/g) and HBTU were obtained from Novabiochem. HOBt was purchased from Molekula, diethylether was from Fisher Chemical. Hydrogenperoxide (30 % in H_2O), anisole, diethylamine, 3-butenoic acid and N-ethylmaleimid were obtained from Fluka, cyclohexane, methanol and ethylacetate were from VWR. Thallium trifluoroacetate was purchased from Aldrich Chemistry, 2-Nitrophenylselenocyanate and tertbutyltrichloroacetimidate from Alfa Aesar. Deuterated solvents were obtained from Deutero GmBH. All other reagents were from Sigma-Aldrich or Merck.
Mpa(Mmt)-OH was kindly donated from Maja Köhn, EMBL Heidelberg.

Peptide synthesis was performed on an automatic peptide synthesizer Syro I from Multisyntech.
HPLC analysis and purification were carried out on a Shimadzu High Performance Liquid Chromatograph/Mass Spectrometer LCMS-2010EV with a UV/Vis Photodiode array detector SPD-M20A Prominence and the solvent delivery module LC-20AD. For RP-HPLC analytical analyses, a Macherey Nagel C18 EC 250/4.0 NUCLEODUR 100-5 C18 ec column was used. RP-semi-preparative runs were carried out on a Macherey Nagel C18 VP 250/10 NUCLEODUR 110-5 C18 ec column.
Mass spectrometry was measured either on the abovementioned LCMS system, a Waters Micromass ZQ ESI mass spectrometer with a Waters 2478 dual λ absorbance detector, or a MALDI micro MX mass spectrometer equipped with a reflectron analyzer, used in positive ion mode with delayed extraction activated (Micromass MS Technologies).
^{1}H and ^{13}C NMR spectroscopy was performed on a 400 MHz Bruker Avance DPX spectrometer.
TLC analysis was carried out on Merck precoated silica gel (Merck 60W F_{254}s) using UV light (254 nm) and a staining solution of ceric ammonium molybdate (consisting of 1 vol H_2SO_4, 9 vol H_2O, 0.25 g/mL ammonium molybdate and 0.1 g/mL ceric sulfate).
For preparative column chromatography, silica gel from Merck (silica 60, grain size 0.063-0.200 mm, 230-400 mesh) was used.

Vacuum concentration was performed on a Büchi Rotavapor R-210 with Büchi Heating bath B-491 and a vacuubrand cvc 3000 vacuum pump.
Measurement of optical rotation was carried out on a Polartronic H532 polarimeter from Schmidt & Haensch.
For peptide lyophilization, a FreeZone 4.5-105°C lyophilizer from Labconco was used.
Single use syringe filters with PTFE membrane and PP housing were from Sartorius Stedim Biotech.
Sonication was performed on a VWR Ultrasonic Cleaner.
Reactions under UV light were carried out using a UVP Pen-Ray® Power Supply and a UVP Pen-Ray® lamp B-39692.
Centrifugation was carried out on a Heraeus Megafuge 1.0R with rotor 7570E Ch. 004063.

2.2 Cloning

I.M.A.G.E. Full Length cDNA clones were purchased from ImaGenes / Source BioScience in a pCR4-TOPO vector (kanamycin and ampicillin resistance) in the host organism CH10B TonA.
DNA purification was performed using HiSpeed Plasmid Maxi Kit and QuickLyse Miniprep Kit from Qiagen.
Concentration measurements were performed on a NanoDROP 1000 Spectrophotometer from Peqlab.
Probes for sequencing were sent to GATC Biotech.
PCR was carried out on an MJ Research PTC-200 Peltier Thermal Cycler using Finnzymes Phusion F530-S polymerase, Fermentas 5X Phusion GC Reaction buffer F-519 and dNTP Mix 2mM from Fermentas, or a Fermentas Maxima Hot Start Green PCR Mastermix (containing Taq polymerase). Primers were ordered from Eurofins MWG Operon.
For agarose gel electrophoresis, 6X DNA Loading dye from Fermentas and O'GeneRuler™ 1kb DNA Ladder were used. TAE buffer contained 40 mM Tris/Acetate and 1 mM EDTA, pH 8.5. All buffer components, agarose and ethidiumbromide were obtained from Merck or Sigma-Aldrich. The gel power supply LKB-EPS 500/400 from Pharmacia was used.
Gel extraction was performed using QIAquick Gel Extraction Kit from Qiagen. Purification of PCR samples was carried out with a QIAquick PCR Purification Kit from Qiagen.
Restriction digestion was carried out with Fermentas FD enzymes *Eco*RI and *Xho*I and buffer Tango™ 10X or FD buffer 10X from Fermentas.

Ligation was performed with 10X T4 DNA ligase buffer and T4 DNA ligase (5 u /µL) from Fermentas. An Eppendorf Thermomixer Comfort was used.
The mammalian vector pmKate2-N was donated from Gregor Reither, EMBL Heidelberg.
E.coli Top10 competent cells were donated from Pablo Rios, EMBL Heidelberg.
LB-medium contained 10 g/l tryptone, 5 g/l yeast extract and 5 g/l NaCl. LB-medium for agar-plates additionally contained 15 g/l agar-agar. 50 µg/mL kanamycin were added for *E. coli* strains containing pmKate2-N or pCR4-TOPO. All media components were obtained from Merck or Sigma-Aldrich.
Centrifugation was carried out on Sorvall RC6 and Eppendorf centrifuge 5415R.

2.3 Cell culture, biological activity assay and microscopy

HEPES was purchased from Biomol, all cell culture media, trypsin, glutamine, FBS and non-essential amino acids as well as Fura-2 AM were obtained from Invitrogen. Penicillin and streptomycin were obtained from Sigma-Aldrich. All other media additives and imaging buffer components were obtained from Merck.

dDAVP and reduced dDAVP for biological activity assay and microscopy studies were kindly donated from Maja Köhn, EMBL Heidelberg.

2.3.1 Cell culture

For cell culture, BD Falcon™ 10 cm tissue culture dishes (polystyrene) and LabTek eight-chambered #1.0 borosilicate dishes with coverglass were used.
HeLa Kyoto cells were donated from Karolina Pavic, EMBL Heidelberg.
Transient transfection was performed using Fugene6 Transfection Reagent from Roche.
Cells were grown in low-glucose DMEM supplemented with 10 % FBS, 1 % glutamine and 1 % penicillin/streptomycin.

2.3.2 Activity assay

Biological activity assays were performed with GeneBLAzer AVPR2 (or AVPR1a) CHO-K1 DA cells, AVPR2 (or AVPR1a)-CRE-bla CHO-K1 Cell-based Assay and LiveBLAzer™ FRET - B/G Loading Kit (with substrate CCF4-AM), all from Invitrogen.

Assay medium contained DMEM without Phenol Red (supplemented with glucose up to 4.5 mg/l), 1 % FBS, 1 % MEM Non-essential amino acids, 2.5 % HEPES pH 7.3, 1 % penicillin/streptomycin and 1 % glutamine.
For assay readout, an Envision HTS fluorescence plate reader with bottom-read capabilities from Perkin Elmer was used, with excitation filter 405 nm (bandwidth 8), emission filter 460 nm (bandwidth 25) and emission filter 535 nm (bandwidth 25), all from Perkin Elmer.
A 384-well Greiner PP plate (black-well) and a clear-bottom 384-well plate from Cornig were used. Plate centrifugation was carried out on Multifuge 3s from Heraeus. Multistep pipetting was conducted on an 8-channel multistep pipette 5-100µL from BioHit.
Results were plotted using Sigma Plot 11.0 from Systat Software Inc.

2.3.3 Microscopy

Microscopy was carried out on a Olympus Biosystems Cell^R, multi-color TIRF equipped with a Hamamatsu Image EM-CCD digital Camera from ImagEM, an MT20 light source, a LUCPLFLN 20x objective and xCELLence software.
Measurements were carried out at 37 °C. 150 pictures at two different excitation wavelengths were taken during each recording, with picture cycles every 5-7 s. EM gain was set to 200 units, the camera was set to 50 ms and the intensity was set to 23.13 %. Excitation (378 nm and 340 nm) and filter wheel (535/50 nm) wavelengths were chosen according to Fura-2 AM requirements.
For mKate-channel observations, 563/9 nm and 617/73 nm were used as excitation and filter wheel settings, respectively. EM gain, camera and intensity settings were adapted according to picture quality.
Imaging buffer contained 20 mM HEPES pH 7.4, 115 mM NaCl, 1.8 mM $CaCl_2$, 1.2 mM $MgCl_2$, 1.2 mM K_2HPO_4 and 2 g/l freshly added glucose.
Fura-2 AM 1 mM stocks were prepared in DMSO containing 10 % pluronic.

Chapter 3

Methods

3 Methods

3.1 Standard methods

Standard techniques like flash chromatography, vacuum concentration or sterile working techniques for bacteria handling and cell culture were performed according to standard protocols and are not discussed here in detail.

3.2 Chemistry

3.2.1 General procedure for automated peptide synthesis and peptide purification

Peptide synthesis was conducted on an automated peptide synthesizer by standard Fmoc-based coupling and deprotection strategies[85].

For all synthesized peptides, Fmoc-protected Rink Amide AM resin (80 mg, loading 0.62 mmol/g) was chosen. Fmoc deprotection was carried out with 40 % piperidine in DMF for 3 min, followed by 20 % piperidine in DMF for 12 min. Peptide couplings were performed by addition of Fmoc-protected L-amino acids (5 eq, dissolved in 0.1M HOBt in DMF), HBTU (5 eq) and DIPEA (10 eq) in DMF for 40 min.

Initially, the resin was swelled in DMF for 2 x 15 min. After deprotection of the first Fmoc group from the resin, the amino acids were coupled stepwise in consecutive cycles of double coupling (2 x 40 min), washing with DMF, Fmoc deprotection and again washing with DMF.

For better solubility reasons, Fmoc-Phe-OH was generally dissolved in 0.1M HOBt in NMP instead of DMF as solvent.

Fmoc-protected cysteines (5 eq) were coupled using DIC (5 eq) instead of HBTU and DIPEA, following the same procedure.

After transferring to manual solid-phase reactor syringes, the resin was washed with DCM (3 x 1 min), dried in HV and either stored at -20 °C for further reactions, or the peptide was cleaved and side chain deprotected using TFA (950 µL) and TIS (50 µL) for 3 h (while shaking). The peptide was then precipitated by filtering the supernatant solution into ice cold Et_2O (20 mL), centrifugation and washing with Et_2O (2 x 20 mL). The crude product was dried at RT and further purified by semi-preparative HPLC. Purified peptides were lyophilized and stored at -20 °C.

Test cleavages using only a small amount of resin were performed according to the cleavage procedure using TFA (20 µL) and TIS (1 µL) and were carried out in 1.5 mL Eppendorf

tubes. After 3 h, 200 µL MeCN/H_2O (1:1) were added to stop the reaction. After short centrifugation, the supernatant containing the cleaved peptide could be used for analysis.

The theoretical loading of peptide on the resin could be calculated according to the following equation:

$$L_{th} = \frac{L_{ini}}{1 + \frac{MW_{pept} - MW_{ini}}{1000} * L_{ini}}$$

with L_{th} being the theoretical loading in mmol/g, L_{ini} being the initial loading of the resin (0.62 mmol/g), MW_{pept} being the molecular weight of the fully protected peptide that has been synthesized on the resin, and MW_{ini} being the molecular weight of the initial group on the resin (Fmoc, 238 g/mol).

3.2.2 High performance liquid chromatography

High performance liquid chromatography (HPLC) was carried out to analyze and/or purify the synthesized compounds. Some analytical runs were performed in combination with mass spectrometry (HPLC-MS).

For both analytical and semi-preparative HPLC, reversed phase systems were chosen. Analytical runs were performed with a pump rate of 1.5 mL/min, semi-preparative runs with 5 mL/min. UV detection was carried out at 215 and 254 nm in both cases.

H_2O and MeCN were used as solvent mixtures, supplemented with 0.05 % TFA. A standard analytical HPLC method started with 10 % MeCN in H_2O for 1 min, then increasing the gradient to 70 % MeCN in 14 min, then to 100 % in 2.5 min and holding 100 % for 2.5 min, then going back to 10 % for 4 min. A standard semi-preparative HPLC method started with 10 % MeCN in H_2O for 1 min, then increasing the gradient to 70 % MeCN in 19 min, then to 100 % in 1 min and holding 100 % for 4 min, then going back to 10 % for 3 min. All mentioned gradients are referred to these standard methods.

3.2.3 Measurement of optical rotation

For compounds **1** - **4**, optical rotation was measured on a polarimeter. The exactly weighed compound (between 2 to 10 mg) was dissolved in 1 mL of solvent and α-values were

measured at least in triplicates. The instrument has thereby been calibrated to the used solvent system.

$[\alpha]_D^{20}$-values were calculated according to the following equation and indicated as averages for each measurement:

$$[\alpha]_D^{20} = \frac{\alpha}{l * d}$$

with α being the rotation angle, l the diameter of the capillary (1 dm) and c the concentration of the compound in g/mL.

Measurements were carried out at 20 °C.

3.2.4 Nuclear magnetic resonance spectroscopy

^{1}H and ^{13}C NMR spectra were recorded on a 400 MHz spectrometer.

The compound to be measured (around 5 mg) was dissolved in deuterated solvent (mixtures). For ^{1}H assignment of compounds **1**-**4** COSY spectra were recorded. Chemical shifts (δ) are given in ppm and coupling constants (J) are given in Hz. Splitting parameters are indicated as follows: s = singlet, d = doublet, t = triplet, m = multiplet, dd = doublet of doublet.

3.2.5 Matrix-assisted laser desorption ionization – mass spectrometry

Matrix-assisted laser desorption ionization (MALDI) - mass spectrometry was carried out for peptide mass analysis.

α-Cyano-4-hydroxycinnamic acid was used as matrix component as a saturated solution in 50 % MeCN in H_2O supplemented with 1 % TFA.

2 µL of matrix were mixed with 2 µL of compound-to-be-analyzed. 2 µL of the mixture were spotted on a MALDI analysis plate and dried before measurement.

3.2.6 N-ethylmaleimid test

An N-ethylmaleimid (NEM) test was performed to analyze the state of sulfhydryl bonds. Free thiol groups can bind the reactant, therefore changing the mass of the compound.

25 µL of peptide or collected HPLC-peak were mixed with 2.5 µL $NaHCO_3$ (sat. aqu.) and 25 µL 1 mM NEM (3.13 µg) and reacted for 15 min. 0.2 µL TFA were added and the mixture was measured by MALDI mass spectrometry.

3.2.7 Syntheses of the various compounds

(1) N-(9-Fluorenylmethoxycarbonyl)-L-homoserine, Fmoc-Hse-OH

1 g (8.4 mmol) of L-homoserine was dissolved (not completely) in MeOH (30 mL), then 2.3 mL (16.8 mmol, 2 eq) TEA were added. After cooling on an ice bath, a mixture of 2.83 g (8.4 mmol, 1 eq) Fmoc-OSu in 6 mL MeOH and 6 mL DCM was added dropwise and the mixture was allowed to stir at 0 °C for 1 h. The reaction was monitored by TLC. The ice bath was removed and the mixture was stirred at RT for 5 h. After adding a few drops of H_2O and stirring for another 30 min, the mixture was concentrated to 50 % under reduced pressure. 2 M HCl was added until pH 3 and the mixture was further concentrated until a white precipitate occurred. H_2O (15 mL) was added and the residue was extracted with tertbutylmethylether (3 x 20 mL). The combined organic phases were dried over Na_2SO_4, filtered and the solvent was removed under reduced pressure. The crude product (2.12 g) was purified by flash chromatography (cyclohexane/EtOAc 2:1, then cyclohexane /EtOAc 1:1, then EtOAC, then MeOH/DCM 1:4, then MeOH for final elution of compound **1**). Identity was confirmed by LC-MS and ^{1}H- and ^{13}C-NMR. The integrity was further supported by measurement of optical rotation.

White solid
$C_{19}H_{19}NO_5$ (341.36 g/mol)
Yield: 1.07 g (9 mmol), 38 %
R_f = 0.4-0.2 (EtOAc)
HPLC (analytical): T_R = 10.8 min (standard gradient)
LC-MS: *m/z* found: 364 $[M+Na]^+$
$[\alpha]_D^{20}$: -12.5 (c = 0.0025, MeOH)
^{1}H-NMR (400 MHz, MeOH-*d4*): δ = 7.47 (d, ^{3}J = 7.6 Hz, 2H, ar-H-Fmoc), 7.33 (d, ^{3}J = 8.0 Hz, 2H, 2 ar-H-Fmoc), 7.10 (t, ^{3}J = 7.2 Hz, 2H, 2 ar-H-Fmoc), 7.01 (t, ^{3}J = 7.4 Hz, 2H, 2 ar-H-Fmoc), 4.11-4.08 (m, 1H, CH_2-Fmoc), 4.07-4.02 (m, 1H, CH_2-Fmoc), 3.92 (t, ^{3}J = 7.0 Hz, 1H, CH-Fmoc), 3.85 (t, ^{3}J = 6.4 Hz, 1H, α-CH-Hse), 3.39 (t, ^{3}J = 5.0 Hz, 2H, CH_2-Hse), 1.80-1.73 (m, 1H, CH_2-Hse), 1.62-1.55 (m, 1H, CH_2-Hse)
^{13}C-NMR (100 MHz, MeOH-*d4*): δ = 141.2 (2 ar-C-Fmoc), 127.4, 126.8, 124.9, 119.5 (8 ar-C-Fmoc), 66.5 (CH2-Fmoc), 58.6 (CH_2-Hse), 53.1 (α-CH-Hse), 47.0 (CH-Fmoc), 35.1 (CH_2-Hse)

(2) N-(9-Fluorenylmethoxycarbonyl)-O-*tert*-butyl-L-homoserine, Fmoc-Hse-*t*Bu

1.23 g (3.6 mmol) of compound **1** were dissolved (not completely) in 34 mL dry EtOAc under argon atmosphere. A mixture of 2.6 mL (14.4 mmol, 4 eq) *tert*-butyltrichloroacetimidate in dry cyclohexane (14.4 mL, ~1 M reagent) was added dropwise and stirred at RT for 24 h. The reaction was monitored by TLC. The reaction was stopped by concentrating under reduced pressure, the crude product was dried in HV and purified by flash chromatography (cyclohexane/EtOAc 2:1, then cyclohexane/EtOAc 1:1). Identity was confirmed by LC-MS and ^{1}H- and ^{13}C-NMR. The integrity was further supported by measurement of optical rotation.

Colorless syrup
$C_{23}H_{27}NO_5$ (397.46 g/mol)
Yield: 394 mg (1 mmol), 28 %
R_f = 0.34 (cyclohexane/EtOAc 1:1)
HPLC (analytical): T_R = 16.3 min (standard gradient)
LC-MS: *m/z* found: 420 $[M+Na]^+$
$[\alpha]_D^{20}$: -5.6 (c = 0.0051, $CHCl_3$)
^{1}H-NMR (400 MHz, $CHCl_3$-*d*, drops of MeOH-*d4*): δ = 7.74 (d, ^{3}J = 7.6 Hz, 2H, ar-H-Fmoc), 7.57 (d, ^{3}J =7.6 Hz, 2H, ar-H-Fmoc), 7.38 (t, ^{3}J = 7.6 Hz, 2H, ar-H-Fmoc), 7.29 (t, ^{3}J = 7.4 Hz, 2H, ar-H-Fmoc), 4.42 (d, ^{3}J = 7.2 Hz, 2H, CH_2-Fmoc), 4.37 (t, ^{3}J = 6.4 Hz, 1H, α-CH-Hse), 4.19 (t, ^{3}J = 6.8 Hz, 1H, CH-Fmoc), 3.68-3.53 (m, 2H, CH_2-Hse), 2.13-2.05 (m, 1H, CH_2-Hse), 1.69-1.59 (m, 1H, CH_2-Hse), 1.45 (s, 9H, 3 CH_3-*t*Bu)
^{13}C-NMR (100 MHz, $CHCl_3$-*d*, drops of MeOH-*d4*): δ = 157.0 (O=C-Fmoc), 143.8, 141.4 (4 ar-C-Fmoc), 127.8, 127.1, 125.0, 120.0 (8 ar-C-Fmoc), 82.4 (C-*t*Bu), 67.2 (CH_2-Fmoc), 58.3 (CH_2-Hse), 51.4 (α-CH-Hse), 47.2 (CH-Fmoc), 36.3 (CH_2-Hse), 28.0 (3 CH_3-*t*Bu)

(3) N-(9-Fluorenylmethoxycarbonyl)-O-*tert*-butyl-L-vinylglycine, Fmoc-Vgl-*t*Bu

215 mg (542 µmol) of compound **2** were dissolved in dry THF (3 mL) under argon atmosphere and stirred at RT for 20 min. Subsequently, 234 mg (1 mmol, 1.9 eq) NO_2PhSeCN and 257 µL (1 mmol, 1.9 eq) PBu_3 were added and the mixture was stirred at RT for 3 h. After cooling down to 0 °C on an ice bath, H_2O_2 (30 % in H_2O, 0.9 mL) was added and the mixture was allowed to warm to RT whilst stirring over night. The reaction was monitored by TLC. The mixture was then rinsed into H_2O (25 mL) and extracted with Et_2O (4

x 20 mL). The combined organic phases were dried over Na_2SO_4, filtered and the solvent was removed under reduced pressure. The crude product (570 mg) was purified by flash chromatography (cyclohexane/EtOAc 4:1). Identity was confirmed by LC-MS and ^{1}H- and ^{13}C-NMR. The integrity was further supported by measurement of optical rotation.

Yellow oil

$C_{23}H_{25}NO_4$ (379.45 g/mol)

Yield: 138 mg (0.4 mmol), 67 %

R_f = 0.55 (cyclohexane/EtOAc 2:1)

HPLC (analytical): T_R = 18.1 min (standard gradient)

LC-MS: *m/z* found: 402 $[M+Na]^+$

$[\alpha]_D^{20}$: -2.6 (c = 0.013, $CHCl_3$)

^{1}H-NMR (400 MHz, $CHCl_3$-*d*, drops of MeOH-*d4*): δ = 7.73 (d, ^{3}J = 7.2 Hz, 2H, ar-H-Fmoc), 7.58 (d, ^{3}J = 7.2 Hz, 2H, ar-H-Fmoc), 7.37 (t, ^{3}J = 7.4 Hz, 2H, ar-H-Fmoc), 7.26 (t, ^{3}J = 7.6 Hz, 2H, ar-H-Fmoc), 5.91-5.82 (m, 1H, CH-Vgl), 5.25 (dd, ^{3}J = 28 Hz, ^{2}J = 42 Hz, 2H, CH_2-Vgl), 4.76 (d, ^{3}J = 4.4 Hz, 1H, α-CH-Vgl), 4.38 (d, ^{3}J = 4.4 Hz, 2H, CH_2-Fmoc), 4.20 (t, ^{3}J =7.0 Hz, 1H, CH-Fmoc), 1.42 (s, 9H, 3 CH_3-*t*Bu)

^{13}C-NMR (100 MHz, $CHCl_3$-*d*, drops of MeOH-*d4*): δ = 169.7 (O=C-Vgl), 155.9 (O=C-Fmoc), 143.7, 141.3 (4 CH-Fmoc), 132.7 (CH-Vgl), 127.7, 127.0, 125.0, 119.9 (8H, CH-Fmoc), 117.1 (CH_2-Vgl), 82.8 (C-*t*Bu), 67.0 (CH_2-Fmoc), 56.6 (α-CH-Vgl), 47.1 (CH-Fmoc), 27.8 (3 CH_3-*t*Bu)

(4) N-(9-Fluorenylmethoxycarbonyl)-L-vinylglycine, Fmoc-Vgl-OH

To a mixture of 105 mg (0.3 mmol) of compound **3** in 1.9 mL DCM, 1.9 mL TFA and 50 µL TIS were added. The solution was stirred at RT for 6 h and the reaction was monitored by TLC. The solvents were removed by coevaporation with toluene under reduced pressure. The vacuum-dried raw product (80 mg) was purified by flash chromatography (cyclohexane/EtOAc 1:1, then EtOAc, then DCM, then MeOH/DCM 1:40 and finally MeOH/DCM 1:3 for elution of compound **4**). Identity was confirmed by LC-MS and ^{1}H- and ^{13}C-NMR. The integrity was further supported by measurement of optical rotation.

White solid

$C_{19}H_{17}NO_4$ (323.34 g/mol)

Yield: 85 mg (0.3 mmol), 95 %

R_f = 0.6-0.1 (cyclohexane/EtOAc 2:1)

HPLC (analytical): T_R = 12.4 min (5 - 100 % MeCN in H_2O in 14 min)

LC-MS: *m/z* found: 346 $[M+Na]^+$

$[\alpha]_D^{20}$: -15.8 (c_1 = 0.008, c_2 = 0.0065, MeOH)

^{1}H-NMR (400 MHz, MeOH-*d4*): δ = 7.79 (d, ^{3}J = 7.6 Hz, 2H, ar-H-Fmoc), 7.67 (d, ^{3}J = 6.6 Hz, 2H, ar-H-Fmoc), 7.38 (t, ^{3}J = 7.4 Hz, 2H, ar-H-Fmoc), 7.30 (t, ^{3}J = 7.6 Hz, 2H, ar-H-Fmoc), 6.09-6.01 (m, 1H, CH-Vgl), 5.16 (dd, ^{3}J = 54.2 Hz, ^{2}J = 68 Hz, 2H, CH_2-Vgl), 5.59 (d, ^{3}J = 4.4 Hz , 1H, α-CH-Vgl), 4.36-4.29 (m, 2H, CH_2-Fmoc), 4.21 (t, ^{3}J = 6.8 Hz, 1H, CH-Fmoc)

^{13}C-NMR (100 MHz, MeOH-*d4*): δ = 143.9, 141.2 (4 CH-Fmoc), 135.8 (CH-Vgl), 127.4, 126.8, 124.8, 119.5 (8 CH-Fmoc), 113.4 (CH_2-Vgl), 66.5 (CH_2-Fmoc), 58.9 (α-CH-Vgl), 47.0 (CH-Fmoc)

(5) H_2N-(Cys-Tyr-Phe-Gln-Asn-Cys)-Pro-Arg-Gly-$COONH_2$ disulfide, vasopressin

The nonapeptide **5** was synthesized and purified according to the general protocol for automated peptide synthesis mentioned in chapter 3.2.1.

After swelling and initial Fmoc-deprotection of the resin, Fmoc-Gly-OH, Fmoc-Arg(N-Pbf)-OH and Fmoc-Pro-OH were consecutively coupled using standard conditions. Fmoc-Cys(S-Acm)-OH was coupled by the special conditions for cysteine couplings. Fmoc-Asn(N-Trt)-OH, Fmoc-Gln(N-Trt)-OH, Fmoc-Phe-OH and Fmoc-Tyr(O-*t*Bu)-OH were then coupled according to the standard protocol, again followed by coupling of Fmoc-Cys(S-Acm)-OH using cysteine coupling conditions. After Fmoc-deprotection of the final residue and drying of the resin, peptide identity was confirmed by a test cleavage using a small amount of resin and subsequent MALDI analysis.

After positively confirmed test cleavage, disulfide bond-formation was performed manually on the solid support. The resin (161 mg, 131 µmol) was swelled in DCM (30 min, shaking) and washed with DMF (4 x 1 min). The tip of the reactor syringe was capped and the syringe was placed into a Falcon tube. 2 mL DMF/anisole (19:1) were added, followed by addition of 85 mg $Tl(CF_3COO)_3$ (1.2 eq, 157 µmol). The mixture was left to stand in an ice bath for 80 min, while manually stirring with a needle from time to time. To stop the reaction, the resin was washed with DMF and DCM (each 5 x 1 min) and dried in HV. Successful disulfide bond-formation was confirmed by MALDI mass spectrometry of a test cleavage.

The peptide was then cleaved and precipitated according to the general procedures described in chapter 3.2.1.

The crude product was dissolved in 5 % MeCN in H_2O, filtered and purified by semi-preparative HPLC (15 - 30 % MeCN in H_2O for 19 min). The purified peptide was lyophilized and identity was confirmed by MALDI mass spectrometry and LC-MS.

Colorless solid
$C_{46}H_{65}N_{15}O_{12}S_2$ (1084.23 g/mol)
Yield: 6.5 mg (7 mol), 12 %
HPLC (analytical): T_R = 8.4 min (5 - 50 % MeCN in H_2O)
MALDI-MS: *m/z* found: 1084.40 $[M]^+$

(6) H_2N-(Cys-Tyr-Ile-Gln-Asn-Cys)-Pro-Leu-Gly-$COONH_2$ disulfide, oxytocin

The disulfide-peptide **6** was synthesized and purified according to the general protocol for automated peptide synthesis (chapter 3.2.1).
After swelling and initial Fmoc-deprotection of the resin, Fmoc-Gly-OH, Fmoc-Leu-OH, Fmoc-Pro-OH, Fmoc-Cys(S-Acm)-OH, Fmoc-Asn(N-Trt)-OH, Fmoc-Gln(N-Trt)-OH, Fmoc-Ile-OH, Fmoc-Tyr(O-*t*Bu)-OH and Fmoc-Cys(S-Acm)-OH were consecutively coupled using standard conditions. Cysteines were coupled using cysteine coupling conditions. After Fmoc-deprotection of the final residue and drying of the resin, peptide identity was confirmed by MALDI analysis of a test cleavage.
Disulfide bond-formation was performed manually on the solid support, exactly as for compound **5**, using the same amounts of solvents and reagents.
After confirmation of successful disulfide bond-formation by MALDI analysis of a test cleavage, the peptide was cleaved and precipitated according to standard procedures (chapter 3.2.1). The crude product was dissolved in 20 % MeCN in H_2O, filtered and purified by semi-preparative HPLC (20 - 30 % MeCN in H_2O for 19 min). The purified peptide was lyophilized and analyzed by HPLC. Identity was confirmed by MALDI mass spectrometry.

Colorless solid
$C_{43}H_{66}N_{12}O_{12}S_2$ (1007.19 g/mol)
Yield: 9 mg (9.1 mol), 18 %
HPLC (analytical): T_R = 5.51 min (20 - 30 % MeCN in H_2O)
MALDI-MS: *m/z* found: 1008.08 $[M+H]^+$

(7) Bta-Tyr-Phe-Gln-Asn-Cys-Pro-D-Arg-Gly-$COONH_2$, linear 1-carba-dDAVP

The first part of peptide **7** was synthesized according to the general protocol for automated peptide synthesis (chapter 3.2.1).

After swelling and initial Fmoc-deprotection of the resin, Fmoc-Gly-OH, Fmoc-D-Arg(N-Pbf)-OH, Fmoc-Pro-OH, Fmoc-Cys(S-Trt)-OH, Fmoc-Asn(N-Trt)-OH, Fmoc-Gln(N-Trt)-OH, Fmoc-Phe-OH and Fmoc-Tyr(O-*t*Bu)-OH were consecutively coupled using standard conditions. Cysteine was coupled using cysteine coupling conditions.

Fmoc-deprotection of the Tyr-residue was performed manually. The preswelled resin (DCM, 30 min) was washed with DMF (3 x 1 min) and treated with 20 % piperidine in DMF (1.5 mL, 3 x 7 min). After washing with DMF (5 x 1 min), 3-butenoic acid (Bta) was coupled manually. The 200 mg resin gave a theoretical loading of 0.295 mmol/g. For preactivation of coupling components, 20 µL 3-butenoic acid (4 eq, 0.2 mmol), 32 mg HOBt (4 eq, 0.2 mmol), 80 mg HBTU (4 eq, 0.2 mmol) and 82 µL DIPEA (8 eq, 0.4 mmol) were added to 1 mL DMF and left to react for 5 min. The mixture was then added to then resin and coupled for 1.5 h. After washing of the resin with DMF (3 x 1 min), the procedure was repeated to perform the second step of the double coupling. The resin was then washed with DMF (3 x 1 min) and DCM (5 x 1 min) and dried in HV. Peptide identity was confirmed by MALDI analysis of a test cleavage.

The peptide was cleaved using standard procedures. The crude product was dissolved in 20 % MeCN in H_2O, filtered and purified by semi-preparative HPLC (23 - 40 % MeCN in H_2O for 19 min). The purified synthesis-product (consisting of three peaks) was lyophilized and peptide identity was analyzed by MALDI and LC-MS. A NEM-test (see chapter 3.2.29) was carried out to analyze the state of the sulfhydryl group. A ^{1}H-NMR spectrum was also recorded. The product was further used and purified in the course of the synthesis of peptide **8**, giving pure compound **7** as well.

Colorless solid

$C_{47}H_{66}N_{14}O_{12}S$ (1051.18 g/mol)

Yield: 3.5 mg (3.7 mol), 20.4 %

HPLC (analytical): T_R = 9.3 min (20 - 35 % MeCN in H_2O)

HPLC-MS: *m/z* found: 1052.58 $[M+H]^+$

(8) (Bta-Tyr-Phe-Gln-Asn-Cys)-Pro-D-Arg-Gly-$COONH_2$ thioether, 1-carba-dDAVP

Thioether formation *via* the thiol-ene reaction was carried out by adding 70 mL degassed H_2O to 6 mg (6 µmol, ~ 0.1 mM) of synthesis-product **7**. The mixture was stirred under argon atmosphere for 7 h while irradiating with UV light (254 nm). The solvent was removed under reduced pressure, the lyophilized crude product was dissolved in 20 % MeCN in H_2O, filtered and purified by semi-preparative HLPC (20 - 35 % MeCN in H_2O for 19 min). The purified products were lyophilized and analyzed by LC-MS and MALDI. Furthermore, a NEM-test and ^{1}H-NMR measurements were carried out.

Colorless solid
$C_{47}H_{66}N_{14}O_{12}S$ (1051.18 g/mol)
Yield: 2.5 mg (2.6 mol), 14.6 %
HPLC (analytical): T_R = 8.0 min (20 - 35 % MeCN in H_2O)
MALDI-MS: *m/z* found: 1052.37 $[M+H]^+$

(9) Fmoc-Vgl-Tyr-Phe-Gln-Asn-Cys-Pro-Arg-Gly-$COONH_2$, linear 1-carba-AVP

The first part of peptide **9** was synthesized according to the general protocol for automated peptide synthesis (chapter 3.2.1).
After swelling and initial Fmoc-deprotection of the resin, Fmoc-Gly-OH, Fmoc-Arg(N-Pbf)-OH, Fmoc-Pro-OH, Fmoc-Cys(S-Trt)-OH, Fmoc-Asn(N-Trt)-OH, Fmoc-Gln(N-Trt)-OH, Fmoc-Phe-OH and Fmoc-Tyr(O-*t*Bu)-OH were consecutively coupled using standard conditions. Cysteine was coupled using cysteine coupling conditions.
Fmoc-deprotection of the Tyr-residue was performed manually. The preswelled resin (DCM, 30 min) was washed with DMF (3 x 1 min) and treated with 20 % piperidine in DMF (1.5 mL, 3 x 7 min). After washing with DMF (5 x 1 min), Fmoc-Vgl-OH (compound **4**) was coupled manually. For preactivation of coupling components, 40 mg compound **4** (2 eq, 0.12 mmol), 16 mg HOBt (2 eq, 0.12 mmol) and 19 µL DIC (2 eq, 0.12 mmol) were added to 1 mL DMF and left to react for 10 min. The mixture was then added to then resin (203 mg, L_{th} 0.295 mmol/g) and coupled over night. The resin was washed with DMF (3 x 1 min) and DCM (5 x 1 min) and dried in HV. Peptide identity was confirmed by MALDI analysis of a test cleavage.
The peptide was cleaved using standard procedures. The crude product was dissolved in 25 % MeCN in H_2O, filtered and purified by semi-preparative HPLC (30 - 60 % MeCN in H_2O for

19 min). The purified products (two fractions) were lyophilized and peptide identity was verified by MALDI analysis and LC-MS. A NEM-test was carried out to analyze the state of the sulfhydryl groups. ^{1}H-NMR spectra were also recorded.

Colorless solid

$C_{62}H_{77}N_{15}O_{14}S$ (1288.43 g/mol)

Yield: I: 9 mg (11.6 mol), 14 %, II: 7.5 mg (9.6 mol), 12 %

HPLC (semipreparative): T_R (I) = 12-13 min, T_R (II) = 13.8 min (30 - 60 % MeCN in H_2O)

MALDI-MS: *m/z* found: 1289.54 $[M+H]^+$ (I), 1289.54 $[M+H]^+$ (II)

(10) H_2N-(Vgl-Tyr-Phe-Gln-Asn-Cys)-Pro-Arg-Gly-$COONH_2$ thioether, 1-carba-AVP

Thioether formation *via* the thiol-ene reaction was carried out by adding each 8 mL dry MeOH to 1 mg (0.8 µmol, ~ 0.1 mM) of each of the two obtained fractions of compound **9**. Each mixture was stirred under argon atmosphere for 7 h while irradiating with UV light (254 nm). The solvent was removed under reduced pressure and peptide identity was analyzed *via* MALDI measurements and NEM-tests of the collected HPLC-peaks (analytical, 30 - 60 % MeCN in H_2O).

Fmoc-deprotection of the vinylglycine residue was then conducted in solution. The former fraction I (1 mg) was dissolved in dry DMF (300 µL), 50 µL DEA were added and the mixture was stirred at RT. After 3 h, a sample was taken (2 µL), shortly dried in HV, dissolved in 20 µL H_2O and analyzed *via* MALDI measurement. Since no starting material could be detected any more, the reaction was stopped by adding 2 mL toluene and coevaporating under reduced pressure. The dried crude product was dissoved in 50 % MeCN in H_2O and purified by HPLC (analytical column, 10 - 50 % MeCN in H_2O; no TFA added). Peptide identity was analyzed by MALDI-MS.

For Fmoc-deprotection of the former fraction II, 1 mg was dissolved in a mixture of 250 µL DMF and 250 µL DCM. After addition of 5 µL DEA, the mixture was stirred at RT for 2.5 h. The reaction was again stopped by addition of toluene and coevaporation under reduced pressure. The dried crude product was dissoved in 50 % MeCN in H_2O and purified by HPLC (analytical column, 30 - 60 % MeCN in H_2O). The purified product was lyophilized and peptide identity was analyzed by MALDI-MS.

Colorless solid

$C_{47}H_{67}N_{15}O_{12}S$ (1066.19 g/mol)

HPLC (analytical): T_R (I) = 11.5 min (10 - 50 % MeCN in H_2O), T_R (II) = 2.8 min (30 - 60 % MeCN in H_2O)
MALDI-MS: *m/z* found: 1068.35 (I), 1068.35 (II) (identities unclear)

(11a) Mpa-Tyr-Phe-Gln-Asn-Hse-Pro-D-Arg-Gly-●, 6-carba-dDAVP precursor Ia

The first part of compound **11a** was synthesized according to the general protocol for automated peptide synthesis (chapter 3.2.1).
After swelling and initial Fmoc-deprotection of the resin, Fmoc-Gly-OH, Fmoc-D-Arg(N-Pbf)-OH, Fmoc-Pro-OH, Fmoc-Hse(O-Trt)-OH, Fmoc-Asn(N-Trt)-OH, Fmoc-Gln(N-Trt)-OH, Fmoc-Phe-OH and Fmoc-Tyr(O-*t*Bu)-OH were consecutively coupled using standard conditions.
3-Mercaptopropionic acid (Mpa) was then coupled manually. For preactivation of coupling components, 11.2 mg Mpa(Mmt)-OH (4 eq, 0.03 mmol), 4.5 mg HOBt (3 eq, 0.03 mmol) and 5 µL DIC (3 eq, 0.03 mmol) were added to 1 mL DMF/DCM (1:1) and left to react for 5 min. The mixture was then added to then resin (85 mg, L_{th} 0.295 mmol/g) and coupled for 2 h. After washing of the resin with DMF (3 x 1 min), the procedure was repeated to perform the second step of the double coupling. The resin was then washed with DMF (3 x 1 min) and DCM (5 x 1 min) and dried in HV. Peptide identity was confirmed by MALDI analysis and ESI-MS of a test cleavage.

(11b) Mpa-Tyr-Phe-Gln-Asn-Vgl-Pro-D-Arg-Gly-● , 6-carba-dDAVP precursor Ib

The homoserine(Trt) residue of compound **11a** was selectively side chain-deprotected. After swelling of the resin in DCM (30 min), a mixture of 3 % TFA and 3 % TIS in DCM (1.5 mL) was added. After 10 min reaction, the resin was washed with DCM (6 x 1 min) and dried in HV.
Conversion of homoserine to vinylglycine was carried out on the solid support similar to the procedure described for compound **3**. 21 mg of resin (L_{th} 0.33 mmol/g) were dried in a Schlenk tube and THF anh. (330 µL) was added under argon atmosphere. After 30 min of slow stirring, 13.3 mg $NO_2PhSeCN$ (59 µmol, 8.5 eq) were added, followed by addition of 11 µL Bu_3P (59 µmol, 8.5 eq) after 15 min. The mixture was stirred for 6 h under argon atmosphere and then cooled to 0 °C on an ice bath. A few drops of H_2O_2 were added and the mixture was stirred over night while warming to RT. The mixture was then transferred into a solid-phase reactor syringe, the resin was rinsed with EtOAc, ACN, EtOAc, cyclohexane,

DCM and again with EtOAc and dried in HV. The product was analyzed by MALDI-MS of a test cleavage.

(12a) H_2N-Tyr-Phe-Gln-Asn-Hse-Pro-D-Arg-Gly-● , 6-carba-dDAVP precursor IIa

Compound **12a** was synthesized according to the general protocol for automated peptide synthesis (chapter 3.2.1).

After swelling and initial Fmoc-deprotection of the resin, Fmoc-Gly-OH, Fmoc-D-Arg(N-Pbf)-OH, Fmoc-Pro-OH, Fmoc-Hse(O-Trt)-OH, Fmoc-Asn(N-Trt)-OH, Fmoc-Gln(N-Trt)-OH, Fmoc-Phe-OH and Fmoc-Tyr(O-*t*Bu)-OH were consecutively coupled using standard conditions.

Fmoc-deprotection was carried out manually as described for compound **9** using 20 % piperidine in DMF (1.5 mL, 3 x 7 min). The resin was then washed with DMF (3 x 1 min) and DCM (5 x 1 min) and dried in HV.

(12b) H_2N-Tyr-Phe-Gln-Asn-Vgl-Pro-D-Arg-Gly-● , 6-carba-dDAVP precursor IIb

The homoserine(Trt) residue of compound **12a** was selectively side chain-deprotected the same way as for compound **11b**, but using 5 % of TFA and TIS.

Conversion of homoserine to vinylglycine was also carried out the same way as for compound **11b**, having 25 mg of resin (L_{th} 0.318 mmol/g), 176 µL THF anh., 15.4 mg $NO_2PhSeCN$ (68 µmol, 8.5 eq), 17 µL Bu_3P (68 µmol, 8.5 eq) and 17 µL H_2O_2.

The product was analyzed by MALDI-MS and LC-MS of a test cleavage.

(13a) Fmoc-Tyr-Phe-Gln-Asn-Hse-Pro-D-Arg-Gly-● , 6-carba-dDAVP precursor IIIa

Compound **13a** was synthesized according to the general protocol for automated peptide synthesis (chapter 3.2.1).

After swelling and initial Fmoc-deprotection of the resin, Fmoc-Gly-OH, Fmoc-D-Arg(N-Pbf)-OH, Fmoc-Pro-OH, Fmoc-Hse(O-Trt)-OH, Fmoc-Asn(N-Trt)-OH, Fmoc-Gln(N-Trt)-OH, Fmoc-Phe-OH and Fmoc-Tyr(O-*t*Bu)-OH were consecutively coupled using standard conditions. The final Fmoc group was left on the tyrosine residue by leaving out the step for Fmoc deprotection.

The resin was then washed with DCM (5 x 1 min) and dried in HV.

(13b) Fmoc-Tyr-Phe-Gln-Asn-Vgl-Pro-D-Arg-Gly-● , 6-carba-dDAVP precursor IIIb

The homoserine(Trt) residue of compound **13a** was selectively side chain-deprotected using the same procedure as for compound **11b**, but using 5 % of TFA and TIS.
Conversion of homoserine to vinylglycine was also carried out the same way as for compound **11b**, having 115 mg of resin (L_{th} 0.297 mmol/g), 2 mL THF anh., 69.5 mg $NO_2PhSeCN$ (0.3 mmol, 9 eq) and 76 µL Bu_3P (0.3 mmol, 9 eq). The reaction was stirred for 30 h before adding 500 µL H_2O_2 to react for 24 h.
The product was analyzed by HPLC of a test cleavage. The reaction was repeated once more and analyzed by HPLC and MALDI.

(13c) Mpa-Tyr-Phe-Gln-Asn-Vgl-Pro-D-Arg-Gly-$COONH_2$, 6-carba-dDAVP precursor IIIc

Compound **13b** was Fmoc-deprotected as described for compound **9** using 20 % piperidine in DMF and analyzed by HPLC and MALDI-MS.
For coupling of 3-mercaptopropionic acid (Mpa), 38 mg Mpa(Mmt)-OH (0.1 mmol, 3 eq), 13.5 mg HOBt (0.1 mmol, 3 eq) and 15 µL DIC (0.1 mmol, 3 eq) were added to 1 mL DMF and preactivated for 5 min, before the mixture was added to the resin (110 mg, L_{th} 0.034 mmol/g). After 2 h of first coupling, the resin was washed with DMF (2 x 1 min) and the procedure was repeated with fresh reagents. The resin was washed with DMF and DCM (each 5 x 1 min), dried in HV and analyzed *via* MALDI-MS and HPLC of a test cleavage.
Fmoc-deprotection was then repeated by addition of piperidine/DBU/DMF 2:2:96 to the preswelled resin (DCM, 30 min, then washed 3 x 1 min with DMF) for 5 min. After washing with DMF (5 x 1 min), Mpa was again coupled as before. The product was analyzed by HPLC and MALDI-MS of a test cleavage.
The product was then cleaved off the resin as previously described (chapter 3.2.5) and the crude product was analyzed by HPLC, MALDI-MS and ^{1}H-NMR.

(14a) Fmoc-Cys-Tyr-Phe-Gln-Asn-Hse-Pro-Arg-Gly-●, 6-carba-AVP precursor Ia

Compound **14a** was synthesized according to the general protocol for automated peptide synthesis (chapter 3.2.1).
After swelling and initial Fmoc-deprotection of the resin, Fmoc-Gly-OH, Fmoc-Arg(N-Pbf)-OH, Fmoc-Pro-OH, Fmoc-Hse(O-Trt)-OH, Fmoc-Asn(N-Trt)-OH, Fmoc-Gln(N-Trt)-OH, Fmoc-Phe-OH and Fmoc-Tyr(O-*t*Bu)-OH were consecutively coupled using standard

conditions. Fmoc-Cys(S-Trt)-OH was then coupled using the special cysteine conditions. The final Fmoc group was left on the cysteine residue by leaving out the step for Fmoc deprotection.
The resin was washed with DCM (5 x 1 min) and dried in HV.

(14b) Fmoc-Cys-Tyr-Phe-Gln-Asn-Vgl-Pro-Arg-Gly-● , 6-carba-AVP precursor Ib

The homoserine(Trt) residue of compound **14a** was selectively side chain-deprotected the same way as for compound **11b**, but using 7 % of TFA and TIS.
Conversion of homoserine to vinylglycine was also carried out the same way as for compound **11b**, having 25 mg of resin (L_{th} 0.269 mmol/g), 317 µL THF anh., 12.9 mg $NO_2PhSeCN$ (57 µmol, 8.5 eq), 14 µL Bu_3P (57 µmol, 8.5 eq) and 14 µL H_2O_2.
The product was analyzed by MALDI-MS and HPLC of a test cleavage.

(15a) H_2N-Tyr-Phe-Gln-Asn-Hse-Pro-Arg-Gly-● , 6-carba-AVP precursor IIa

Compound **15a** was synthesized according to the general protocol for automated peptide synthesis (chapter 3.2.1).
After swelling and initial Fmoc-deprotection of the resin, Fmoc-Gly-OH, Fmoc-Arg(N-Pbf)-OH, Fmoc-Pro-OH, Fmoc-Hse(O-Trt)-OH, Fmoc-Asn(N-Trt)-OH, Fmoc-Gln(N-Trt)-OH, Fmoc-Phe-OH and Fmoc-Tyr(O-*t*Bu)-OH were consecutively coupled using standard conditions.
The resin was washed with DCM (5 x 1 min) and dried in HV.

(15b) H_2N-Tyr-Phe-Gln-Asn-Vgl-Pro-Arg-Gly-● , 6-carba-AVP precursor IIb

The homoserine(Trt) residue of compound **15a** was selectively side chain-deprotected the same way as for compound **11b**, but using 5 % of TFA and TIS.
Conversion of homoserine to vinylglycine was also carried out the same way as for compound **11b**, having 24 mg of resin (L_{th} 0.318 mmol/g), 361 µL THF anh., 14.7 mg $NO_2PhSeCN$ (65 µmol, 8.5 eq), 16 µL Bu_3P (65 µmol, 8.5 eq) and 17 µL H_2O_2.
The product was analyzed by MALDI-MS and HPLC of a test cleavage.
The product was then cleaved off the resin using the general procedure and the crude product was analyzed by LC-MS.

(16a) Fmoc-Tyr-Phe-Gln-Asn-Hse-Pro-Arg-Gly-●, 6-carba-AVP precursor IIIa

Compound **16a** was synthesized according to the general protocol for automated peptide synthesis (chapter 3.2.1).

After swelling and initial Fmoc-deprotection of the resin, Fmoc-Gly-OH, Fmoc-Arg(N-Pbf)-OH, Fmoc-Pro-OH, Fmoc-Hse(O-Trt)-OH, Fmoc-Asn(N-Trt)-OH, Fmoc-Gln(N-Trt)-OH, Fmoc-Phe-OH and Fmoc-Tyr(O-*t*Bu)-OH were consecutively coupled using standard conditions. The final Fmoc group was left on the tyrosine residue by leaving out the step for Fmoc deprotection.

The resin was washed with DCM (5 x 1 min) and dried in HV.

(16b) H_2N-Tyr-Phe-Gln-Asn-Vgl-Pro-Arg-Gly-● , 6-carba-AVP precursor IIIb

The homoserine(Trt) residue of compound **16a** was selectively side chain-deprotected the same way as for compound **11b**, but using 5 % of TFA and TIS.

Conversion of homoserine to vinylglycine was also carried out the same way as for compound **11b**, having 146 mg of resin (L_{th} 0.277 mmol/g), 6 mL THF anh., 153 mg $NO_2PhSeCN$ (0.7 mmol, 15 eq) and 160 µL Bu_3P (0.7 mmol, 15 eq). The reaction was stirred for 24 h before adding 2 mL H_2O_2 to react for 24 h.

The product was analyzed by HPLC and MALDI-MS of a test cleavage. The reaction was repeated once more with fresh reagents, but rinsing the resin with THF, THF/H_2O 1:1, THF, EtOAc, cyclohexane, DCM and again with EtOAc before drying in HV. The product was analyzed by HPLC and MALDI-MS of a test cleavage.

For Fmoc-deprotection, the resin was first swelled in DCM (30 min) and washed with DMF (5 x 1 min), before it was treated with 1 ml of piperidene/DBU/DMF 2:2:96 for 5 min. The resin was washed with DMF and DCM (each 5 x 1 min), dried in HV and a test cleavage was analyzed by HPLC and MALDI measurement.

3.3 Cloning

3.3.1 DNA isolation of purchased cDNA clones

Purchased cDNA clones AVPR1a-pCR4-TOPO, AVPR2-pCR4-TOPO and OTR-pCR4-TOPO in the host organism DH10B TonA containing the inserts for the human receptors AVPR1a, AVPR2 and OTR, respectively, were plated on LBK plates according to the product information sheet. 5 mL-ONCs (LBK medium) were prepared for one colony of each

respective clone and incubated at 37 °C over night. The ONCs were centrifuged at 5000 rpm for 30 min and plasmid DNA was isolated according to the QuickLyse Miniprep Kit protocol, but eluting with sterile H_2O (2 x 25 µL) instead of elution buffer. DNA concentration was measured on a NanoDrop spectrophotometer.
cDNA insert identity was verified by sequencing with sequencing primers M13-FP and M13-RP from GATC Biotech.

3.3.2 PCR of isolated cDNA

Polymerase chain reaction (PCR) was carried out to amplify the cDNA inserts of the isolated clones with simultaneous introduction of restriction digestion sites at the beginning and the end of the inserts.
PCR reaction mix for the AVPR1a insert contained 15.75 µL H_2O, 5 µL 5X GC buffer, 2.5 µL AVPR1a-pCR4-TOPO template (10 ng), 0.5 µL dNTPs, 0.5 µL forward primer (primer 1, 5 pmol), 0.5 µL reverse primer (primer 2, 5 pmol) and 0.25 µL Phusion polymerase.
PCR reaction mix for the OTR insert contained 9 µL H_2O, 2.5 µL OTR-pCR4-TOPO template (10 ng), 0.5 µL forward primer (primer 3, 5 pmol), 0.5 µL reverse primer (primer 4, 5 pmol) and 12.5 µL 2X Fermentas Maxima Hot Start Green PCR Mastermix.
The following cycling parameters were used:

Table 1: Cycling parameters for PCR.

AVPR1a insert			**OTR insert**		
Cycles	Temperature	Time	Cycles	Temperature	Time
1	95 °C	2 min	1	95 °C	4 min
30	95 °C	20 sec	30	95 °C	1 min
	54 °C	10 sec		57 °C	30 sec
	72 °C	1 min		72 °C	1.5 min
1	72 °C	10 min	1	72 °C	15 min
	4 °C	∞		4 °C	∞

Used primers are listed in Table 2. Primers were designed in order to introduce restriction digestion sites for the enzymes *Xho*I (forward primers) and *EcoR*I (reverse primers).

PCR reactions were resolved by agarose gel electrophoresis, positive bands were cut out of the gel and purified according to the QIAquick Gel Extraction Kit protocol.

Table 2: Primers and their respective Tm values for the overlapping region. Bold – insert sequence, italic – restriction site, underlined – base insert for frameshift maintenance.

Primer	Insert	Sequence	Tm
Primer 1 (forw)	AVPR1a	5' ccg *ctc gag* **atg cgt ctc tcc gcc gg** 3'	58 °C
Primer 2 (rev)	AVPR1a	5' c*gg aat tc*g **agt tga aac agg aat gaa ttt gat** 3'	62 °C
Primer 3 (forw)	OTR	5' ccg *ctc gag* **atg gag ggc gcg ctc gca** 3'	62 °C
Primer 4 (rev)	OTR	5' c*gg aat tc*g **cgc cgt gga tgg ctg gga** 3'	62 °C

3.3.3 Agarose gel electrophoresis

Agarose gel electrophoresis was conducted on 0.8 % agarose gels prepared by dissolving the agarose in TAE buffer in a microwave oven and adding ethidiumbromide with a final concentration of 0.1 µg/mL after cooling down to RT.

Gels were run at 80 V and DNA bands were visualized through the intercalated ethidiumbromide in a UV transillumination chamber.

DNA samples were loaded together with 6X loading dye. 5 µL O'Gene Ruler 1 kb DNA Ladder were loaded on each gel as a standard for visualization of band sizes.

3.3.4 Restriction digestion

Restriction digestion using restriction enzymes *Xho*I and *EcoR*I was carried out on the mammalian vector pmKate2-N (a scheme is shown in the appendix, chapter 6.1) and the purified PCR products AVPR1a and OTR.

The vector-batch contained 13 µL H_2O, 4 µL 10X buffer tango, 1 µL of each restriction enzyme and 1 µL of vector DNA (5 µg), was incubated at 37 °C for 5 h and then stored at - 20 °C.

The PCR product-containing batches contained 2 µL H_2O, 6 µL 10X FD buffer (OTR) or 6 µL 10X buffer tango (AVPR1a), 1 µL of each restriction enzyme and 50 µL of PCR product (1.2 µg OTR / 0.6 µg AVPR1a), was incubated at 37 °C for 4 h (OTR) or 2 h (AVPR1a).

pmKate2-N–*Xho*I/*EcoR*I was purified by agarose gel electrophoresis and QIAquick Gel Extraction of the cut-out band.

AVPR1a–*Xho*I/*EcoR*I and OTR–*Xho*I/*EcoR*I were purified using the PCR Purification Kit.

3.3.4 Ligation

Ligation of the digested PCR products with the digested pmKate2-N vector was carried out by mixing 15 µL of the digested PCR product (AVPR1a–*Xho*I/*EcoR*I or OTR–*Xho*I/*EcoR*I) with

5 µL of digested vector (pmKate2-N–*Xho*I/*EcoR*I), 2.5 µL 10X T4 buffer, 1.5 µL H_2O and 1 µL T4 ligase. The mixture was incubated at 22 °C for 10 min.

3.3.5 Transformation into competent cells

The ligated vector constructs were transformed into *E. coli* competent cells to enable plasmid amplification.
15 µL of ligation product ([pmKate2-N–AVPR1a] or [pmKate2-N–OTR]) were merged with 150 µL newly defrosted competent cells and incubated on ice for 30 min. After heat shock at 42 °C for 2 min and short cooling on ice, 300 µL LB medium were added and the mixture was incubated at 37 °C for 45 min. The samples were plated on LBK plates and incubated at 37 °C over night.
A negative control was done accordingly by using 5 µL of the digested vector pmKate2-N–*Xho*I/*EcoR*I instead of the 15 µL ligation product.
Selected transformants were transferred into adequate media for ONC preparation and subsequent Miniprep plasmid DNA isolation. Receptor construct identity was verified by sequencing with forward sequencing primer CMV-F from GATC Biotech and the following reverse sequencing primer: 5’ ttg att ctc atg gtc tgg gtg 3’, covering bases 812 to 792 of the mKate sequence.

3.4 Cell culture

3.4.1 Splitting cells

HeLa Kyoto cell cultures were split according to standard techniques. Growth medium was gently removed from the cell culture dish and cells were washed once with prewarmed PBS-buffer. 2 mL trypsin were added and incubated for 5 min at 37 °C. The now deattached cells were transferred into a Falcon tube by adding 5 mL prewarmed growth medium and centrifuged at 600 rpm for 3 min. The supernatant was removed and the cell pellet was resuspended in 10 mL growth medium. Cells were seeded onto new dishes in appropriate dilutions. For 8-well dishes for microscopy, 20 µL of the resuspended pellet were added to 250 µL growth medium per well. Cells were grown by incubation at 37 °C in a humidified atmosphere containing 5 % CO_2.

3.4.2 Transient transfection

HeLa Kyoto cells (not containing endogenous vasopressin or oxytocin receptors) were transiently transfected with the generated constructs [pmKate2-N–AVPR1a] or [pmKate2-N–OTR].

Growth medium was gently removed from the cells grown in 8-well dishes and 380 µL prewarmed OptiMEM medium were added in each well.

Transfection cocktails contained 1 µg plasmid DNA and 3 µL transfection reagent Fugene6 per 100 µL OptiMEM. The cocktail was prepared by carefully adding the transfection reagent to the OptiMEM and incubating the mixture for 5 min. DNA was then added and incubated for 20 min, before adding 20 µL of the mixture per cell culture well. One well was left untransfected for each microscopy experiment as a negative control.

Cells were incubated for 24 h at 37 °C in a humidified atmosphere containing 5 % CO_2.

3.5 Microscopy

For measuring the effect of hormone (analogs) on receptor construct AVPR1a-mKate2 or OTR-mKate2, dilution series of the respective peptides were prepared in concentration ranges between 6000 and 0.023 nM, depending on the peptide species (see Table 3). Dilutions were prepared in imaging buffer, except of peptides **7** and **8**, which were diluted in imaging buffer containing 2 % DMSO.

For each individual microscopy measurement, 4 wells (one row of an 8-well dish) were measured simultaneously. Growth medium containing the transfection cocktail was gently removed from the transfected cells of the respective wells, the cells were washed once with imaging buffer and incubated with the Ca^{2+}-sensor Fura-2 AM (2 µM in imaging buffer, 300 µL per well) at 37 °C. After 20 – 30 min, the sensor mix was reused once by transferring to new cell-containing wells. Former sensor-incubated wells were washed with imaging buffer, then 150 µL imaging buffer were added in each well.

Transfected cells were located by observing the mKate-channel. A picture frame was selected for each well (taking a snapshot for later comparison) and recording of the Fura-2 channels was started. After 2 min, the recording was paused briefly for adding 50 µL of peptide in each well.

Table 3: Measured compounds and concentrations for the two receptor constructs.

Compound (nM)	AVPR1a-mKate2				OTR-mKate2				
	5	**dDAVP**	**7**	**8**	**6**	**5**	**dDAVP**	**7**	**8**
6000			x	x				x	x
4000			x	x				x	x
2800			x	x				x	x
2000			x	x		x		x	x
1200				x		x			x
800	x	x		x	x	x	x		x
720				x					
480				x					
400	x	x		x	x	x	x		x
40	x	x		x	x	x	x		x
10	x	x			x	x	x		
2.5	x	x			x	x	x		
0.625	x	x			x		x		
0.208	x	x			x		x		
0.068	x	x			x		x		
0.023	x	x			x		x		

Data analysis was performed by selecting approximately ten transfected and ten untransfected cells per recording (using the program ImageJ) and calculating the maximal amplitude for the 340/378 ratio in relation to the baseline (when plotted time *versus* ratio intensity). Significant values were taken as baseline plus thrice the standard deviation. The median of the amplitudes was then plotted against the concentration to obtain the concentration values leading to half-maximal amplitude (using the sigmoidal dose response-fit of the Sigma Plot software).

3.6 Activity assay

Biological activity of hormone (analogs) was also tested *via* Invitrogen AVPR2 (or AVPR1a)-CRE-bla CHO-K1 Cell-based Assay, strictly following the manufacturer's protocol.

Briefly, CHO division-arrested cells stably expressing human receptors AVPR1a or AVPR2 were thawed, centrifuged and resuspended in assay medium to get a final concentration of 312500 cells/mL. 10000 cells/well (32 µL) were seeded into the cell-containing wells of a 384-well plate (cell-free control wells contained only 32 µL assay medium) and incubated for 20 h at 37 °C in a humidified atmosphere containing 5 % CO_2. 8 µL assay medium with 2 % DMSO (unstimulated wells and cell-free wells) or 8 µL of previously prepared 5X test compound dilution series in assay medium with 2 % DMSO (stimulated wells) were added

and incubated for 5 h. 8 µL of 6X substrate mix were added on each well and incubated for 1-2 h at RT in the dark. Fluorescence-readout was measured at 535 and 460 nm.

Compounds **5**, **7**, **8**, **10-I**, **10-II**, dDAVP and reduced dDAVP were measured in duplicates or triplicates in one or more separate experiments in concentration ranges between 2000 and 0.001 nM, depending on the peptide species and the experiment.

Data analysis was performed on Sigma Plot software. The 460/535 ratio was calculated for background-subtracted values and related to the one for unstimulated wells. Results were indicated as percent of maximal response versus compound concentration. Concentrations of peptides leading to half-maximal response (EC_{50} values) were obtained by using the sigmoidal dose response model from Sigma Plot. Where possible, EC_{50} values were calculated as averages of different experiments.

Chapter 4

Results

4 Results

4.1 Chemistry

4.1.1 Synthesis of N-(9-Fluorenylmethoxycarbonyl)-L-vinylglycine

For the synthesis of peptide **9**, an N-terminal-protected L-vinylglycine residue had to be introduced in position 1 of the peptide. We chose to follow the approach of Pellicciari and coworkers for the racemization-free conversion of L-homoserine into L-vinylglycine *via* a water-elimination reaction[94]. A scheme of the complete reaction procedure is shown in Figure 16.

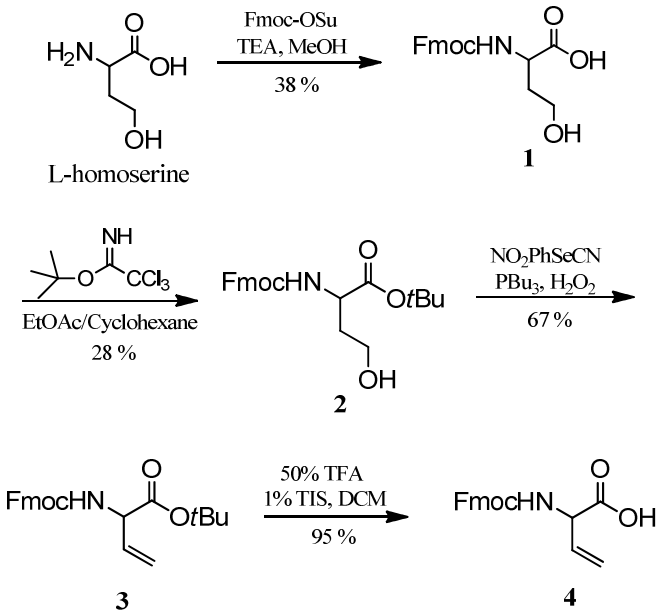

Figure 16: Scheme of the synthesis of L-vinylglycine (**4**) out of L-homoserine.

In the first step of the synthesis, the amino group of L-homoserine was protected with an Fmoc moiety by reaction with Fmoc-OSu in the presence of TEA. The protecting group was chosen because of its acid-stable properties. After incorporation of the final amino acid residue **4** into peptide **9**, the protecting group has to resist the acidic conditions during peptide-cleavage in order to avoid racemization of the vinylglycine residue. After in total 6 h reaction, subsequent aqueous workup and column chromatography (R_f 0.4-0.2, side-products at 0.5, 0.68 and 0.73, EtOAc), 1.07 g (38 %) of compound **1** were isolated. The relatively low yield resided from incomplete extraction and loss of product. Extraction had to be performed at an acidic pH in order to hold the product – a carboxylic acid – into the organic phase. The

workup procedure should undergo improvement to gain better yields, as well as the reaction time could be modulated.

The second reaction involved protection of the carboxylic acid moiety of compound **1** with a *tert*-butyl group using *tert*-butyltrichloroacetimidate as reagent. This reaction included the formation of unavoidable side-products (including protection of the hydroxyl moiety instead of the carboxylic acid moiety and protection of both –OH groups; side-products at R_f 0.3, 0.5, 0.6, 0.68, cyclohexane/EtOAc 1:1) and therefore led to poor yields of compound **2** (394 mg, 18 %; R_f 0.34). Also, remaining starting material could be detected by TLC even after stirring for 24 h (R_f 0.1-0.02). Elongating the reaction time or starting the reaction at 0 °C did not lead to any improvement.

The third step of the synthesis was the elimination of water from homoserine (**2**) leading to vinylglycine (**3**) adapted from Pellicciari *et.al.*, using $NO_2PhSeCN$ and PBu_3 as reagents[94]. $NO_2PhSeCN$ thereby activates PBu_3 which binds to hydroxyl groups and easily can be eliminated as $Bu_3P{=}O$ upon attack of $ArSe^-$ [95]. Hydrogen peroxide oxidation then forms the desired β-γ unsaturated product[94]. After 3 h reaction and aqueous workup, complete conversion of the starting material could be monitored by TLC (R_f 0.2; product at 0.55, side-product at 0.45, cyclohexane/EtOAc 2:1). Column chromatography gave 138 mg (67 %) of product **3**.

The last step of the synthesis was the deprotection of the carboxylic acid of **3** leading to Fmoc-Vgl-OH (**4**) by treatment with 50 % TFA. TIS additionally served as scavenger of the *t*Bu leaving group. Reaction of 6 h led to almost quantitative yields after column chromatography (85 mg, 95 %; R_f 0.6-0.1, cyclohexane/EtOAc 2:1).

Optical rotation was measured for all intermediates in order to exclude racemization. All compounds showed negative $[\alpha]_D^{20}$ values (see Table 4).

The identity of all intermediates was confirmed by LC-MS and ^{1}H- and ^{13}C-NMR. For two of the intermediates (**1** and **2**), some of the quarternary ^{13}C signals could not be resolved on the used 400 MHz spectrometer.

HPLC analysis of the flash-chromatography-purified intermediates gave single product peaks with very good or good purity. Figure 17 shows a comparison of HPLC chromatograms before and after flash chromatography of compound **2**. The final compound **4** could be determined in 100 % purity.

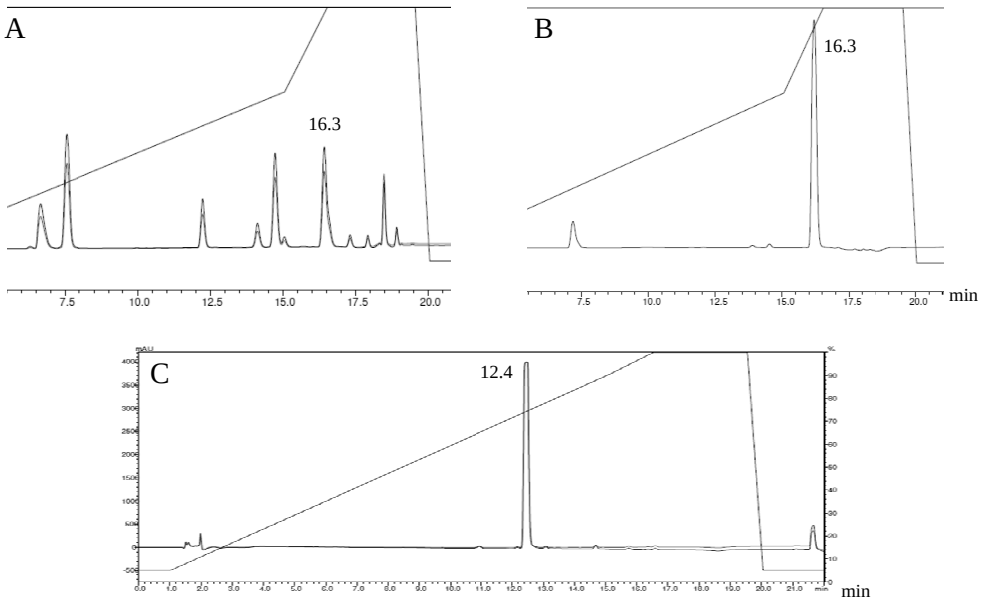

Figure 17: Analytical HPLC chromatograms of crude compound **2** (A) and after flash-chromatography (B) (T_R = 16.3 min (standard gradient)). (C) Analytical HPLC chromatogram of pure compound **4** (T_R = 12.4 min (5 - 100 % MeCN in H2O)).

Table 4 summarizes the properties of the purified intermediates **1** - **4**.

Table 4: Properties of the purified intermediates of N-Fmoc-L-vinylglycine synthesis.

Compound	Yield (%)	TLC R_f	HPLC T_R (min)	HPLC gradient (%)	MW	*m/z*	$[\alpha]_D^{20}$
1	38	0.4-0.2[a]	10.8	10-70	341.36	364[d]	-12.5[e]
2	28	0.34[b]	16.3	10-70	397.46	420[d]	-5.6[f]
3	67	0.55[c]	18.2	10-70	379.18	402[d]	-2.6[f]
4	95	0.6-0.1[c]	12.4	5-100	323.12	346[d]	-15.8[e]

[a] EtOAc, [b] cyclohexane/EtOAc 1:1, [c] cyclohexane/EtOAc 2:1, [d] $[M+Na]^+$, [e] in MeOH, [f] in $CHCl_3$

4.1.2 Peptide synthesis

Rink amide AM resin was chosen for peptide synthesis because cleavage of peptides from this resin using 95 % TFA leaves C-terminal carboxamides which are also present in native vasopressin and oxytocin[85].

HOBt/HBTU/DIPEA as coupling reagent mixture was generally used for coupling of all amino acids except of cysteine. Due to risk of racemization, cysteines were coupled free of base using DIC/HOBt as reagent mixture. Fmoc-Vgl-OH (compound **4**) was also coupled using the same mixture.

The coupling took place efficiently for both automated and manual peptide couplings. HPLC and MS analysis of the synthesized peptides indicated no fragments due to inaccurate coupling efficiency. Albeit the good quality of the couplings and due to unknown reasons, the

yield of the cleaved peptides was generally quite low. Cleavage of peptides after performance of reactions on the solid support (like conversion of homoserine into vinylglycine and subsequent coupling reactions) reduced the yield drastically – however, the reason for that should be sought in low reaction efficiencies due to improper reaction conditions.

4.1.2.1 Synthesis of vasopressin and oxytocin

Vasopressin (compound **5**) and oxytocin (compound **6**) were synthesized according to equal procedures. Peptide synthesis was performed with acetamidomethyl (Acm) as special cysteine side-chain protecting group enabling Tl^{3+}-catalyzed disulfide bond formation directly on the solid support[96]. The resin with the synthesized peptide was incubated with $Tl(CF_3COO)_3$ for 80 min and the completed peptide could be cleaved from the resin yielding the desired peptide and some side-products which could be separated by HPLC. Disulfide-bond formation was confirmed by MALDI mass spectrometry, since the two Acm groups protecting the cysteine residues do not get cleaved upon peptide cleavage (performed here on test cleavage scale) and hence the open vasopressin and oxytocin forms (still holding two Acm groups) can easily be distinguished from the respective oxidized products[86]. Figure 18 shows the MALDI mass spectra of open and oxidized vasopressin, respectively. The open form thereby also showed an additional mass of the peptide holding only one Acm group. However, this did not have an effect on the subsequent on-resin oxidation and the cleaved peptide was purified by HPLC chromatography anyway.

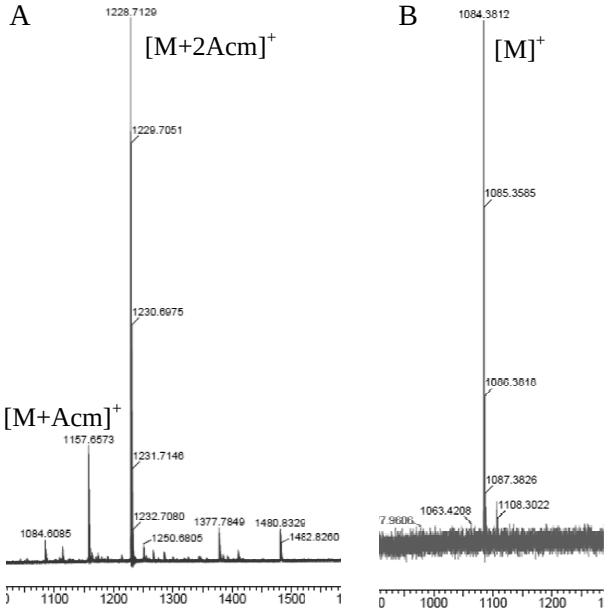

Figure 18: MALDI mass spectra of open vasopressin (A) and the oxidized product **5** (B).

Table 5 summarizes the properties of the HPLC-purified products **5** (vasopressin) and **6** (oxytocin).

Table 5: Properties of purified vasopressin and oxytocin.

Compound	Peptide	Yield (%)	HPLC T_R (min)	HPLC gradient	MW	*m/z*
5	AVP	12[a]	8.4	5-50 %	1084.23	1084.40[b]
6	OT	18[a]	5.51	20-30 %	1007.19	1008.08[c]

[a] referenced to 80 mg resin with 0.62 mmol/g loading, [b] $[M]^+$, [c] $[M+H]^+$

4.1.2.2 Synthesis of 1-carba-AVP and 1-carba-dDAVP

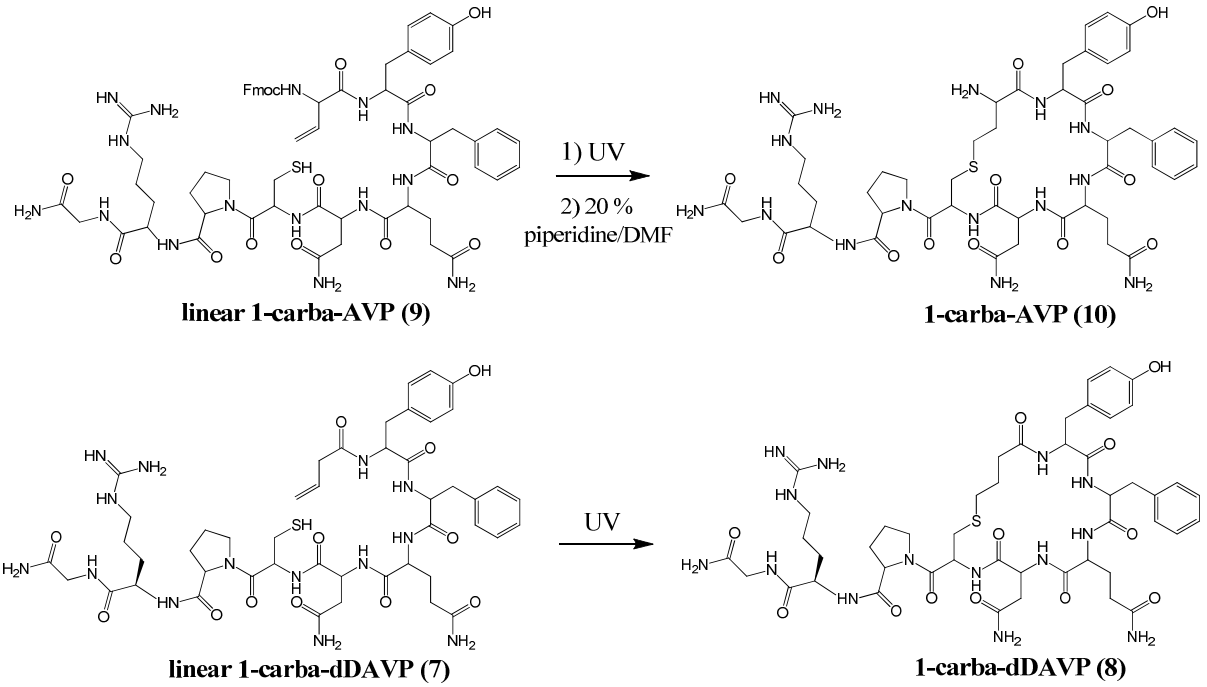

Figure 19: Scheme of the synthesis of 1-carba-AVP (compound **9**) and 1-carba-dDAVP (compound **7**).

The first eight residues of peptides **9** (linear 1-carba-AVP) and **7** (linear 1-carba-dDAVP) were synthesized on the solid support using general procedures for automated peptide synthesis. The respective last amino acids were then coupled manually – Fmoc-Vgl-OH (compound **4**) for peptide **9** and 3-butenoic acid for peptide **7**. Fmoc-Vgl-OH was thereby coupled by cysteine-coupling conditions in order to avoid racemization-inducing basic conditions. The Fmoc group was left on the peptide for the same reason and was not removed until the thiol-ene reaction was carried out successfully. The finished peptides **9** and **7** were cleaved from the resin and purified by semipreparative HPLC. Synthesis-product **9** was

thereby purified as two distinct fractions sharing the same mass for the desired peptide. Synthesis-product **7** was purified as one single fraction – however, HPLC-MS analysis of this fraction revealed the existence of several peaks, two of them sharing the mass of the monomeric peptide, one of them having the mass of the dimeric form. Figure 20 shows HPLC traces and masses of **9** and **7**.

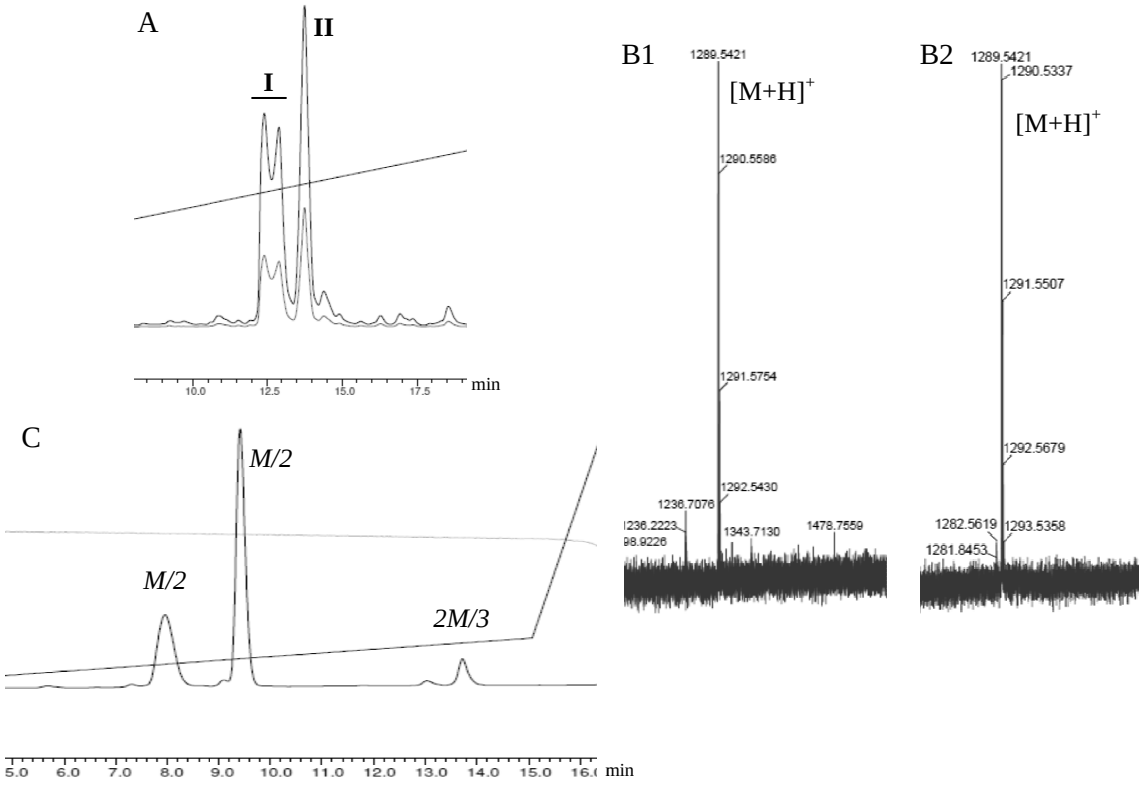

Figure 20: A) Semipreparative HPLC chromatogram of crude product **9** (gradient 30-60 %). The two collected fractions are indicated as **I** and **II**. B) MALDI spectra of purified products **9-I** (B1) and **9-II** (B2). C) Analytical HPLC-MS chromatogram of purified synthesis-product **7** (gradient 20-35 %) with masses indicated as *m/z*.

In order to analyze the two fractions of peptide **9**, N-ethylmaleimid tests were carried out with both fractions to determine the state of the sulfhydryl groups. Free thiol groups thereby undergo a reaction with the maleimid reactant, changing the mass of the peptide. Figure 21 shows the results of this test. Fraction **9-I** showed a mass of the peptide plus bound maleimid, indicating a former free thiol group, whereas fraction **9-II** only showed a mass of the peptide alone, indicating that the thiol group was not free to react with the reactant.

Light-induced thiol-ene reactions of peptides **9** (linear 1-carba-AVP) and **7** (linear 1-carba-dDAVP) in order to gain peptides **10** (1-carba-AVP) and **8** (1-carba-dDAVP), respectively, were carried out under argon atmosphere by irradiation with UV light for 7 h. Synthesis-

product **7** was thereby dissolved in degassed water, whereas the two fractions of peptide **9** (**9-I** and **9-II**) were separately dissolved in dry methanol.

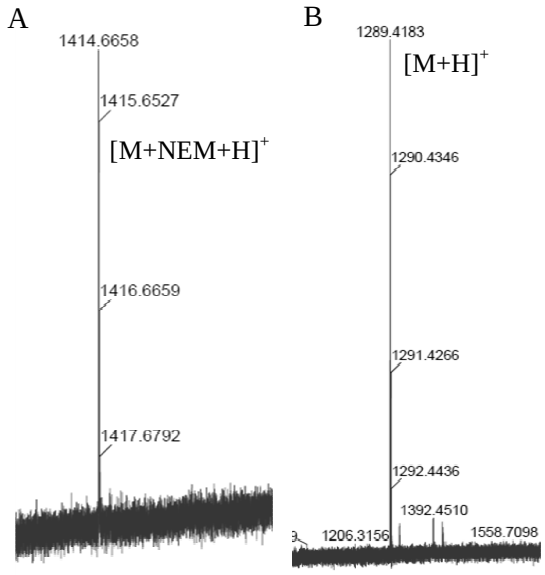

Figure 21: MALDI spectra of peptides **9-I** (A) and **9-II** (B) after reaction with N-ethylmaleimid (NEM).

Figure 22 shows the analytical HPLC-MS chromatogram of crude peptide **8**. Compared to Figure 20C (the same peptide before thiol-ene reaction), the areas of the peaks changed, indicating that a reaction has happened. (Although using the same gradient, the retention times of the respective peaks differ due to changes in TFA content of the solvents.) HPLC-purification of the peaks and subsequent MALDI analysis followed by N-ethylmaleimid tests revealed the existence of two monomeric peptides – one of them binding NEM, the other one not – and a dimeric peptide. This result suggests that the monomeric peptide not binding NEM is the cyclic peptide with the formed thioether group, representing pure peptide **8** (1-carba-dDAVP). The monomeric peptide able to bind NEM is the linear form having a free thiol group, therefore representing pure peptide **7** (linear 1-carba-dDAVP). The results also show that the cyclic form already formed spontaneously to a certain extent upon cleavage from the resin and that performing the thiol-ene reaction increased the amount of cyclic peptide while decreasing the amount of the linear one. Moreover, the reaction obviously favored the unexpected formation of selective dimers.

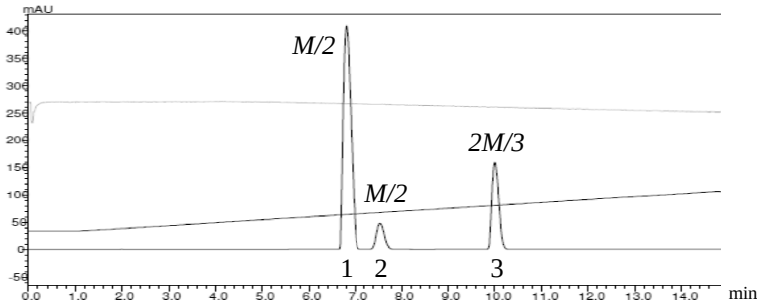

Figure 22: Analytical HPLC-MS chromatogram of crude product **8** (gradient 20-35 %) with masses indicated as *m/z*. Number 1 indicates the cyclic form (final compound **8**), number 2 the linear form (final compound **7**), number 3 the dimeric form.

HPLC chromatograms after thiol-ene reaction of the two fractions **9-I** and **9-II** (**10-I** and **10-II**) are shown in Figure 23. Fraction **II** did not change in retention time (respective chromatogram not shown), suggesting that this fraction already represents the cyclic form of 1-carba-AVP. This result is further supported by an N-ethylmaleimid test performed with this peak (result similar to Figure 21B). For fraction **I**, a clear shift in retention time took place with two obtained peaks sharing the mass of the desired peptide. However, retention times do not fit to the one of the presumable cyclic peptide **II**. A NEM-test performed with the two peaks was of no avail.

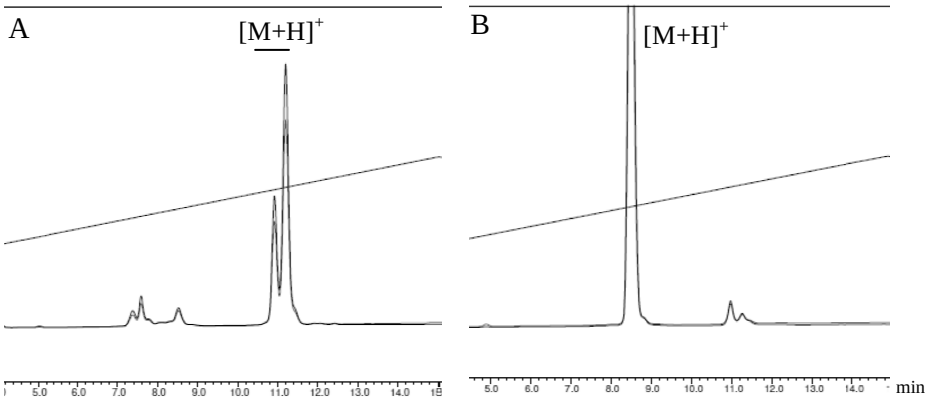

Figure 23: Analytical HPLC chromatograms of crude compounds **10-I** (A) and **10-II** (B) after thiol-ene reaction (gradient 30-60 %).

In order to gain the final compound **10**, solution-phase Fmoc-deprotection had to be performed on the crude fractions **I** and **II** after thiol-ene reaction. Figure 24 shows the chromatograms of the crude products after Fmoc-deprotection. HPLC-purification of the indicated peaks led to the purified final compounds **10-I** (inidentified 1-carba-AVP analog) and **10-II** (supposedly 1-carba-AVP). Since the amounts of the purified peaks were so little, identity could only be analyzed *via* MALDI mass spectrometry. NMR studies could not be

performed. Alongside measured NEM tests did not lead to any result. Especially the Fmoc-deprotection of **10-II** was very inefficient, leading to a very small product peak hard to purify by HPLC. Separation of the product-peak of **10-I** was only possible when omitting TFA in the solution systems. It has to be pointed out that MALDI analysis of both peptides revealed masses of *m/z* 1068 for a theoretical mass of 1066 g/mol. It is therefore not clear if any of the two products are the desired peptide.

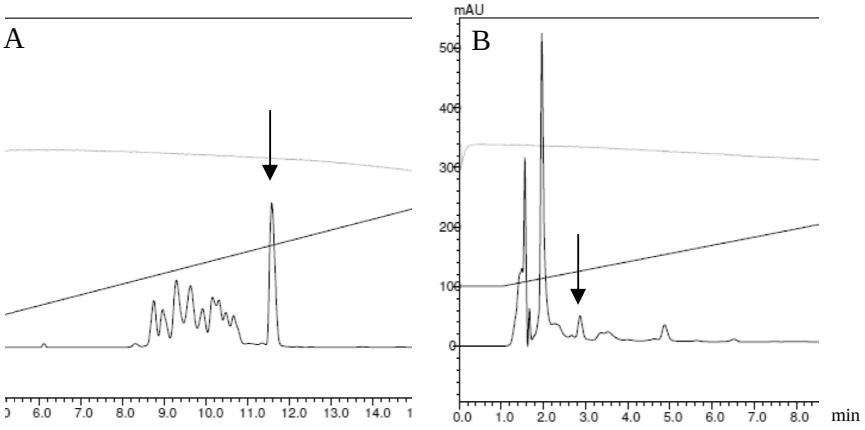

Figure 24: Analytical HPLC chromatograms of crude compounds **10-I** (A) and **10-II** (B) after Fmoc-deprotection (A – gradient 10-50 %, B – gradient 30-60 %). Peaks representing the final peptides destined for purification are marked with arrows.

^{1}H-NMR measurements (results not shown) were performed on products **9-I**, **9-II**, synthesis-product **7** and all purified fractions of product **8** (including pure peptide **7**). Unfortunately, the quality of the spectra was unsatisfactory – albeit good resolution of peaks –, since the strongly required existence or absence of very typical peaks for the double bonds of the respective linear peptides could not be determined free of doubt. Hence, the real identity of the purified products remains speculation since information on the peptides could only be consulted from MALDI and NEM analyses and HPLC-retention times.

Table 6 shows characteristics of the purified peptides. Peptides **7**, **8**, **10-I** and **10-II** were further tested for biological activity.

Table 6: Properties of the purified 1-carba-peptides.

Compound	Peptide	Yield (%)	HPLC T_R (min)	HPLC gradient (%)	MW	*m/z*	NMR
7	linear 1-carba-dDAVP	20.4	9.3	20-35	1051.18	1052.58[c]	n.c.[b]
8	1-carba-dDAVP	14.6	8.0	20-35	1051.18	1052.37[c]	n.c.[b]
10-I	1-carba-AVP analog[a]	n.c.[b]	11.5	10-50	1066.19	1068.35[d]	n.d.[e]
10-II	1-carba-AVP[a]	n.c.[b]	2.8	30-60	1066.19	1068.35[d]	n.d.[e]

[a] presumably because unidentified, [b] n.c. – not clear, [c] $[M+H]^+$, [d] not clear, [e] n.d. – not determined

4.1.2.3 Synthesis of 6-carba-AVP and 6-carba-dDAVP

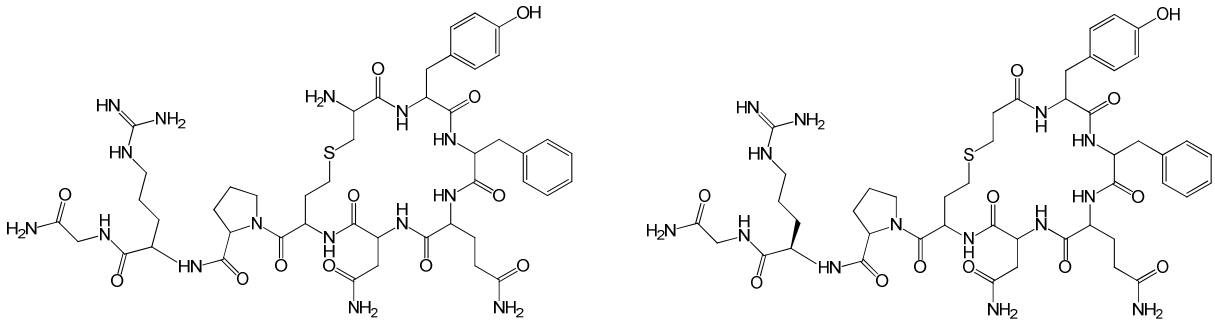

Figure 25: Structures of 6-carba-AVP and 6-carba-dDAVP.

Synthesis of the two analogs where the vinylglycine residue is located in the middle of the synthesized linear peptides was performed equally for 6-carba-AVP and 6-carba-dDAVP. The idea was to perform the conversion of L-homoserine into L-vinylglycine – using the same reagents as for compound **3** according to Pelliciari *et.al.*[94] *– in situ* on the peptide directly on the solid support. The principle of the reaction is already shown in Figure 15. Table 7 lists all synthesized precursor peptides.

Table 7: Synthesized 6-carba-peptide precursors.

Compound	Peptide	Sequence on the resin
11a	6-carba-dDAVP precursor Ia	Mpa-Tyr-Phe-Gln-Asn-Hse-Pro-D-Arg-Gly-
11b	6-carba-dDAVP precursor Ib	Mpa-Tyr-Phe-Gln-Asn-Vgl-Pro-D-Arg-Gly-
12a	6-carba-dDAVP precursor IIa	H_2N-Tyr-Phe-Gln-Asn-Hse-Pro-D-Arg-Gly-
12b	6-carba-dDAVP precursor IIb	H_2N-Tyr-Phe-Gln-Asn-Vgl-Pro-D-Arg-Gly-
13a	6-carba-dDAVP precursor IIIa	Fmoc-Tyr-Phe-Gln-Asn-Hse-Pro-D-Arg-Gly-
13b	6-carba-dDAVP precursor IIIb	Fmoc-Tyr-Phe-Gln-Asn-Vgl-Pro-D-Arg-Gly-
13c	6-carba-dDAVP precursor IIIc	Mpa-Tyr-Phe-Gln-Asn-Vgl-Pro-D-Arg-Gly-
14a	6-carba-AVP precursor Ia	Fmoc-Cys-Tyr-Phe-Gln-Asn-Hse-Pro-Arg-Gly-
14b	6-carba-AVP precursor Ib	Fmoc-Cys-Tyr-Phe-Gln-Asn-Vgl-Pro-Arg-Gly-
15a	6-carba-AVP precursor IIa	H_2N-Tyr-Phe-Gln-Asn-Hse-Pro-Arg-Gly-
15b	6-carba-AVP precursor IIb	H_2N-Tyr-Phe-Gln-Asn-Vgl-Pro-Arg-Gly-
16a	6-carba-AVP precursor IIIa	Fmoc-Tyr-Phe-Gln-Asn-Hse-Pro-Arg-Gly-
16b	6-carba-AVP precursor IIIb	H_2N-Tyr-Phe-Gln-Asn-Vgl-Pro-Arg-Gly-

The reaction has first been tried with the two fully synthesized peptides **11a** (6-carba-dDAVP precursor Ia) and **14a** (6-carba-AVP precursor Ia) by selectively side chain-deprotecting the homoserine(Trt) residue using small percentages of TFA and TIS, respectively, followed by reaction of the peptide with $NO_2PhSeCN$ and Bu_3P in dry THF under argon atmosphere for 6 h and subsequent reaction with H_2O_2 over night. Analysis of the washed and dried products

11b (6-carba-dDAVP precursor Ib) and **14b** (6-carba-AVP precursor Ib) revealed sole (**11b**) or part (**14b**) elimination of the -SH group of the mercaptopropionic acid (**11b**) or cysteine (**14b**) residue of the respective peptide instead of (**11b**) or additionally to (**14b**) elimination of the desired -OH group. The products therefore held the vinylglycine moiety at the wrong position in the peptides due to favored elimination of -SH instead of the desired -OH. The results of the MALDI analyses are shown in Figure 26.

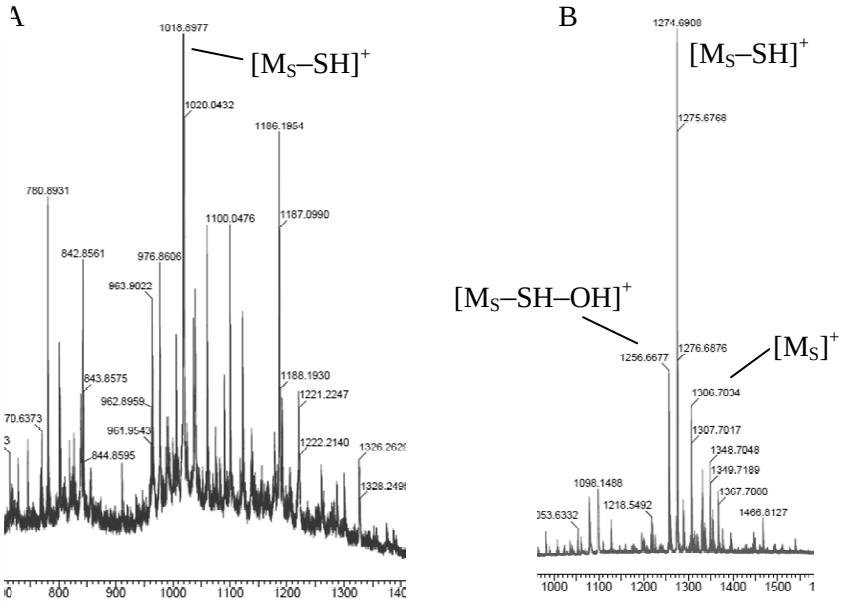

Figure 26: MALDI spectra of test cleavages of **11b** (A) and **14b** (B) after conversion of homoserine into vinylglycine of the fully synthesized linear analogs. M_S – starting mass.

As a consequential step, the same conversion was now tried with peptides **12a** (6-carba-dDAVP precursor IIa) and **15a** (6-carba-AVP precursor IIa), lacking the respective final thiol-containing (amino) acid residues. Analysis of products **12b** and **15b** revealed formation of the desired product peptide with elimination of the right alcohol moiety. Besides, however, the starting material could still be observed and, most importantly, some unidentifiable higher masses appeared additionally (see Figure 27).

Since performing the reaction on peptides holding a free amino group at the end led to the uncontrolled formation of undesired higher masses, the very same reaction was consequentially performed on the same peptides lacking the last (amino) acids but this time being Fmoc-protected on the former free N-terminus. The elimination reaction was performed on peptides **13a** (6-carba-dDAVP precursor IIIa) and **16a** (6-carba-AVP precursor IIIa) as before but this time using longer reaction times (about 24 h), yielding the desired products **13b** and **16b**.

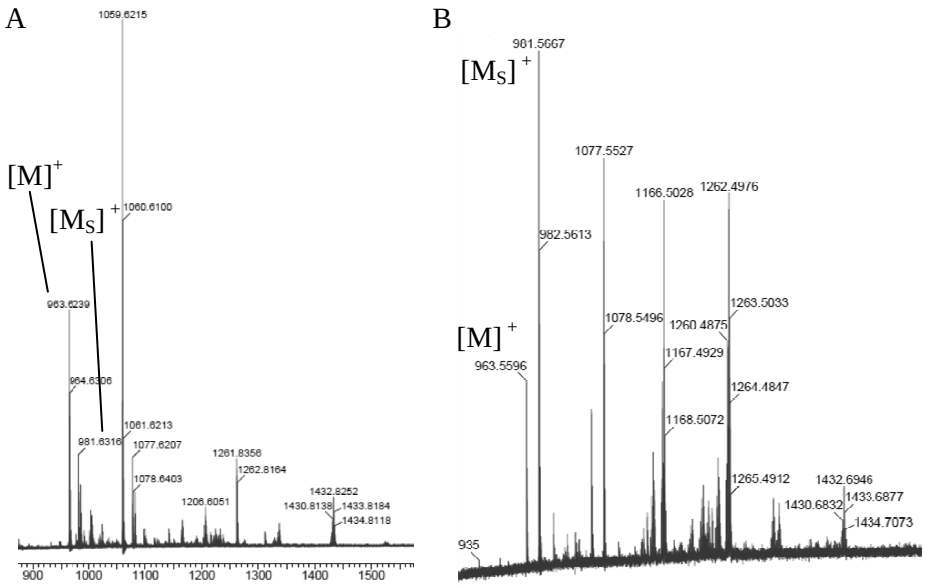

Figure 27: MALDI spectra of test cleavages of **12b** (A) and **15b** (B) after conversion of homoserine into vinylglycine of the partly synthesized linear analogs. M – product mass, M_S – starting mass.

As shown in Figure 28, no higher masses have been formed with the now Fmoc-protected peptides, but the mass of the starting materials could still be observed in varying extents. Therefore, the very same procedure has been performed a second time with fresh reagents to drive the reaction to more completion. Figure 29 shows the HPLC chromatograms of the first and second conversion of **13a**.

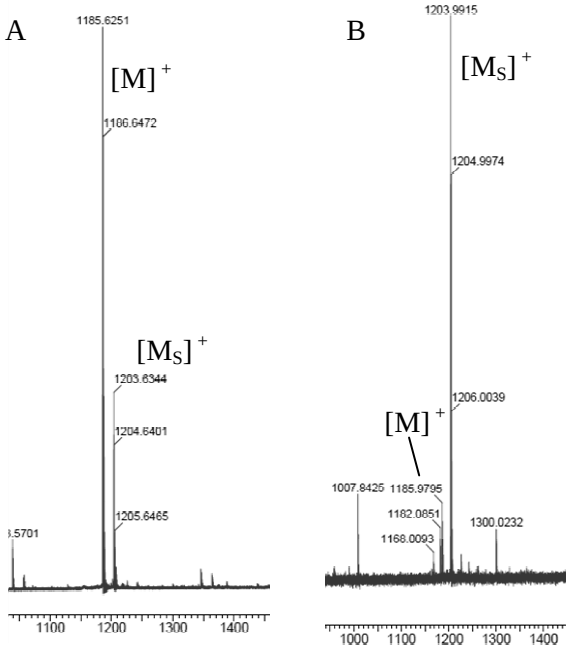

Figure 28: MALDI spectra of test cleavages of **13b** (A) and **16b** (B) after first conversion of homoserine into vinylglycine of the partly synthesized Fmoc-protected linear analogs. M – product mass, M_S – starting mass.

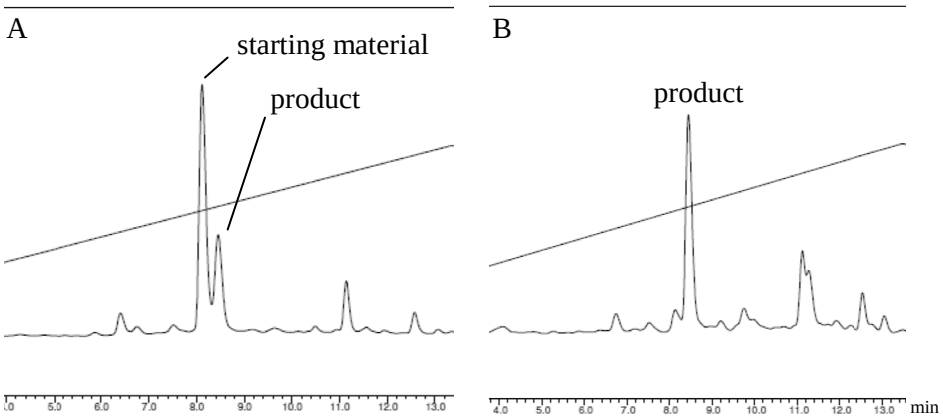

Figure 29: Analytical HPLC chromatograms of test cleavages of **13b** after first (A) and second (B) conversion of homoserine into vinylglycine. Starting compound and product are indicated.

After double conversion of homoserine into vinylglycine and satisfactory product formation, peptide **13b** was Fmoc-deprotected and 3-mercaptopropionic acid was coupled to yield peptide **13c** (6-carba-dDAVP precursor IIIc), the direct precursor of the final ring-closed product 6-carba-dDAVP. Fmoc-deprotection using 20% piperidine in DMF did not lead to satisfactory results, as shown in Figure 30A. The subsequent coupling of 3-mercaptopropionic acid worked just as poorly (Figure 30B). Fmoc-deprotection using piperidine/DBU/DMF 2/2/96 instead of 20 % piperidine did not improve the reaction (results not shown).

^{1}H-NMR spectroscopy of crude product **13c** after cleavage from the resin approved the presence of vinylglycine (results not shown), indicating at least successful conversion of homoserine into vinylglycine.

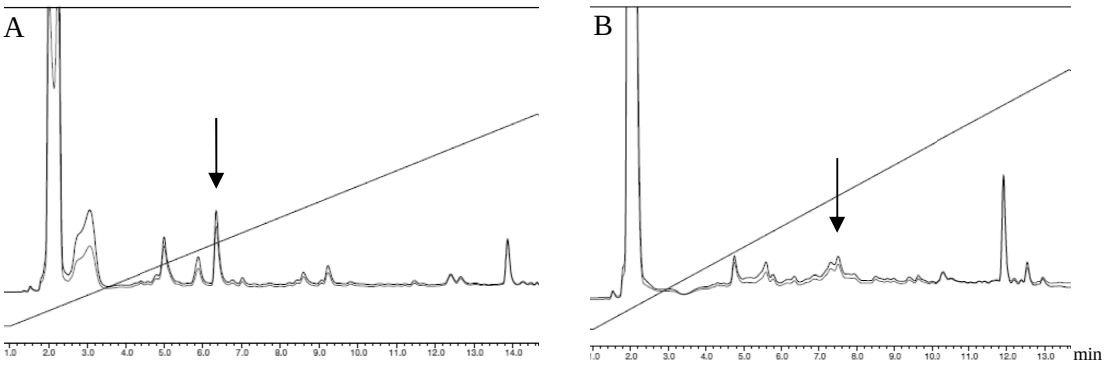

Figure 30: Analytical HPLC chromatograms of test cleavages of **13c** after Fmoc-deprotection (A) and coupling of 3-mercaptopropionic acid (B). Products are indicated with arrows.

Since this last step did not work as expected and the yield was extremely poor, thiol-ene ring-closing reactions to yield the final analog 6-carba-dDAVP could not be performed.

Fmoc-deprotection of **16b** (6-carba-AVP precursor IIIb) worked very poorly as well, hence attempts to couple the last cysteine residue could not be performed.

4.2 Cloning

In order to express the human receptors AVPR1a and OTR in cells for microscopy studies, fluorescently labeled constructs had to be made to be able to visualize them on the cells and monitor the transfected ones. Since Fura-2 was used as fluorescent Ca^{2+} sensor, the fluorescent protein tag mKate2 was chosen for the constructs in order not to interfere with the absorbance properties of Fura-2. It has been reported that receptors containing fluorescent protein tags at their C-terminal ends are active and behave like wild-type receptors[97].
The mammalian vector pmKate2-N was chosen as final vector to insert the receptor genes so that the fluorescent tag would be expressed at the C-terminus of the gene and therefore be located at the inner side of the plasma membrane, leaving the N-terminus at the outer side free – and thereby also the entrance side for hormones/peptides into the receptor.
The PCR-amplified genes encoding AVPR1a and OTR with attached restriction sites at both ends as well as the vector pmKate2-N were all digested by the same restriction enzymes in order to be able to ligate them afterwards and form the desired vector constructs. For that purpose, *Xho*I and *EcoR*I were chosen as restriction enzymes, because neither of the genes nor the vector showed to possess intragenic restriction sites of the same kind, which was important in order not to additionally perform cuts inside the genes. After successful ligation and transformation into *E.coli* competent cells for plasmid amplification, the DNA of the final constructs [pmKate2-N–AVPR1a] and [pmKate2-N–OTR] could be isolated. The generated plasmids were sequenced before applying them to further transfection into mammalian cells and microscopic analyses.

The additionally purchased cDNA clone AVPR2-pCR4-TOPO turned out not to be the desired clone after sequencing and therefore could not be used for PCR and further applications. Hence, only the final constructs [pmKate2-N–AVPR1a] and [pmKate2-N–OTR] could be used for microscopy studies.

4.3 Microscopy

The effect of various concentrations of hormone (analogs) on HeLa Kyoto cells transiently expressing the fluorescent receptor constructs AVPR1a-mKate2 or OTR-mKate2 on their

surface was monitored by measuring Ca^{2+} levels *via* the fluorescent Ca^{2+} sensor Fura-2 AM. This ratiometric sensor exhibits a shift in its excitation spectrum from 378 to 340 nm when binding Ca^{2+} (see Figure 31)[98], which makes it an ideal indicator for the calcium changes introduced by activation of $G\alpha_q$-linked GPCR signaling, like it is occurring for AVPR1a and OTR[65,99]. The AM ester form of Fura-2 makes it able to passively diffuse across cell membranes and holding it inside cells by cleavage of the ester by intracellular esterases[98].

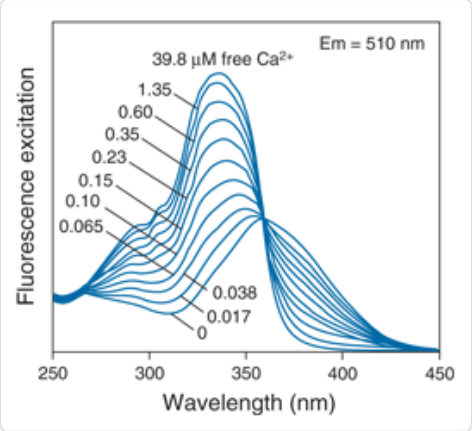

Figure 31: Fluorescence excitation spectra of Fura-2 at different Ca^{2+} concentrations[98].

The effect of peptides on receptor AVPR1a should reflect the results of the more reproducible activity assay from Invitrogen (chapter 4.3), giving therefore more reliability to the microscopy results of receptor OTR.

The results of the microscopic measurements with AVPR1a and OTR are shown in Table 8. Signals for active peptides increased in a dose-dependent manner, indicating normal activity of the receptors (see Figure 32). Peptides **7**, **8** and dDAVP did not show significant activity neither to AVPR1a nor to OTR, therefore leading to the same result as the Invitrogen assay for AVPR1a (chapter 4.3). Vasopressin (AVPR1a and OTR) and oxytocin (OTR) showed activities towards the respective receptors, with lower activity of vasopressin against OTR than oxytocin, as expected[71]. Therefore, the inactivity of vasopressin analogs against OTR was not surprising. Since the results are indicated as peptide-concentration leading to half-maximal signal amplitude and measurements were carried out on only transiently transfected cells, the obtained values cannot be directly compared to previously published EC_{50} values of functional assays or to the results obtained by the Invitrogen assay. However, the general trends can be confirmed, although our results showed activities about one or two degrees higher in magnitude than the published data[71,76].

Figure 32 shows characteristic plots of selected peptides against AVPR1a or OTR.

Table 8: Concentrations of peptides leading to half-maximal signal amplitude.

		AVPR1a	OTR
Compound	**Peptide**	**EC_{50} (nM)**	**EC_{50} (nM)**
5	AVP	0.13 ± 0.05[a]	> 32.61
	dDAVP	not resp.[b]	not resp.[b]
6	OT	-	0.04
7	linear 1-carba-dDAVP	not resp.[b]	not resp.[b]
8	1-carba-dDAVP	not resp.[b]	not resp.[b]

[a] average of two experiments, [b] not resp. – not responding

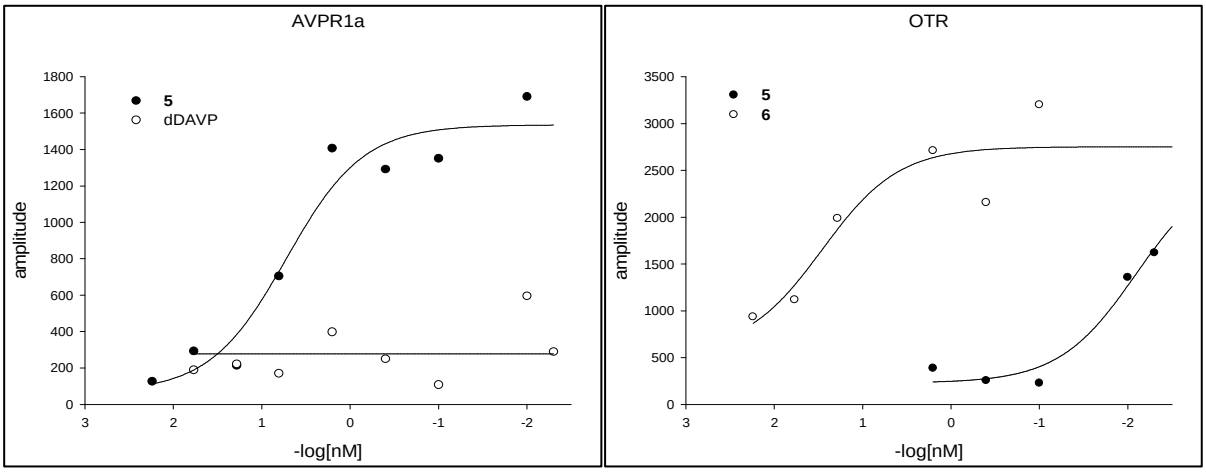

Figure 32: Activity of selected peptides against AVPR1a and OTR, plotted as peptide concentration (-log[nM]) against signal amplitude.

The results in Table 8 reflect the overall behavior of 10-15 cells per peptide and measured concentration. Especially for the inactive peptides and the active peptides at low concentrations, few cells out of a population of non-responding cells were always showing more or less strong signals of response, which remained insignificant when calculating the median of the response of all cells. Furthermore, also few considered untransfected cells sometimes showed responses. Those cells may be very faintly transfected or heavily stressed because of local high compound concentrations.

Most of the activated cells showed responses as depicted in Figure 33 with a strong amplitude directly at the point of addition of the peptide and subsequent oscillating smaller amplitudes after depletion of the initial response. However, some curves showed their maximal amplitudes much later after peptide addition due to diffusion issues. On the whole, smaller peptide concentrations led to smaller initial amplitudes and weaker oscillations.

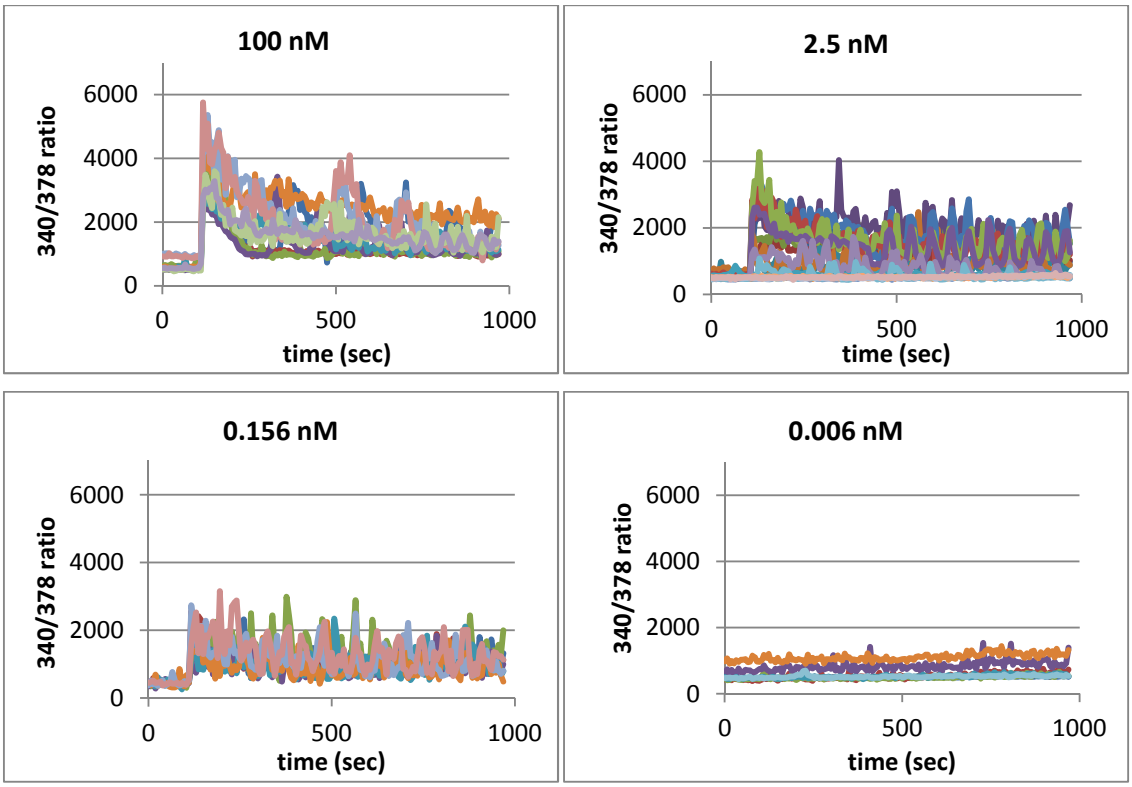

Figure 33: Vasopressin (**5**) added to AVPR1a-expressing cells at four different concentrations. Each color represents an individual cell. Graphs are shown as 340/378 ratio of the two Fura-2 AM signals against time.

Figure 34 shows snapshots of cells expressing AVPR1a-mKate before and after addition of vasopressin.

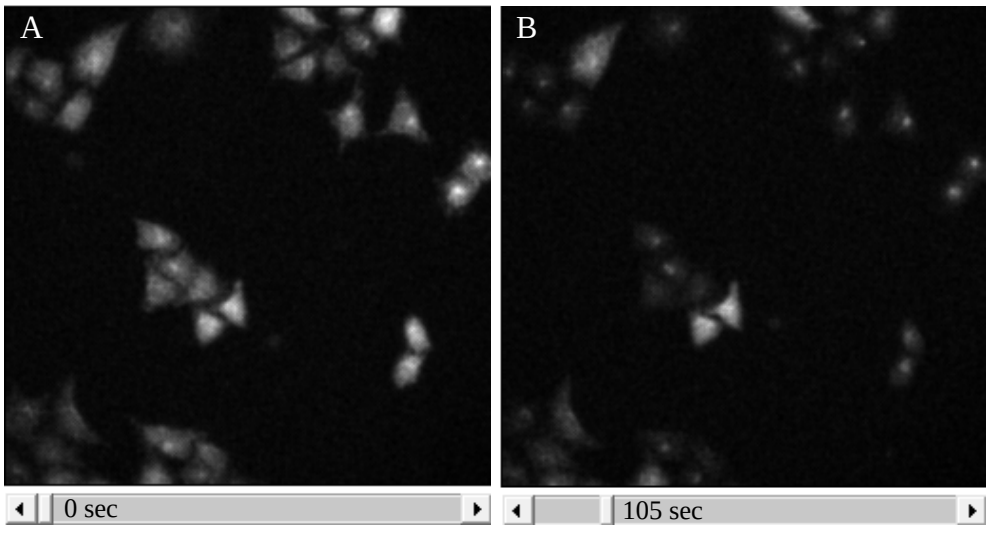

Figure 34: HeLa Kyoto cells observed in the 378-Fura-channel before (A) and immediately after (B) addition of 100 nM vasopressin (**5**). Cells transiently expressing receptor AVPR1a-mKate undergo darkening upon peptide stimulation when observed in the 378-Fura-channel, due to calcium-release and therefore shifting of the excitation spectrum of the calcium-sensor Fura-2 AM to lower wavelengths.

4.3 Activity assay

Screening of biological activity of the various synthesized peptides against human vasopressin receptors AVPR2 and AVPR1a was performed on cell-based assays from Invitrogen having the receptor AVPR2 or AVPR1a stably integrated in division-arrested CHO cells containing a beta-lactamase reporter gene. Upon binding of (active) peptides to the receptors controlling this reporter gene, beta-lactamase gets expressed and a beta-lactamase FRET substrate can be cleaved, leading to diminishment of the FRET acceptor signal (green) and appearance of the donor signal (blue)[100]. Figure 35 demonstrates this principle.

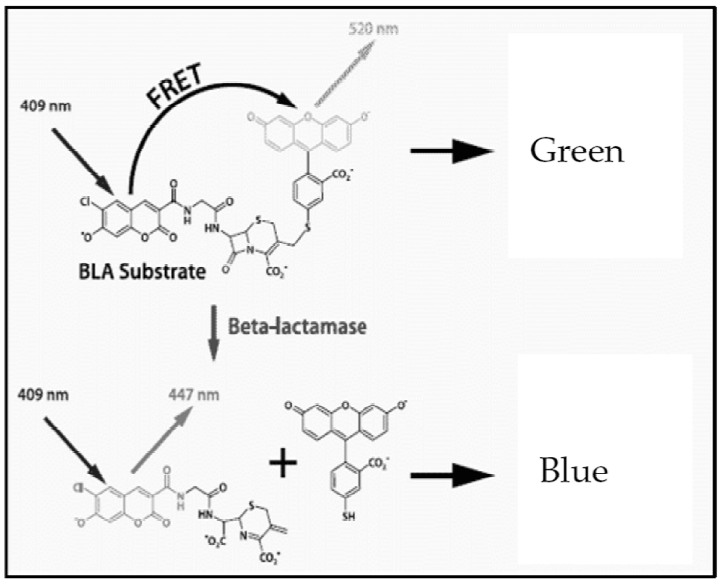

Figure 35: Fluorescent detection of beta-lactamase reporter gene response by a FRET-enabled substrate[100].

The assays were performed with the peptides mentioned in Figure 36 and Table 9 for the receptors AVPR2 and AVPR1a. The blue and green signals were measured for each peptide in a dose-dependent manner in duplicates or triplicates and the ratio was plotted against the concentration as percent of maximal response. For active peptides, EC_{50} values could be obtained.

The results indicate that peptide analogs **8** (1-carba-dDAVP), **10-I** and **10-II** (both unidentified 1-carba-AVP analogs) did not show any activity against receptor AVPR2 in the measured concentration range.

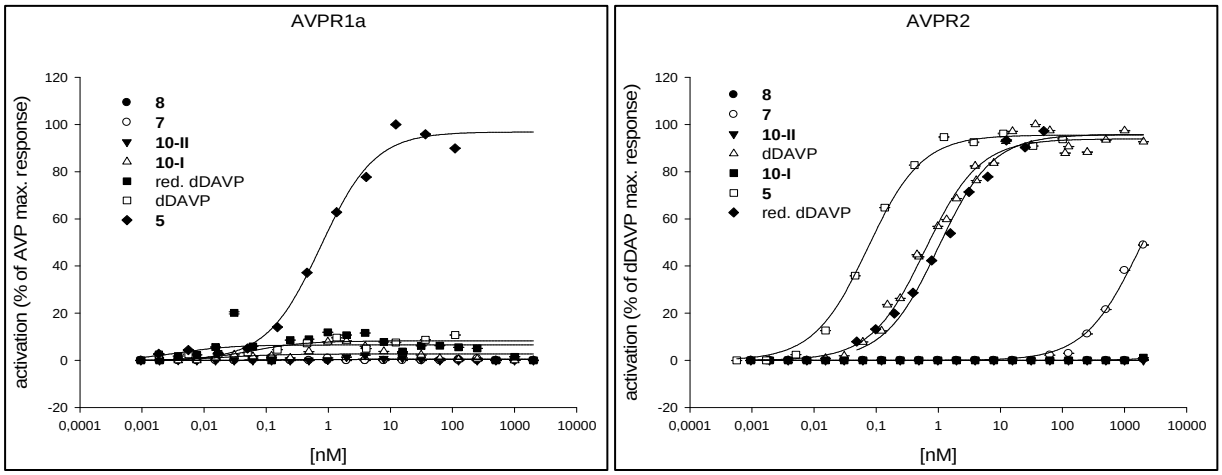

Figure 36: Activity of peptides against AVPR1a and AVPR2. Results are indicated as percent of maximal AVP activation (AVPR1a) or percent of maximal dDAVP activation (AVPR2).

Table 9: Obtained EC_{50} values for peptides against AVPR2 and AVPR1a.

		AVPR2	**AVPR1a**
Compound	**Peptide**	**EC_{50} (nM)**	**EC_{50} (nM)**
5	AVP	0.04 ± 0.02[b]	0.79
	dDAVP	0.70 ± 0.41[c]	not resp.[d]
	red. dDAVP	1.48 ± 0.23[b]	not resp.[d]
7	linear 1-carba-dDAVP	> 1621	not resp.[d]
8	1-carba-dDAVP	not resp.[d]	not resp.[d]
10-I	1-carba-AVP analog[a]	not resp.[d]	not resp.[d]
10-II	1-carba-AVP[a]	not resp.[d]	not resp.[d]

[a] presumably, [b] average of two experiments, [c] average of five experiments, [d] not resp. – not responding

Interestingly, the linear form of 1-carba-dDAVP (peptide **7**) started to show activity at higher concentrations. Due to the limited concentration range, an exact EC_{50} value could not be obtained for this analog. A much higher concentration of this analog would be necessary to reach maximal activity. The activity of dDAVP was slightly weaker than the one of AVP (compound **5**), with EC_{50} values of 0.7 and 0.04 nM, respectively. This result is in good agreement with the values obtained by Cotte *et.al.* with 0.049 nM for AVP and 0.37 nM for dDAVP[64]. However, Invitrogen itself got EC_{50} values of 0.3 nM for dDAVP – which is similar to our result – and importantly the much higher 110 nM for AVP[100]. Also Pena *et.al.* obtained a much stronger activity of dDAVP compared to AVP[101]. Reduced dDAVP (EC_{50} 1.48 nM) showed activity in the range of its oxidized counterpart dDAVP.

Except of vasopressin itself (compound **5**), all other measured peptides were inactive towards receptor AVPR1a in the measured concentration range. The obtained EC_{50} value of AVP,

0.79 nM, is in good agreement with the literature (around 1.0 nM)[102]. The lack of activity of dDAVP towards AVPR1a was anticipated, considering its agonistic activity only towards the human AVPR2 and AVPR1b receptors[66]. Therefore, also the inactivity of dDAVP analogs was anticipated.

Chapter 5

Discussion

5 Discussion

As a form of disulfide bond-engineering, thioether bond-formation represents an opportunity to stabilize disulfide-containing peptides against degradation, while only minimally disturbing the native structure of the peptides[71]. In the course of this master's thesis project, thioether analogs of the neurohypophyseal hormone vasopressin and of its analog desmopressin (1-deamino-8-D-arginine-vasopressin) have been synthesized by a novel approach using the thiol-ene reaction by reacting thiol groups with alkene moieties. Therefore, L-vinylglycine as a suitable amino acid holding a double bond had to be incorporated into the respective peptides. The synthesized analogs were further tested for their ability to activate human vasopressin receptors AVPR1a, AVPR2 and receptor OTR of the closely related hormone oxytocin in order to investigate the impact of the exchange of one respective sulfur atom by a carbon atom on peptide activity.

Synthesis of L-vinylglycine out of L-homoserine was adapted from earlier reports with selection of appropriate protecting groups for our needs[94]. The four-stepped synthesis yielded Fmoc-vinylglycine in very good purity, however, especially steps one and two of the synthesis procedure – coupling of the N-terminal Fmoc-group and coupling of the C-terminal *tert*-butyl-group to homoserine – should undergo improvement due to loss of product during workup and extensive formation of side-products, respectively. Whereas the first step could be improved by changing parts of the workup procedure and strictly maintaining the required acidic pH conditions, the second step would be hard to improve due to unavoidable side-protection of the alcoholic –OH group of homoserine as well as double-protection of both carboxylic and alcoholic –OH groups. Maybe choosing another type of protecting group would be worth trying here.

Synthesis of linear 1-carba-AVP (with the incorporated Fmoc-vinylglycine residue) and linear 1-carba-dDAVP already showed partial formation of the desired cyclic products 1-carba-AVP and 1-carba-dDAVP. Subsequently performed thiol-ene reactions shifted the relation of the products to the favored formation of the respective cyclic peptides. The obtained products were confirmed by MALDI analyses and NEM-tests. However, the conducted ^{1}H-NMR studies did not lead to the desired clear structural evidence, since assignment of the peaks to the right amino acids was impossible with the performed operations and characteristic signals for the double bonds of the linear peptides could not be obtained unambiguously. For definite structural confirmation, extensive NMR studies for clear assignments would be required.

Synthesis of the final 1-carba-AVP required one more step, namely the final solution-phase Fmoc-deprotection of the cyclic peptide. The thiol-ene reaction had already revealed unidentified fractions, Fmoc-deprotection worked so poorly that NMR-studies could not even be performed due to the small amounts, and NEM-tests did not lead to any result, hence the identities of the two isolated peptides remain pure speculation. Also, the revealed masses were one digit too high. Consequently, any results obtained by activity studies with these peptides have to be taken with severe caution. The inefficient Fmoc-deprotection definitely has to be improved in order to gain greater peptide amounts for more detailed analyses.
Despite of the vague NMR results, synthesis of linear and cyclic 1-carba-dDAVP was supposed to be successful, since masses and NEM-test-analyses of the state of the thiol groups were positive. An additional possibility would here be the analysis of the existence or absence of a double-bond, respectively, for example by metathesis reactions. Synthesis of this analog additionally revealed the appearance of a peptide-dimer – a very interesting case, since selective formation of peptide dimers is not easy to achieve due to uncontrollable polymerization. NMR-analyses of this dimer would be very interesting in order to understand the exact structural features. It is not clear if a double-thioether bond and therefore a "double-dimerization" has been achieved, or if two peptides are held together by a single interface. It is also not clear if they are connected by thioether or disulfide bonds.

Synthesis of the 6-carba-analogs of vasopressin and desmopressin turned out to be tricky. On-resin conversion of homoserine into vinylglycine was not successful with peptides holding the final N-terminal thiol-containing (amino) acid residue due to elimination of H_2S instead of the desired H_2O. Omitting this residue led to the favored conversion, although uncontrollable side-products with higher masses appeared when the N-termini were free and not Fmoc-protected. The reaction performed on Fmoc-protected peptides lacking the last residue led to the desired results, however, it was never quantitative and had to be repeated on the same peptide with fresh reactants in order to gain satisfactory product formation. Besides and due to unknown reasons, the portion of formed product varied with every experiment. Sometimes, performing the conversion with still Trt-protected homoserine worked comparatively well, other times, the homoserine residue had to be selectively deprotected first in order to gain any conversion at all. Usage of higher amounts of equivalents of the required reagents only led to improvements to a certain extent, since parts of the reagents started to precipitate at a certain concentration. Nevertheless, on-resin vinylglycine-formation worked satisfactory in the end. However, subsequent Fmoc-deprotection and coupling of the respective last residue –

standard procedures known to be unproblematic – led to inevitable problems due to extremely poor yields and loss of nearly the whole product. Somehow, the products are not stable at the used standard conditions, or some during the vinylglycine-conversion generated side-products – which were always there to a certain extent and may have remained albeit extensive washing steps – interfered with the reactions. Therefore, new methods for Fmoc-deprotection will have to be tried out in order to gain the final linear products. Some effort should also be laid in improvement of the conversion-step, although acceptable product amounts were achieved in the end.

The finally completed analogs 1-carba-dDAVP, linear 1-carba-dDAVP and two unidentified 1-carba-AVP analogs (one of them may represent the desired 1-carba-AVP) have been tested for their biological activities by two different approaches. The beta-lactamase reporter gene-based assay from Invitrogen with cells stably expressing human AVPR1a or AVPR2 revealed the expected results for the control peptides AVP and dDAVP. 1-carba-dDAVP turned out to be inactive towards AVPR2 and AVPR1a, whereas the linear form of this analog showed initiating activity towards AVPR2 at higher concentrations, suggesting *in situ*-folding into a pseudocyclic conformation. Linear 1-carba-dDAVP is obviously able to adopt a conformation more suitable to the AVPR2-binding pocket, whereas the cyclic form of this analog is somehow hindered. A similar result was obtained for linear (reduced) dDAVP which showed activity in the range of the original dDAVP, suggesting folding into a conformation similar to the one of the ring-closed dDAVP. The concept of linear analogs adopting pseudocyclic conformations has already been demonstrated by Cotte *et.al.*[63]. Also, the cyclic version of 1-carba-dDAVP does not have a free thiol group anymore, so maybe the ability to retain a thiol group in position 6 of desmopressin is important for activity. Nevertheless, 1-carba-oxytocin, 6-carba-dDAVP and 6-carba-dAVP have been shown to retain their biological activities[71,80], hence this assumption has to be made with caution. The unidentified 1-carba-AVP analogs were inactive towards both receptors. It has nevertheless to be pointed out that all measurements were performed in limited peptide-concentration ranges – although adapted by comparison with the literature – hence the (small) possibility exists that presumable inactive analogs could start to show some activity at very high concentrations out of the here measured range, or could have an antagonistic effect.

The results of peptide activity studies measured by microscopic analysis on cells transiently expressing human AVPR1a or OTR supported the expectations. Since native dDAVP is neither active against AVPR1a nor against OTR, also the two tested dDAVP-analogs did not

show any surprising activity towards the two receptors. Due to time and sample amount restrictions, the unidentified AVP-analogs were not tested in these experiments. Interestingly, the obtained EC_{50} values for vasopressin and oxytocin were in all cases a little lower than the respective results in literature or our result from the Invitrogen assay. However, activity results obtained from the usage of only transiently transfected cells are not totally reliable due to at times massive concentration differences between the individual cells, hence these values should rather represent an orientation value. For more and reproducible information to gain out of such microscopic studies, it is indispensable to use stably transfected cell lines. Furthermore, microscopic analysis with observation of 15 to 20 cells per well will never gain the reliability of assays like the one from Invitrogen with observation of a whole population of cells at a time. It has further to be pointed out that the EC_{50} values found in literature often vary between the performing groups and between the types of assays.

For further studies, it would be interesting to examine the effect of the peptides on the here not tested because not available vasopressin receptor AVPR1b. Especially the performance of the dDAVP-analogs on this receptor would be interesting to investigate, since dDAVP itself is an agonist for both human AVPR2 and AVPR1b receptors[66]. It would have further been extremely interesting to see the effect of the 6-carba-analogs, especially 6-carba-dDAVP, on the receptors, because this analog has shown to possess increased antidiuretic activity in the rat[80]. The effect on the respective human receptor would therefore be interesting to investigate. Unfortunately, these analogs could not be finished due to problems with some synthetic steps.
Furthermore, binding studies could additionally be performed to investigate the affinity of the different analogs against the respective receptors. This would be especially important for examining the inactive analogs in order to investigate loss or retention of binding affinity. The next step of assay analysis would, however, be antagonistic activity studies of the synthesized inactive peptides against all receptors, in order to examine their potential to counteract the activity of the native peptide hormones by binding to the respective receptors and blocking the binding pockets.

Conclusion

It could be shown that thioether-containing 1-carba-desmopressin was inactive towards human vasopressin receptors AVPR1a, AVPR2 and oxytocin receptor OTR, indicating that exchange of the sulfur atom in residue 1 of desmopressin by a carbon atom had a striking

impact on this peptide's activity. It has already been reported by Knerr *et.al*. that the position of the sulfur atom within the disulfide bridge of a bioactive peptide is important for its activity and that thioether analoga of this peptide retain or lose their activity, depending on the site of the sulfur-to-carbon exchange[81]. It would therefore be interesting to see the effect of 6-carba-desmopressin on the respective receptors with its sulfur-to-carbon exchange at the respective other position. It could further be shown that the linear form of 1-carba-desmopressin, on the other hand, very well retained some activity at higher concentrations, indicating that this linear peptide could adopt a conformation similar to the native desmopressin which the cyclic 1-carba-analog could not achieve.

These results show that already minimal perturbations of the conformation of an active peptide can lead to loss of activity and that such modifications are therefore an important tool to modulate peptide activities.

Chapter 6

Appendix

6 Appendix

6.1 pmKate2-N vector

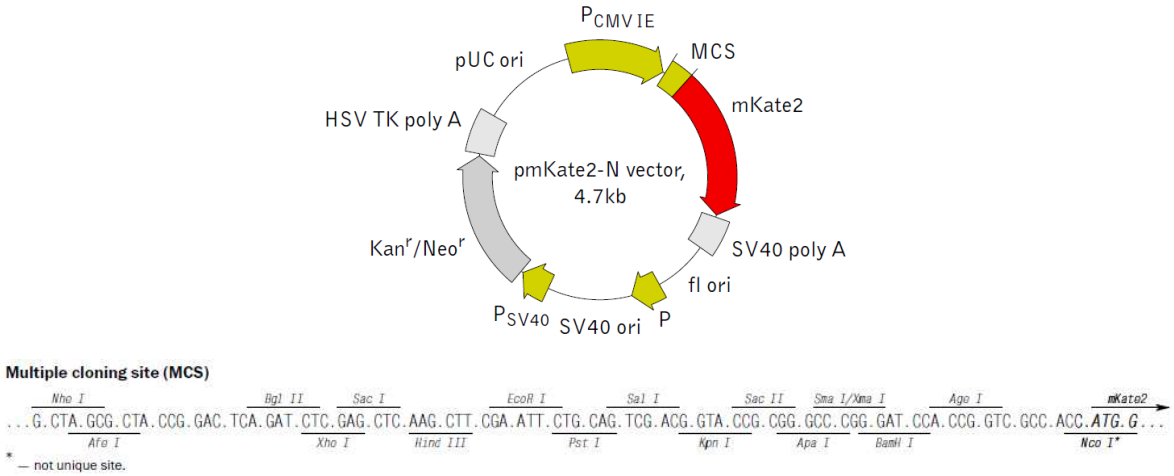

Figure 37: Scheme of the mammalian vector pmKate2-N and its multiple cloning site (Evrogen).

6.2 Figure and table index

Abbreviations

Acm	acetamidomethyl
AM	acetoxymethyl
anh.	anhydrous
AVP	arginine vasopressin
AVPR	arginine vasopressin receptor
BLA	beta-lactamase
Boc	*tert*-butoxycarbonyl
Bta	3-buteinoic acid
CHO	chinese hamster ovary
COSY	correlation spectroscopy
DBU	1,8-diazabicycloundec-7-ene
DCM	dichloromethane
dDAVP	desmopressin
DEA	diethylamine
DIC	diisopropylcarbodiimid
DIPEA	diisopropylethylamine
DMEM	Dulbecco’s modified Eagle’s medium
DMF	dimethylformamide
eq	equivalents
FBS	fetal bovine serum
Fmoc	9-fluorenylmethyloxycarbonyl
FRET	fluorescence resonance energy transfer
GDP	guanosine diphosphate
GPCR	G-protein coupled receptor
GTP	guanosine triphosphate
HBTU	O-(benzotriazol-1-yl)-*N*,*N*,*N*',*N*'-tetramethyluroniumhexafluorophosphate
HEPES	2-[4-(2-hydroxyethyl)piperazin-1-yl]-ethanesulfonic acid
HF	hydrofluoric acid
HOBt	1-hydroxy-benzotriazole
HPLC	high performance liquid chromatography
Hse	homoserine
HV	high vacuum

L_{th}	theoretical loading of resin
MALDI	matrix-assisted laser desorption ionization
MHz	Megahertz
Mmt	4-methoxytrityl
Mpa	3-mercaptopropionic acid
MS	mass spectrometry
NEM	N-ethylmaleimid
NMR	nuclear magnetic resonance
ONC	over night culture
OT	oxytocin
OTR	oxytocin receptor
Pbf	pentafluorophenyl
PBS	phosphate buffered saline
PCR	polymerase chain reaction
R_f	rate of flow
RP(-HPLC)	reversed phase(-HPLC)
Rpm	rounds per minute
RT	room temperature
sat. aqu.	saturated aqueous solution
SPPS	solid-phase peptide synthesis
*t*Bu	*tert*-butyl
TFA	trifluoroacetate
THF	tetrahydrofuran
TIS	triisopropylsilane
TLC	thin layer chromatography
Tm	melting temperature
T_R	retention time
Trt	triphenylmethyl, trityl
Vgl	vinylglycine
	resin

References

[1] Frank E, Landgraf R (2008) The vasopressin system – from antidiuresis to psychopathology. *Eur. J. Pharmacol.* **583**, 226-242

[2] Derick S, Cheng LL, Voirol MJ, Stoev S, Giacomini M, Wo NC, Szeto HH, Ben Mimoun M, Andres M, Gaillard RC, Guillon G, Manning M (2002) [1-Deamino-4-cyclohexylalanine] arginine vasopressin: A potent and specific agonist for vasopressin V1b receptors. *Endocrinology* **143** (12), 4655-4664.

[3] De Wied D, Diamant M, Fodor M (1993) Central nervous system effects of the neurohypophyseal hormones and related peptides. *Front. Neuroendocrinol*. **14**, 251-302.

[4] Land H, Schutz G, Schmale H, Richter D (1982) Nucleotide sequence of cloned cDNA encoding bovine arginine vasopressin-neurophysinII precursor. *Nature* **295**, 299-303.

[5] Christensen JH, Rittig S (2006) Familial neurohypophyseal diabetes insipidus – an update. *Semin. Nephrol*. **26**, 209-223.

[6] Walse B, Kihlberg J, Drakenberg T (1998) Conformation of desmopressin, an analogue of the peptide hormone vasopressin, in aqueous solution as determined by NMR spectroscopy. *Eur. J. Biochem*. **252**, 428-440.

[7] Jard S (1998) Vasopressin receptors. A historical survey. In *Advances in experimental medicine and biology*. Zingg HH, Bourque CW, Bichet DG, Eds. *Plenum Press: New York*, 1-13.

[8] Tanoue A (2009) New topics in vasopressin receptors and approach to novel drugs: Effects of vasopressin receptor on regulations of hormone secretion and metabolisms of glucose, fat and protein. *J. Pharmacol. Sci.* **109**, 50-52.

[9] Hiroyama H, Aoyagi T, Fujiwara Y, Oshikawa S, Sanbe A, Endo F, et.al. (2007) Hyperammonemia in V1a vasopressin receptor knockout mice caused by the promoted proteolysis and reduced intrahepatic blood volume. *J. Physiol.* **581**, 1183-1192.

[10] Birumachi JI, Hiroyama M, Fujiwara Y, Aoyagi T, Sanbe A, Tanoue A (2007) Impaired arginine-vasopressin-induced aldosterone release from adrenal gland cells in mice laching vasopressin V_{1a} receptor. *Eur. J. Pharmacol*. **566**, 226-230.

[11] Hiroyama M, Aoyagi T, Fujiwara Y, Birumachi J, Shigematsu Y, Kiwaki K, et.al. (2007) Hypermetabolism of fat in V1a vasopressin receptor knockout mice. *Mol. Endocrinol*. **21**, 247-258.

[12] Zing HH (1996) Vasopressin and oxytocin receptors. *Baillieres Clin. Andocrinol. Metab.* **10**, 75-96.

[13] Engelmann M, Landgraf R (2004) Microdialysis administration of vasopressin into the septum improves social recognition in Brattleboro rats. *Physiol. Behav.* **55**, 145-149.

[14] Oshikawa S, Tanoue A, Koshimizu T, Kitagawa Y, Tsujimoto G (2004) Vasopressin stimulated insulin release from islet cells through V1b receptors: A combined pharmacological/knockout approach. *Mol. Pharmacol.* **65**, 623-629.

[15] De Wied D, van Ree JM (1989) Neuropeptides: animal behavior and human psychopathology. *Eur. Arch. Psychiatry Neuro. Sci.* **238**, 232-331.

[16] Insel TR, Wang ZX, Ferris CF (1994) Patterns of brain vasopressin receptor distribution associated with social organization in microtine rodents. *J. Neurosci.* **14,** 5381-5392.

[17] Winslow JT, Hastings N, Carter CS, Harbaugh CR, Insel TR (1993) A role for central vasopressin in pair bonding in monogamous prairie voles. *Nature* **365**, 545-548.

[18] Antoni FA (1993) Vasopressinergic control of pituitary adrenocorticotropin secretion comes of age. *Front. Neuroendocrinol.* **14**, 76-122.

[19] Koshimizu T, Tsujimoto G (2009) New topics in vasopressin receptors and approach to novel drugs: Vasopressin and pain perception. *J. Pharmacol. Sci*. **109**, 33-37.

[20] Ostrowski NL, Lolait SJ, Young 3rd WS (1994) Cellular localization of vasopressin V1a receptor messenger ribonucleic acid in adult male in rat brain, pineal, and brain vasculature. *Endocrinol*ogy **135**, 1511-1528.

[21] Hernando F, Schoots O, Lolait SJ, Burbach JP (2001) Immunohistochemical localization of the vasopressin V1b receptor in the rat brain and pituitary gland: anatomical support for its involvement in the central effects of vasopressin. *Endocrinology* **142**, 1659-1668.

[22] Manning M, Olma A, Klis WA, L´Kolodziejczyk AM, Seto J, Sawer WH (1982) Design of more potent antagonists of the antidiuretic responses to arginine-vasopressin. *J. Med. Chem.* **25**, 45-50.

[23] Gimpl G, Fahrenholz F (2001) The oxytocin receptor system: structure, function and regulation. *Physiol. Rev.* **81**, 629-683.

[24] Young LJ, Wang Z, Insel TR (1998) Neuroendocrine bases of monogamy. *Trends Neurosci.* **21**, 71-75.

[25] Ring RH (2005) The central vasopressinergic system: examining the opportunities for psychiatric drug development. *Curr. Pharm. Des.* **11**, 205-225.

[26] Ma P, Zemmel R (2002) Value of novelty? *Nat. Rev. Drug Discov.* **1**, 571-572.

[27] Pierce KL, Premont RT, Lefkowitz RJ (2002) Seven-transmembrane receptors. *Nature Rev. Mol. Cell Biol.* **3**, 639-650.

[28] Marinissen M, Gutkind JS (2001) G protein-coupled receptors and signaling networks: emerging paradigms. *Trends Pharmacol. Sci.* **22**, 268-276.

[29] Lappano R, Maggiolini M (2011) G protein-coupled receptors: novel targets for drug discovery in cancer. *Nature Reviews* **10**, 47-60.

[30] Woehler A, Ponimaskin E (2009) G protein-mediated signaling: Same receptor, multiple effectors. *Curr. Mol. Pharmacol.* **2**, 237-248.

[31] Cabrera-Vera TM, Vanhauwe J, Thomas TO, Medkova M, Preininger A, Mazzoni MR, Hamm HE (2003) Insights into G protein structure, function and regulation. *Endocr. Rev*. **24**, 765-781.

[32] Freissmuth M, Casey PJ, Gilman AG (1989) G-proteins control diverse pathways of transmembrane signaling. *FASEB J.* **3**, 2125-2131.

[33] Gruber C, Mutenthaler M, Freissmuth M (2010) Ligand-based peptide design and combinatorial peptide libraries to targert G protein-coupled receptors. *Curr. Pharm. Des.* **16**, 3071-3088.

[34] Roychowdhury S, Panda D, Wilson L, Rasenick MM (1999) G protein alpha subunits activate tubulin GTPase and modulate microtubule polymerization dynamics. *J. Biol. Chem.* **274**, 13485-13490.

[35] Peleg S, Ivanina T, Dessauer CW, Dascal N (2002) G(aiGDP) regulated the basal activity of G protein-activated K+ channels (GIRK, KIR3). *Biophys J.* **82**, 592A-592A.

[36] Hall RA, Premont RT, Chow CW, Blitzer JT, Pitcher JA, Claing A, Stoffel RH, Barak LS, Shenolikar S, Weinman EJ, Grinstein S, Lefkowitz RJ (1998) The beta(2)-adrenergic receptor interacts with the Na+/H+ exchange. *Nature* **392**, 626-630.

[37] Tang W, Gilman AG (1991) Tape-specific regulation of adenylyl cyclase by G.protein beta-gamma-subunits. *Science* **254**, 1500-1503.

[38] Camps M, Carozzi A, Schnabel P, Scheer A, Parker PJ, Gierschik P (1992) Isozyme-selective stimulation of phospholipase C-beta-2 by G-protein beta-gamma-subunits. *Nature* **360**, 684-686.

[39] Wickman KD, Iniguezlluhi JA, Davenprot PA, Tausig R, Krapivinsky GB, Linder ME, Gilman AG, Clapham DE (1994) Recombinant G-protein beta-gamma-subunits activate the muscarinic-gated atrial potassium channel. *Nature* **368**, 255-257.

[40] Crespo P, Xu NZ, Simonds WF, Gutkind JS (1994) Ras-dependent activation of Map kinase pathway mediated by G-protein beta-gamma-subunits. *Nature* **369**, 418-420.

[41] Neves SR, Ram PT, Iyengar R (2002) G protein pathways. *Science* **296**, 1636-1639.

[42] Moore CAC, Milano SK, Benovic JL (2007) Regulation of receptor trafficking by GRKs and arrestins. *Annu. Rev. Physiol.* **69**, 451-482.

[43] Posner B, Laporte SA (2010) Cellular signaling: peptide hormones and growth factors. In *Progress in brain research*, Martini E, Eds., Vol 181.

[44] McKinley MJ, Cairns MJ, Denton DA, Egan G, Mathai ML, Uschakov A, Wade JD, Weisinger RS, Oldfield BJ (2004) Physiological and pathophysiological influences on thirst. *Physiol. Behav.* **81**, 795-803.

[45] Bourque CW, Oliet SH, Richard D (1994) Osmoreceptors, osmoreception and osmoregulation. *Front Neuroendocrinol.* **15**, 231-274.

[46] Boone M, Deen PMT (2008) Physiology and pathophysiology of the vasopressin-regulated renal water reabsorption. *Eur. J. Physiol.* **456**, 1005-1024.

[47] Nielsen S, Terris J, Andersen D, Acelbarger C, Frokiaer J, Jonassen T, Marples D, Knepper MA, Petersen JS (1997) Congestive heart failure in rats is associated with increased expression and targeting of aquaporin-2 water channel in collecting duct. *Proc. Natl. Acad. Sci. USA* **94**, 5450-5455.

[48] Robben JH, Knoers NV, Deen PM (2006) Cell biological aspects of the vasopressin type-2 receptor and aquaporin 2 water channel in nephrogenic diabetes insipidus. *Am. J. Physiol. Renal Physiol.* **291**, F257-F270.

[49] Ghirardello S, Malattia C, Scagnelli P, Maghnie M (2005) Current perspective on the pathogenesis of central diabetes insipidus. *J. Pediatr. Endocrinol. Metab*. **18**, 631-645.

[50] Siggaard C, Rittig S, Corydon TJ, Andreasen PH, Jensen TG, Andresen BS, Robertson GL, Gregersen N, Bolund L, Pedersen EB (1999) Clinical and molecular evidence of abnormal processing and trafficking of the vasopressin preprohormone in a large kindred with familial neurohypophyseal diabetes insipidus due to signal peptide mutation. *J. Clin. Endocrinol. Metab*. **84**, 2933-2941.

[51] Makaryus AN, McFarlane SI (2006) Diabetes insipidus: diognosis and treatment of a complex disease. *Cleve. Clin. J. Med.* **73**, 65-71.

[52] Robben JH, Knoers NV, Deen PM (2005) Characterization of vasopressin V2 receptor mutants in nephwogenis diabetes insipidus in a polarized cell model. *Am. J. Physiol. Renal Physiol.* **289**, F265-F272.

[53] Deen PMT, Croes H, van Aubel RH, Ginsel LA, van Os CH (1995) Water channels encoded by mutant aquaporin-2 genes in nephrogenic diabetes insipidus are impaired in their cellular routing. *J. Clin. Invest.* **95**, 2291-2296.

[54] Wood SP, Tickle IG, Treharne AM, Pitts JE, Mascarenhas Y, Li JY, Husain J, Cooper S, Blundell TL, Hruby VJ, Buku A, Fischman AJ, Wyssbrod HR (1986) Crystal structure analysis of deamino-oxytocin: conformational flexibility and receptor binding. *Science* **232**, 633-636.

[55] Iwadate M, Nagao E, Williamson MP, Ueki M, Asakura T (2000) Structure determination of [Arg8]vasopressin methylenedithioether in dimethyl sulfoxide using NMR. *Eur. J. Biochem.* **267**, 4504-4510.

[56] Schmidt JM, Ohlenschläger O, Rüterjans H, Grzonka Z, Kojro E, Pavo I, Fahrenholz F (1991) Conformation of [8-arginine]vasopressin and V1 antagonists in dimethyl sulfoxide solution derived from two-dimensional NMR spectroscopy and molecular dynamics simulation. *Eur. J. Biochem.* **201**, 355-371.

[57] Hempel JC (1987) The conformation of neurohypophyseal hormones, In *The peptides: Analysis, synthesis, biology*, Smith CW, Eds., Vol. 8, *Academic Press: New York*, 209-237.

[58] Hruby VJ, Lebl M (1987) I. Conformational properties of neurohypophyseal hormone analogs in solution as determined by NMR and laser Ramam spectroscopies, In *CRC handbook of neurohypophyseal homone analogs*, Jost K, Lebl M, Brtnik F, Eds., Vol. 1, *CRC Press: Boca Raton FL*, 105-155.

[59] Slusarz MJ, Gieidon A, Slusarz R, Ciarowski J (2006) Analysis of onteractions responsible for vasopressin binding to human neurohypophyseal hormone receptors – molecular dynamics study of the activated receptor-vasopressin-Gα systems. *J. Peptide Sci.* **12**, 180-189.

[60] Lu Z-L, Saldanha JW, Hulme EC (2002) Seven-transmembrane receptors: crystals clarify. *Trends Pharmacol. Sci.* **23**, 140-146.

[61] Hibert M, Hoflack J, Trumpp-Kallmeyer S, Mouillac B, Chini B, Mahé E, Cotte N, Jard S, Manning M, Barberis C (1999) Functional analysis of vasopressin/oxytocin receptors. *J. Recept. Signal Transduct. Res.* **19**, 589-596.

[62] Chini B, Mouillac B, Ala Y, Balestre MN, Trumpp-Kallmeyer S, Hoflack J, Elands J, Hibert M, Manning M, Jard S, Barberis C (1997) Identification of a single residue responsible for agonist selectivity in the oxytocin-vasopressin receptors. *Ann. N. Y. Acad. Sci.* **812**, 218-221.

[63] Cotte N, Balestre M-N, Aumelas A, Mahé E, Phalipou S, Morin D, Hibert M, Manning M, Durroux T, Barberis C, Mouillas B (2000) Conserved aromatic residues in the transmembrane region VI of the V1a vasopressin receptor differentiate agonist vs. antagonist ligand binding. *Eur. J. Biochem.* **267**, 4253-4263.

[64] Cotte N, Balestre M-N, Phalipou S, Hibert M, Manning M, Barberis C, Mouillac B (1998) Identification of residues responsible for the selective binding of peptide antagonists and agonists in the V2 vasopressin receptor. *J. Biol. Chem.* **273**/45, 29462-29468.

[65] Barberis C, Mouillac B, Durroux T (1998) Structural bases of vasopressin/oxytocin receptor function. *J. Endocrinol.* **156**, 223-229.

[66] Saito M, Tahara A, Sugimoto T (1997) 1-Desamino-8-D-arginine vasopressin (dDAVP) as an agonist on V_{1b} vasopressin receptor. *Biochem. Pharmacol.* **53**, 1711-1717.

[67] Zaoral M, Kolc J, Sorm F (1967) Amino acids and peptides LXXI. Synthesis of 1-deamino-8-D-γ-aminobutyrine-vasopressin, 1-deamino-8-D-lysine-vasopressin and 1-deamino-8-D-arginine-vasopressin. *Coll. Czech. Chem. Commun.* **32**, 1250-1257.

[68] Manning M, Cheng LL, Stoev S, Wo NC, Chan WY, Szeto HH, Durroux T, Mouillac B, Barberis C (2005) Design of peptide oxytocin antagonists with strikingly higher affinities and selectivities for the human oxytocin receptor than anrisoban. *J. Pept. Sci.* **11**, 593-608.

[69] Thibonnier M, Coles P, Thibonnier A, Shoham M (2001) The basic and clinical pharmacology of nonpeptide vasopressin receptor antagonists. *Ann. Rev. Pharmacol. Toxicol.* **41**, 175-202.

[70] Manning M, Stoev S, Chini B, Durroux T, Mouillac B, Guillon G (2008) Peptide and non-peptide agonists and antagonists for the vasopressin and oxytocin V1a, V1b, V2 and OT receptors: research tools and potential therapeutic agents. *Prog. Brain Res.* **170**/37, 473-512.

[71] Muttenthaler M, Andersson A, de Araujo A, Dekan Z, Lewis RJ, Alewood PF (2010) Modulating oxytocin activity and plasma stability by disulfide bond engineering. *J. Med. Chem.* **53**, 8585-8596.

[72] Jarvis D, DuVigneaud V (1964) Cristalline deamino-oxytocin. *Science* **143**, 545-548.

[73] Chini B, Manning M, Guillon G (2008) Affinity and efficacy of selective agonists and antagonists for vasopressin and oxytocin receptors: an "easy guide" to receptor pharmacology. *Prog. Brain Res.* **170**/38, 513-517.

[74] Meraldi JP, Hruby VJ, Brewster AIR (1977) Relative conformational rigidity in oxytocin and [1-penecillamine]oxytocin: A proposal for the relation of conformational flexibility to peptide hormone agonism and antagonism. *Proc. Natl. Acad. Sci. USA* **74**, 1373-1377.

[75] Panijpan B (1977) Chirality of the disulfide bond in biomolecules. *J. Chem. Ed.* **54**/11, 670-672.

[76] Stymiest JL, Mitchell BF, Wong S, Vederas JC (2005) Synthesis of oxytocin analogues with replacement of sulfur by carbon gives potent antagonists with increased stability. *J. Org. Chem.* **70**, 7799-7809.

[77] Hase S, Morikawa T (1969) Synthesis of a biologically active analog of deamino-8-arginine-vasopressin which does not contain a disulfide bond. *Experientia* **25**/12, 1239-1240.

[78] Mayer JP, Heil JR, Zhang J, Munson MC (1995) An alternative solid-phase approach to C1-oxytocin. *Tetrahedron Lett.* **36**/41, 7387-7390.

[79] Rudinger J, Jost K (1964) A biologicallx active analogue of oxytocin not containing a disulfide group. *Experiantia* **XX**/10, 570-571.

[80] Jost K, Prochazka Z, Cort JH, Barth T, Skopkova J, Prusik Z, Sorm F (1974) Synthesis and some biological activities of analogues of deamino-vasopressin with the disulpfide bridge altered to a thioether bridge. *Coll. Czech. Chem. Commun.* **39**, 2835-2856.

[81] Knerr PJ, Tzekou A, Ricklin D, Qu H, Chen H, van der Donk WA, Lambris JD (2011) Synthesis and activity of thioether-containing analogues of the complement inhibitor compstatin. *ACS Chem. Biol.* **6**/7, 753-760.

[82] Kelleman A, Mattern R-H, Pierschbacher MD, Goodman M. (2003) Incorporation of thioether building blocks into an $\alpha_v\beta_3$-specific RGD peptide: Synthesis and biological activity. *Biopolymers* **71**, 686-695.

[83] Merrifield RB (1963) Solid phase peptide synthesis. I. The synthesis of a tetrapeptide. *J. Am. Chem. Soc.* **85**, 2149-2154.

[84] El-Faham A, Albericio F (2011) Peptide coupling reagents, more than a letter soup. *Chem. Rev.* **111**/11, 6557-6602.

[85] Amblard M, Fehrentz J-A, Martinez J, Subra G (2006) Methods and protocols of modern solid phase peptide synthesis. *Mol. Biotechnol*. **33**, 239-254.

[86] Sewald N, Jakubke H-D (2009) In *Peptides: Chemistry and biology*, 2nd edition, Wiley-VCH.

[87] Moss JA (2005) Guide for resin and linker selection in solid-phase peptide synthesis. *Curr. Protoc. Prot. Sci.* Chapter 18, Unit 18.7

[88] Du Vigneaud V, Gish DT, Katsoyannis PG (1954) A synthetic preparation possessing biological properties associated with arginine-vasopressin. *J. Am. Chem. Soc.* **76**, 4751-4752.

[89] Triola G, Brunsveld L, Waldmann H (2008) Racemization-free synthesis of S-alkylated cysteines via thiol-ene reaction. *J. Org. Chem*. **73**, 3646-3649.

[90] Hoyle CE, Bowman CN (2010) Thiol-ene click chemistry. *Angew. Chem. Int. Ed*. **49**, 1540-1573.

[91] Killops KL, Campos LM, Hawker CJ (2008) Robust, efficient and orthogonal synthesis of dendrimers via thiol-ene "click" chemistry. *J. Am. Chem. Soc.* **130**, 5062-5064.

[92] Aimetti AA, Shoemaker RK, Lin C-C, Anseth KS (2010) On-resin peptide macrocyclization using thiol-ene click chemistry. *Chem. Commun*. **46**, 4061-4063.

[93] Kolb HC, Finn MG, Sharpless KB (2001) Click chemistry: Diverse chemical function from a few good rections. *Angew. Chem*. **40**, 2004-2021.

[94] Pellicciari R, Natalini B, Marinozzi M (1988) L-vinylglycine from L-homoserine. *Synth. Commun.* **18**/14, 1715-1721.

[95] Grieco PA, Gilman S, Nishizawa M (1976) Organoselenium chemistry: A facile one-step synthesis of alkyl aryl selenides from slcohols. *J. Org. Chem.* **41**/8, 1485-1486.

[96] Fujii N, Otaka A, Funakoshi S, Bessho K, Watanabe T, Akaji K, Yajima H (1987) Studies on peptides. CLI. Syntheses of cystine-peptides by oxidation of S-protected cysteine-peptides with thallium(III) trifluoroacetate. *Chem. Pharm. Bull. (Tokyo)* **35**/6, 2339-2347.

[97] Schülein R, Hermosilla R, Oksche A, Dehe M, Wiesner B, Krause G, Rosenthal W (1998) A dileucine sequence and an upstream glutamate residue in the intracellular carboxyl terminus of the vasopressin V2 receptor are essential for cell surface transport in COS.M6 cells. *Mol. Pharmacol*. **54**, 525-535.

[98] Johnson I, Spence MTZ, Eds. In *The molecular probes handbook – A guide to fluorescent probes and labeling technologies*, 11th edition.

[99] Strakowa Z, Soloff MS (1997) Coupling of oxytocin receptor to G proteins in rat myometrium during labor: Gi receptor interaction. Am. J. Physiol. 272, E870-E876.

[100] Manual (2008) GeneBLAzer® AVPR2 CHO-K1 DA and AVPR2-CRE-*bla* CHO-K1 Cell-based Assay, Invitrogen.

[101] Pena A, Murat B, Trueba M, Ventura MA, Wo NC, Szeto HH, Cheng LL, Stoev S, Guillon G, Manning M (2007) Seding ans synthesis of the first selective agonists for the rat vasopressin V1b receptor: Based on modifications of deamino-[Cys1]arginine vasopressin at positions 4 and 8. *J. Med. Chem*. **50**, 835-847.

[102] Manual (2007) GeneBLAzer® AVPR1a CHO-K1 DA and AVPR2-CRE-*bla* CHO-K1 Cell-based Assay, Invitrogen.